ISSN 2518-7198 (Print)
ISSN 2663-5089 (Online)

№ 3(95)/2019

ФИЗИКА сериясы
Серия ФИЗИКА
PHYSICS Series

ҚАРАҒАНДЫ УНИВЕРСИТЕТІНІҢ ХАБАРШЫСЫ

ВЕСТНИК КАРАГАНДИНСКОГО УНИВЕРСИТЕТА

BULLETIN OF THE KARAGANDA UNIVERSITY

ISSN 2518-7198 (Print)
ISSN 2663-5089 (Online)
Индексі 74616
Индекс 74616

ҚАРАҒАНДЫ УНИВЕРСИТЕТІНІҢ ХАБАРШЫСЫ

ВЕСТНИК КАРАГАНДИНСКОГО УНИВЕРСИТЕТА

BULLETIN OF THE KARAGANDA UNIVERSITY

ФИЗИКА сериясы

Серия ФИЗИКА

PHYSICS Series

№ 3(95)/2019

Шілде–тамыз–қыркүйек
30 қыркүйек 2019 ж.
Июль–август–сентябрь
30 сентября 2019 г.
July–August–September
September, 30, 2019

1996 жылдан бастап шығады
Издается с 1996 года
Founded in 1996

Жылына 4 рет шығады
Выходит 4 раза в год
Published 4 times a year

Қарағанды, 2019
Караганда, 2019
Karaganda, 2019

Қарағанды университетінің хабаршысы. «Физика» сериясы.

ISSN 2518-7198 (Print). ISSN 2663-5089 (Online).

Меншік иесі: «Академик Е.А. Бөкетов атындағы Қарағанды мемлекеттік университеті» РММ.

Қазақстан Республикасының Мәдениет және ақпарат министрлігімен тіркелген. 23.10.2012 ж. № 13111–Ж тіркеу куәлігі.

Басуға 28.09.2019 ж. қол қойылды. Пішімі 60×84 1/8. Қағазы офсеттік. Көлемі 10,75 б.т. Таралымы 300 дана. Бағасы келісім бойынша. Тапсырыс № 109.

Е.А. Бөкетов атындағы ҚарМУ баспасының баспаханасында басылып шықты.
100012, Қазақстан, Қарағанды қ., Гоголь к-сі, 38. Тел. 51-38-20. E-mail: izd_kargu@mail.ru

Адрес редакции: 100024, Казахстан, г. Караганда, ул. Университетская, 28

Тел.: (7212) 77-03-69 (внутр. 1026); факс: (7212) 77-03-84.

E-mail: vestnick_kargu@ksu.kz; tchlv_53@mail.ru (*отв. секретарь*)

Сайт: https://physics-vestnik.ksu.kz/

Вестник Карагандинского университета. Серия «Физика».

ISSN 2518-7198 (Print). ISSN 2663-5089 (Online).

Собственник: РГП «Карагандинский государственный университет имени академика Е.А. Букетова».

Зарегистрирован Министерством культуры и информации Республики Казахстан. Регистрационное свидетельство № 13111–Ж от 23.10.2012 г.

Подписано в печать 28.09.2019 г. Формат 60×84 1/8. Бумага офсетная. Объем 10,75 п.л. Тираж 300 экз. Цена договорная. Заказ № 109.

Отпечатано в типографии издательства КарГУ им. Е.А. Букетова.
100012, Казахстан, г. Караганда, ул. Гоголя, 38, тел.: (7212) 51-38-20. E-mail: izd_kargu@mail.ru

Postal address: 28, University Str., 100024, Karaganda, Kazakhstan
Tel.: (7212) 77-03-69 (add. 1026); fax: (7212) 77-03-84.
E-mail: vestnick_kargu@ksu.kz; tchlv_53@mail.ru (*secretary*)
Web-site: https://physics-vestnik.ksu.kz/

Editors

Zh.T. Nurmukhanova, I.N. Murtazina

Computer layout

V.V. Butyaikin

Bulletin of the Karaganda University. «Physics» series.

ISSN 2518-7198 (Print). ISSN 2663-5089 (Online).

Proprietary: RSE «Academician Ye.A. Buketov Karaganda State University».

Registered by the Ministry of Culture and Information of the Republic of Kazakhstan. Registration certificate No. 13111–Zh from 23.10.2012.

Signed in print 28.09.2019. Format 60×84 1/8. Offset paper. Volume 10,75 p.sh. Circulation 300 copies. Price upon request. Order № 109.
Printed in the Ye.A. Buketov Karaganda State University Publishing house.
100012, Kazakhstan, Karaganda, Gogol Str., 38, Tel.: (7212) 51-38-20. E-mail: izd_kargu@mail.ru

МАЗМҰНЫ

КОНДЕНСАЦИЯЛАНҒАН КҮЙДІҢ ФИЗИКАСЫ

ЖЫЛУ ФИЗИКАСЫ ЖӘНЕ ТЕОРИЯЛЫҚ ЖЫЛУ ТЕХНИКАСЫ

ТЕХНИКАЛЫҚ ФИЗИКА

ФИЗИКАНЫ ОҚЫТУ ӘДІСТЕМЕСІ

ЕСКЕ АЛУ

СОДЕРЖАНИЕ

ФИЗИКА КОНДЕНСИРОВАННОГО СОСТОЯНИЯ

ТЕПЛОФИЗИКА И ТЕОРЕТИЧЕСКАЯ ТЕПЛОТЕХНИКА

ТЕХНИЧЕСКАЯ ФИЗИКА

МЕТОДИКА ФИЗИКИ

ПАМЯТИ УЧЕНОГО

CONTENTS

PHYSICS OF THE CONDENSED MATTER

THERMOPHYSICS AND THEORETICAL THERMOENGINEERING

TECHNICAL PHYSICS

METHODOLOGY OF PHYSICS

IN MEMORY OF THE SCIENTIST

DOI 10.31489/2019Ph 3/8-16

UDC 535.3, 544.77, 546.57

D.A. Afanasyev[1,2], N.Kh. Ibrayev[1], E.Zh. Alikhaidarova[1]

[1]Ye.A. Buketov Karaganda State University, Kazakhstan;
[2]Institute of Applied Mathematics, Kazakhstan
(E-mail: a_d_afanasyev@mail.ru)

Charge transfer and properties of localized plasmon resonance in Ag-TiO_2 nanostructures

In the paper the results of the synthesis of Ag – TiO2 nanostructures are presented. Nanostructures consist of a silver core and a TiO_2 semiconductor shell. The size of nanostructures (NSs), determined by the method of dynamic light scattering, was 20 nm and 50 nm in different medias. The effect of the semiconductor shell of TiO_2 on the properties of the localized plasmon resonance of silver nanoparticles is investigated. The quantitative index of localized plasmon resonance in NSs (electron density) was deteriorated, while the qualitative indicator of localized plasmon resonance (attenuation coefficient of plasma oscillations) can improve in the case of a thin TiO_2 shell. After the synthesis of the TiO_2 shell an additional luminescence band of the Ag – TiO_2 NS is observed. The observed luminescence is associated with charge transfer from TiO_2 on Ag. The dependence of the maximum recombination luminescence band on the value of the charge on silver nanoparticles is observed.

Keywords: localized plasmon resonance, silver nanoparticle, nanostructures, charge transfer, titanium dioxide.

Introduction

The number of applied applications of plasmon resonance observed in nanoparticles (NPs) and nanostructures (NSs) of metals increases every year [1]. Compositions of the interrelated components of various substances, one or several of which have linear dimensions in the nanorange are taken to nanostructures. However, the wider practical application of metal NPs and NSs is limited by their chemical activity [2]. This is due to the increase in the specific surface of the particles with a decrease in their size [3]. One of the main ways to protect NPs from destruction is the synthesis of the protective shell. A schematic plot of the core-shell NS and their main geometrical parameters are shown in Figure 1. The shell can be from both organic and inorganic materials. The most commonly used substances are oxide materials, such as TiO_2 and SiO_2 [1]. They are highly stable. Core-shell nanostructures can be used for photocatalysis, in medicine, electronics and photovoltaics [4–6]. An important positive quality of NS core-shell is the ability to change the characteristics of the resulting nanoparticles. In particular, it is possible to change the characteristics of localized plasmon resonance (LPR) of metal nanoparticles.

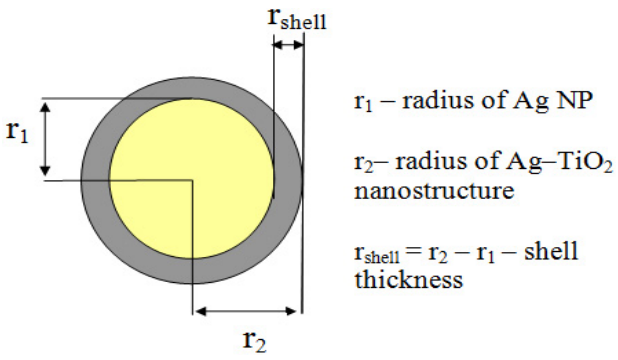

Figure 1. Schematic plot of Ag-TiO_2 nanostructures

Also for core-shell NSs can be observed that weren't observed for metals NPs. One such effect is charge transfer across the semiconductor/metal interface. Charge transfer can occur both from a metal nanoparticle to semiconductor when LPR is excited in it [7] and from TiO_2 when a semiconductor absorbs light and electrons transfer to the conduction band of silver [8]. If a large amount of work is devoted to charge transfer from metal to semiconductor, then the process of charge transfer from TiO_2 to metal is few understood.

The aim of the present work was to study the charge transfer process in nanostructures of the «plasmon core-semiconductor shell» and to study the influence of the semiconductor shell on the LPR of silver nanoparticles.

Method of experiment

The method of synthesis of Ag-TiO_2 NSs, used in the work, is described in detail in [9]. Originally, silver NPs were synthesized. To reduce the concentration of additional reagents in the solution, the production of silver nanoparticles in water was carried out by laser ablation in a liquid. The setup diagram for the production of nanoparticles and the conditions for carrying out the synthesis are given in [10].

After the synthesis of silver NPs, titanium dioxide semiconductor shells (TiO_2) were synthesized. The core-shell nanostructures are synthesized by adding a solution of titanium tetraisopropoxide (TIPT) to an ethanol solution of silver NPs. All of these components are added during vigorous stirring of the solution. During the synthesis, the following ratio between the reagents was mainly chosen: 6 μl of TIPT was added to 1 ml of ethanol. In 10 ml of silver NP solution was added 1 ml of TIPT solution. After this, the reaction mixture is stirred for 12 hours at room temperature in the dark. Also, besides the standard concentration of TIPT, concentrations were used 2 times and 3 times less than the standard (concentrations TIPT of 50 % and 30 % of the standard respectively).

The average sizes of the obtained NPs and NSs were determined by the method of dynamic light scattering on the Zetasizer Nano ZS (Malvern) particle size analyzer. The morphology of the NPs was studied on a Tescan Mira 3 scanning electron microscope (SEM). Absorption spectra were recorded on a Cary 300 spectrophotometer (Agilent), and fluorescence was recorded on an Eclipse spectrofluorometer (Agilent).

Results and its discussion

Originally, silver NPs were synthesized. Their size was $r_1 \sim 20$ nm (Fig. 2, a), r_1 as pointed in Figure 1. Then, an Ag-TiO_2 NSs with different thicknesses of the semiconductor shell was synthesized in an ethanol solution (r_{shell} in Fig. 1). The obtained TiO_2 shell thickness in synthesized NSs was equal to r_{shell}=23 nm (Fig. 2, b) and r_{shell}=63 nm (Fig. 2, c). The use of NSs with a shell of different thickness will allow you to determine the degree of influence of the semiconductor shell on the properties of decision maker silver NPs. The concentration of NSs in solution was $4{,}1 * 10^{-8}$ mol/l. The sizes of NPs and NSs in aqueous solution are shown in Figure 2 and Table.

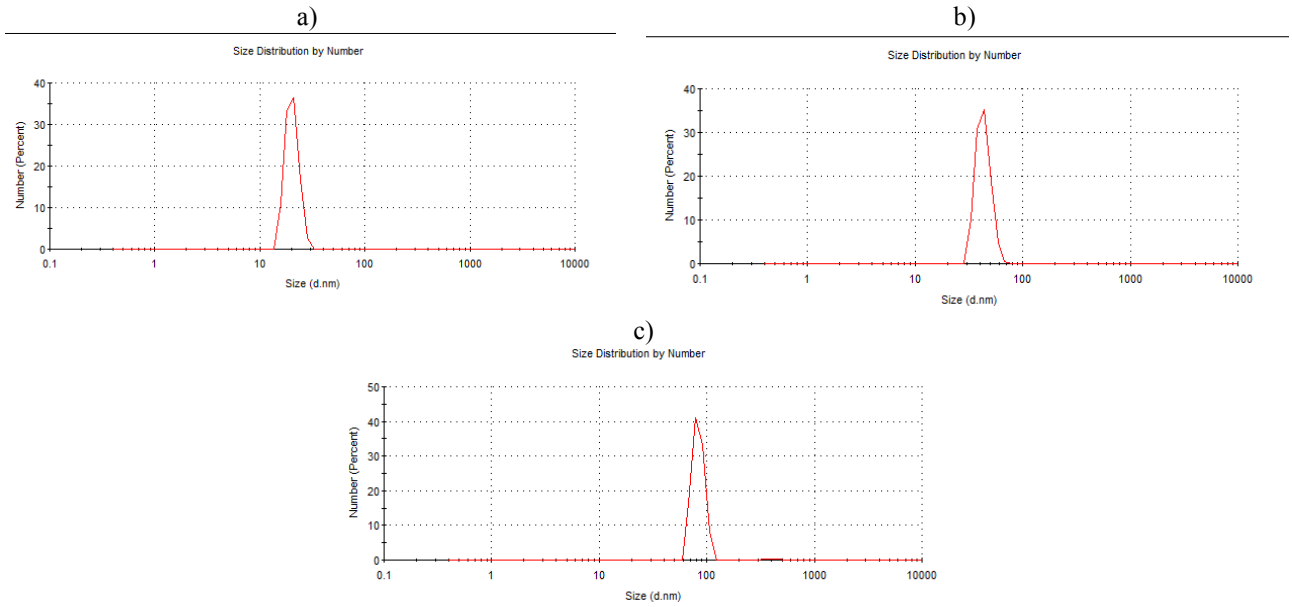

Figure 2. The size distribution of Ag (a) and Ag-TiO_2 nanoparticles with a concentration TIPT of 30 % of the standard (b) and 50 % (c) in water

Table

Size and main characteristics of the absorption spectra of the NSs «plasmon core/semiconductor shell»

Characteristics of solutions NP and NS	Particle size, nm	λ_{abs}^{max}, nm	$\Delta\lambda_{1/2}$, nm	N,·10^{22} cm^{-3}	γ,·10^{15} s^{-1}
Aqueous solution Ag	20	416	45	7,46	3,64
Aqueous solution Ag-TiO_2 (concentration of TIPT 30 %)	43	420	62	7,35	3,04
Aqueous solution Ag-TiO_2 (concentration of TIPT 50 %)	84	424	58	7,20	3,86
Ethanol solution Ag	50	407	65	-	-
Ethanol solution Ag-TiO_2	130	-	-	-	-

Electron-microscopic studies of NPs and NSs showed that they are predominantly spherical in shape and correspond to the results obtained in [9]. The Ag NPs and Ag-TiO_2 NSs in ethanol were also synthesized. The main characteristics of the obtained NPs and NSs are shown in Table.

The absorption spectra of silver NPs and Ag-TiO_2 NSs in ethanol and aqueous solutions are shown in Figure 3. It is seen from the figure that the maximum plasmon resonance of silver NPs is in the range 410–415 nm (curve 1). The absorption spectra of the NSs solutions are observed. As it is known, the absorption band of TiO_2 is located in the ultraviolet part of the spectrum, starting at 360 nm. Therefore, the change in the absorption spectrum is due to the formation of TiO_2 particles in a solution with silver NPs. With an increase of shell thickness in NSs from 23 nm (curve 2) to 63 nm (curve 3) a significant decrease in the intensity of the plasmon resonance band of NPs in aqueous solution occurs (Fig. 3, a). The formation of the TiO_2 semiconductor shell is indicated by a decrease in the intensity of the plasmon resonance of silver NPs and the red–shift of its maximum. A similar result was obtained for the absorption spectra of NPs and NSs in ethanol (Fig. 3, b).

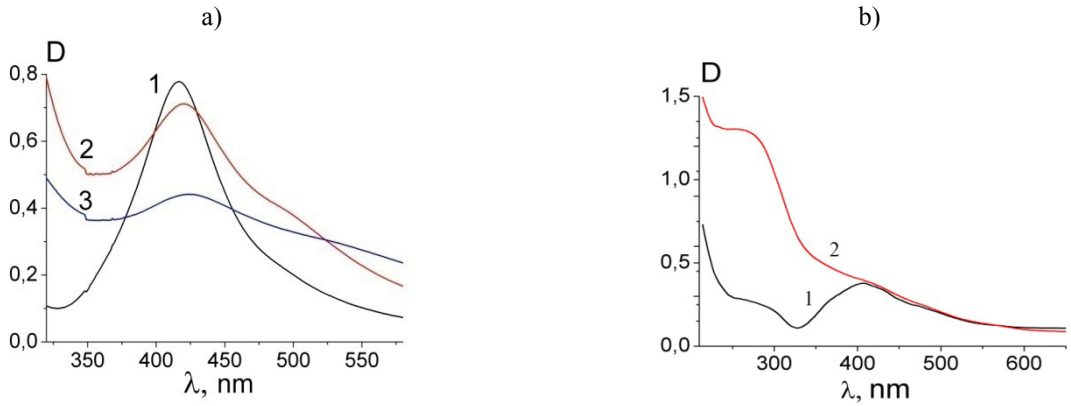

Figure 3. Absorption spectra of the Ag (1) and Ag-TiO_2 (2, 3) with r_{shell}=23 nm (2) and r_{shell}=63 nm (3) in aqueous (a) and ethanol (b) solutions

For spherical NPs, the frequency (ω) corresponding to the maximum of the absorption spectrum is related to the plasmon resonance frequency (ω_p) by the following formula:

$$\omega = \frac{\omega_p}{\sqrt{3}}. \quad (1)$$

The half–width of the absorption spectrum is also one of the main characteristics of plasmon resonance. It carries information on the distribution of LPR by size. The values λ_{abs}^{max} and Δλ1/2 contain information on the relaxation of plasmon oscillations, electron density, and other characteristics of LPR. Thus, knowledge of the maximum of the absorption spectrum and the shape of NPs makes it possible to determine the frequency of plasmon resonance of NPs and a number of important parameters characterizing the properties of LPR.

For metals NPs, the position of the plasmon absorption band can be described by the following formulas [11, 12]:

$$\lambda_{peak}^2 = \lambda_p^2 (\varepsilon^\infty + 2\varepsilon_m) \quad (2)$$

$$\lambda_p^2 = 4\pi^2 c^2 m\varepsilon_0 / Ne^2, \quad (3)$$

where, λ^2_p is the volume plasma wavelength in terms of the electron mass, ε_0 is the vacuum dielectric constant, e is the charge of the electron, and N is the electron density in the particle; ε^∞ is the high–frequency dielectric constant (for silver – about 4,9 ± 0,3, for gold – 6,9 [13]) ε_m is the numerical value equivalent to the square of the refractive index of the solvent. For ethyl alcohol, ε_m was taken equal to 3,7 [9].

In the formation of a shell of titanium dioxide on the surface of NPs, the electron density N will decrease. This, in turn, will lead to an increase in λ^2_p (formula 3). This is expressed in the long–wavelength shift of the maximum of the LPR. A decrease in the electron density N will lead to a decrease in the absorption intensity of the LPR, which is observed in Figure 3. These results show that the formation of the TiO_2 film occurs on the surface of the Ag NPs.

As shown in [11, 12], under the condition that the radius is lower than the wavelength of the incident radiation, a linear dependence of the form is applicable:

$$\frac{1}{k} = \frac{\theta_2}{\theta_1} + \frac{1}{\theta_1}\left(\frac{\lambda^2_{peak}}{\lambda} - \lambda\right)^2. \quad (4)$$

From the graph of the dependence of $\frac{1}{k}$ on $\left(\frac{\lambda^2_{peak}}{\lambda} - \lambda\right)^2$, the parameters of the linear dependence (formula 4) θ_1 and θ_2 were determined. Figure 4 shows the dependence of $\frac{1}{k}$ on $\left(\frac{\lambda^2_{peak}}{\lambda} - \lambda\right)^2$ for solutions

of silver NPs and NSs Ag-TiO_2. Using the parameters θ_1 and θ_2, the attenuation coefficient of plasma oscillations γ was determined by the formula:

$$\gamma = \frac{2\pi c \theta_2^{1/2}}{\lambda_{peak}^{2}} \tag{5}$$

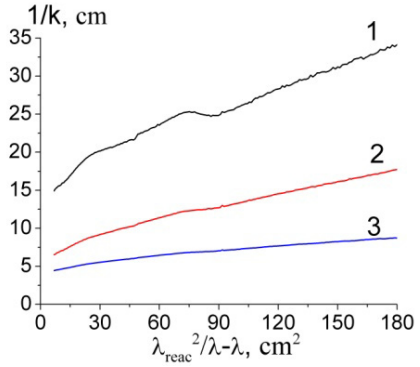

Figure 4. Dependence of 1/k on λ for a colloidal solution of silver NPs (1) and Ag-TiO_2 NSs (2,3) with r_{shell}=23 nm (2) and r_{shell}=63 nm (3)

The electron density N (formula 3) and the damping coefficient of plasma oscillations γ are given in Table. From the data in the table it can be seen that during the formation of the TiO_2 semiconductor shell, the concentration of electrons participating in the formation of LPR in silver decreases. This indicates deterioration in the quality of LPR in plasmon NPs when depositing a semiconductor shell on them. The rate of damping of plasma oscillations varies in different ways depending on the thickness of the TiO_2 shell. At small thicknesses of TiO_2, the rate of damping of plasma oscillations decreases. This can be seen both in the results given in Table and in [9]. With increasing shell thickness, the value of γ for Ag-TiO_2 (r_{shell}=63 nm) increases. This leads to an increase in the damping plasma of plasma oscillations. In the case of NPs obtained in ethanol, the above calculation algorithm could not be used due to the inability to determine the value λ_{abs}^{max} from the absorption spectrum of the obtained NS (Fig. 3, b, curve 2).

Titanium dioxide NPs have their own luminescence [8, 14]. However, because the luminescence occurs with indirect optical transitions of an electron, the intensity of the glow is quite low. Figure 5 (a) shows the luminescence spectra of ethanol solutions of TiO_2 NPs and Ag-TiO_2 NSs. The excitation was carried out by ultraviolet radiation with λ_{excit}=300 nm. The concentration of TiO_2 NPs and Ag-TiO_2 NSs was chosen in such a way that the optical absorption of TiO_2 remained unchanged. The size of silver NPs was 50 nm. It can be seen from Figure 6 (a) that the luminescence spectra of Ag-TiO_2 nanostructures are significantly different from the TiO_2 luminescence spectra. In the luminescence spectrum of Ag-TiO_2, a new band appears with a maximum at 575 nm. This corresponds to the energy of 2,16 eV. This band was registered by the authors of [8] and is explained by them as the luminescence of silver NPs during charge transfer from TiO_2 to silver. The luminescence intensity of Ag-TiO_2 is much lower than the luminescence intensity of TiO_2, which is also explained by the transfer of electrons from the conduction band of titanium dioxide to the conduction band of silver NPs.

In the case of an aqueous solution of Ag and Ag-TiO_2 NPs, the luminescence of Ag NPs was recorded (Fig. 5, b). For silver NPs, luminescence can be observed [15, 16] if their size is sufficiently small. This luminescence is explained by the emission of small silver clusters [15]. An additional luminescence band with a maximum at 540 nm appears in the luminescence spectrum for an aqueous solution of Ag-TiO_2 NSs, as for an ethanol solution of Ag-TiO_2 NSs (Fig. 5 b, curve 2, 3).

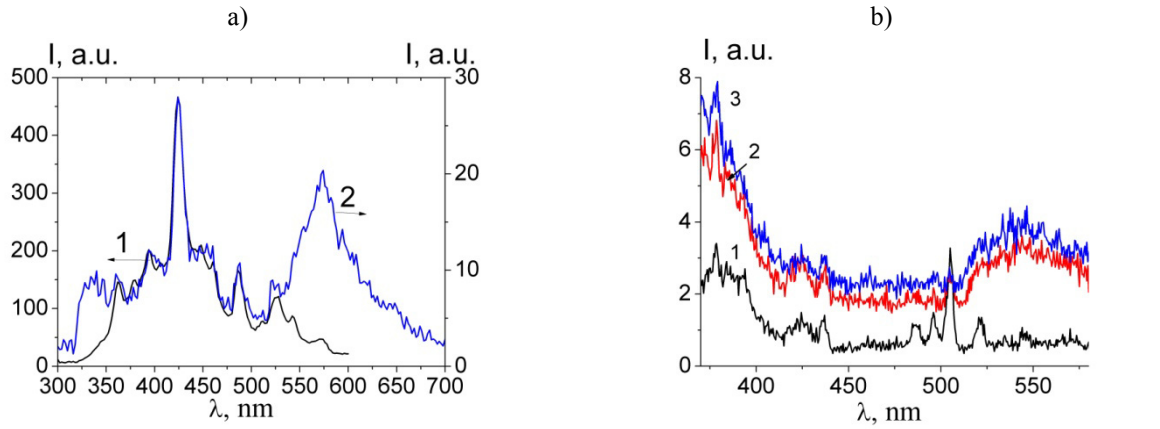

1 –TiO_2 NPs; 2 – Ag-TiO_2

1 –Ag NPs; 2 – Ag-TiO_2 with r_{shell}=23 nm; 3 – Ag-TiO_2 with r_{shell}=63 nm

Figure 5. Luminescence spectra of solutions of Ag, TiO_2 and Ag-TiO_2 in ethanol (a) and in water (b)

A possible mechanism of charge transfer is described in [9] and is shown in Figure 5. In the first stage of the process, the light quantum of TiO_2 is absorbed and the electron is transferred from the conduction band of TiO_2 to the Fermi level (E_F) of the metal NPs (Fig. 6, a). In the second stage, the electron returns from the Fermi level to the valence band of the semiconductor (E_v). In this case, recombination luminescence with the wavelength of the corresponding transition energy $\Delta E = E_F – E_v$ can occur (Fig. 6, b). The value of ΔE for the transition between the Fermi level of the solid body of Ag and Au and the valence band of TiO_2 is 2,9 eV [17]. At the same time, as shown in [18], the Fermi level of gold NPs can vary from the value observed for atomic gold of 9,2 eV to a value corresponding to a bulk material (5,3 eV). However, the value of the Fermi level depends both on the size and on the charge of the NPs [16].

The transfer energy ΔE from the Fermi level is 2,3 eV. At the same time, the increase in the thickness of the TiO_2 shell from 23 nm to 63 nm does not lead to a significant increase in luminescence with a maximum at 540 nm or a shift in the maximum of the luminescence band at 540 nm. This suggests that the luminescence at 540 nm is formed by transferring a charge from a layer of titanium dioxide bordering on silver. In this case, the thickness of the TiO_2 shell does not have a large effect on the value of ΔE. Therefore, the outlying TiO_2 layer from the silver does not participate in the charge transfer process. In the luminescence spectrum of aqueous solutions of Ag-TiO_2 NSs, no luminescence of TiO_2 is observed. Perhaps this is due to the low value of the quantum yield of the luminescence of TiO_2 in comparison with the luminescence of Ag clusters.

As shown in [18], the value of the Fermi level (E_F) depends both on the size and on the charge of the low frequency. The decrease in the value of E_F should occur with a decrease in the size of the NPs. In our case, the value of ΔE increases with decreasing size of the low frequency. Silver NPs with a diameter of 50 nm have ΔE = 2,16 eV, silver NPs with a diameter of 20 nm have ΔE = 2,3 eV. The observed values of ΔE for different Ag-TiO_2 NSs are related to the charge value for silver NPs. At the NPs with d=20 nm, a more negative charge should be presented compared to the NPs with d = 50 nm.

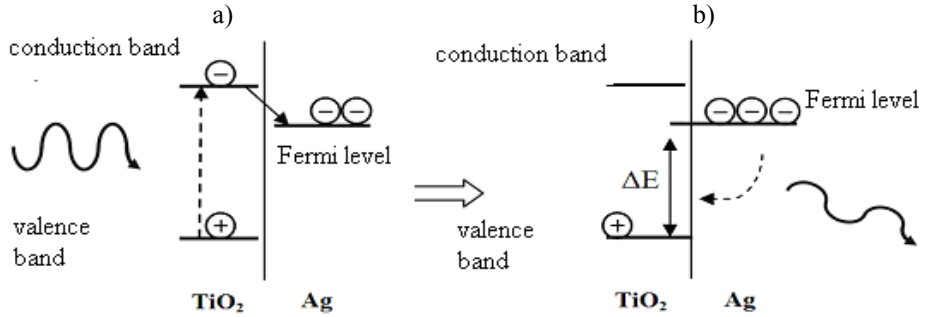

Figure 6. Mechanism of charge transfer and luminescence in the Ag-TiO_2 NSs

Thus, the paper presents the results of the synthesis of Ag-TiO_2 nanostructures. Measurement of the size and shape of the obtained NSs. The size of the NSs was determined using the method of dynamic light scattering. When using the absorption spectra of solutions of NPs and NSs, the electron density and attenuation coefficient of plasma oscillations γ were determined. It is shown that the TiO_2 semiconductor shell reduces the electron density concentration of plasmon NPs. In this case, the damping rate of plasma oscillations varies in different ways and depends on the thickness of the synthesized shell. With a small thickness (r_{shell}=23 nm), the decay rate decreases. With a large shell thickness (r_{shell}=63 nm), the oscillation damping rate γ increases. The obtained results show that the quantitative indicator of NPs in NSs (electron density) is deteriorating, while the qualitative indicator of LPR (attenuation coefficient of plasma oscillations) can improve in the case of a thin TiO_2 shell (r_{shell}=23 nm). Also, after the synthesis of the TiO_2 shell, an additional luminescence band of the Ag-TiO_2 NSs occurs. This luminescence is associated with charge transfer from TiO_2 to Ag. The dependence of the maximum recombination luminescence band on the value of the charge on silver NPs is observed.

This work was supported as part of scientific-research grants of the Ministry of education and science of the Republic of Kazakhstan (AP05133724) and (BR05236691).

References

1 Ghosh R. Core/Shell Nanoparticles: Classes, Properties, Synthesis Mechanisms, Characterization, and Applications / Ch.Paria, S.Paria // Chemical Reviews, — 2012. — 112. — P. 2373–2433.

2 Рыжонков Д.И. Наноматериалы / Д.И. Рыжонков, В.В. Лёвина, Э.Л. Дзидзигури. — 2–е изд. — М.: БИНОМ; Лаборатория знаний, 2010. — 365 с.

3 Зимон А.Д. Коллоидная химия НЧ / А.Д. Зимон, А.Н. Павлов. — М.: Научный мир, 2012. — 224 с.

4 Yin X. Ag/TiO2 nanocomposites with improved photocatalytic properties prepared by a low temperature process in polyethylene glycol / Que W., Y. Liao // Colloids and surf. A: Physicochem. eng. Aspects, — 2012. — 410. — P. 153–158.

5 Qi J. Highly efficient plasmon–enhanced dye–sensitized solar cells through metal@oxide core–shell Nanostructure / J. Qi, X. Dang, P.T. Hammond, A.M. Belcher // ACS Nano. — 2011. — 5, 9. — P. 7108–7116.

6 Zhang R. Influence of SiO2 shell thickness on power conversion efficiency in plasmonic polymer solar cells with Au nanorod@SiO2 core–shell structures / R. Zhang, Y. Zhou, L. Peng // Scientific Reports. — 2016. — 6, 25036. — P. 1–9.

7 Clavero C. Plasmon-induced hot-electron generation at nanoparticle/metal-oxide interfaces for photovoltaic and photocatalytic devices / C. Clavero // Nature Photonics. — 2014. — 8. — P. 95–103.

8 Calandra P. Structural and optical properties of novel surfactant coated TiO2–Ag based nanoparticles / P. Calandra, A. Ruggirello, A. Pistone, V.T.J. Liveri // Clust. Sci. — 2010. — 21. — P. 767–778.

9 Afanasyev D.A. Effect of the titanium dioxide shell on the plasmon properties of silver nanoparticles / D.A. Afanasyev, N.Kh. Ibrayev, T.M. Serikov, A.K. Zeinidenov // Russian Journal of Physical Chemistry. — 2016. — 90. — 4. — P. 833–837.

10 Afanasyev D.A. Synthesis of aluminum-aluminium oxide nanostructures by laser ablation / D.A. Afanasyev, N.Kh. Ibrayev, M.E. Kasymov // Bulletin of the Karaganda University, physics series. — 2018. — 3, 91. — P. 8–15.

11 Toporko, A.V. Change of the properties of copper small particles during sulfur-containing ions adsorption from solutions / A.V. Toporko, V.V. Tsvetkov, V.D. Yagodovskii, A. Issa // Zhurnal fizicheskoi khimii. — 1995. — 5, 69. — P. 867–870.

12 Подлегаева Н.Л. Исследование свойств НЧ серебра, полученных восстановлением из растворов и термическим напылением в вакууме / Н.Л. Подлегаева, Д.М. Руссаков, С.А. Созинов, Т.В. Морозова, И.Л. Швайко, Н.С. Звиденцова, Л.В.Колесников // Вестн. Кемер гос. ун-та. Сер. Химия. — 2009. — № 2. — С. 95–99.

13 Shklyarevskii I.N. Separation of the contribution of free and bound electrons into real and imaginary parts of the dielectric constant of gold / I.N. Shklyarevskii, P.L. Pakhmov // Optika i Spektroskopia. — 1973. — 34, 1. — P. 163–166.

14 Serpone N. Size Effects on the Photophysical Properties of Colloidal Anatase $Ti0_2$ Particles: Size Quantization or Direct Transitions in This Indirect Semiconductor / N. Serpone, D. Lawless, R.J. Khairutdinov // Phys. Chem. — 1995. — 99, 16646–16654.

15 Bulavchenko, A.I. Photon correlation spectroscopic and spectrophotometric studies of the formation of cadmium sulfide nanoparticles in ammonia-thiourea solutions / A.I. Bulavchenko, A.N. Kolodin, T.Yu. Podlipskaya, M.G. Demidova, E.A. Maksimovskii, N.F. Beizel', S.V. Larionov, A.V. Okotrub // Russian Journal of Physical Chemistry A. — 2015. — 90, 5, 1034–1038.

16 Ping H. Photoluminescence phenomenon during the formation of silver nanoparticles / H. Ping, Sh. Xing–Hai, G. Hong–Cheng // Acta Phys. Chim. Sin. — 2004. — 20, 10, 1200–1203.

17 Kasap S.O. Principles of Electronic Materials and Devices, Third Edition McGraw–Hill, 2002. 768 p.

18 Scanlon M.D. Charging and discharging at the nanoscale: Fermi level equilibration of metallic nanoparticles / M.D. Scanlon, P. Peljo, M.A. Méndez, E. Smirnov, H.H. Girault // Chem. Sci, 2015. 6, 5, 2705–2720.

Д.А. Афанасьев, Н.Х. Ибраев, Э.Ж. Алихайдарова

$Ag–TiO_2$ наноқұрылымдарында зарядты тасымалдау және локалды плазмондық резонанс қасиеттері

Мақалада $Ag–TiO_2$ наноқұрылымдары синтезінің нәтижелері келтірілген. Наноқұрылымдар күміс ядросынан және TiO_2 жартылайөткізгіш қабыршағынан тұрады. Қолданылған еріткіштің тәуелділігіне байланысты жарықтың динамикалық шашырау әдісімен анықталған наноқұрылымдардың (НҚ) өлшемі 20 нм және 50 нм құрады. TiO_2 жартылайөткізгіш қабыршағының күміс нанобөлшектерінің локалды плазмондық резонанс қасиеттеріне әсері зерттелді. НҚ-да локалды плазмондық резонанстың сандық көрсеткіші (электрондық тығыздығы) нашарлайды, алайда локалды плазмондық резонанстың сапалық көрсеткіші (плазмалық тербелістердің өшу коэффициенті) TiO_2 қабықшасы жұқа болғанда жақсаратыны дәлелденді. Сонымен қатар TiO_2 қабықшасының синтезінен кейін $Ag\text{-}TiO_2$ НҚ-да люминесценцияның қосымша жолағы байқалды. Бақыланатын жарқырау TiO_2-ден Ag-ға зарядтың тасымалдалуына байланысты болып табылады. Күміс НБ-де зарядтың мәніне тәуелді рекомбинациялық люминесценция жолағының максимумы байқалды.

Кілт сөздер: локалды плазмондық резонанс, күміс нанобөлшектері, наноқұрылымдар, заряд тасымалдау, титан диоксиді.

Д.А. Афанасьев, Н.Х. Ибраев, Э.Ж. Алихайдарова

Перенос заряда и свойства локализованного плазмонного резонанса в наноструктурах $Ag–TiO_2$

В статье приведены результаты синтеза наноструктур $Ag–TiO_2$. Наноструктуры состоят из серебряного ядра и полупроводниковой оболочки TiO_2. Размер наноструктур (НС), определенный методом динамического рассеяния света, составил 20 нм и 50 нм в зависимости от использованного растворителя. Исследовано влияние полупроводниковой оболочки TiO_2 на свойства локализованного плазмонного резонанса наночастиц серебра. Установлено, что количественный показатель локализованного плазмонного резонанса в НС (электронная плотность) ухудшается, в то время как качественный показатель локализованного плазмонного резонанса (коэффициент затухания плазменных колебаний) может улучшиться в случае тонкой оболочки TiO_2. Также после синтеза оболочки TiO_2 наблюдается дополнительная полоса люминесценции НС $Ag\text{-}TiO_2$. Наблюдаемое свечение связано с переносом заряда с TiO_2 на Ag. Наблюдается зависимость максимума полосы рекомбинационной люминесценции от значения заряда на НЧ серебра.

Ключевые слова: локализованный плазмонный резонанс, наночастица серебра, наноструктуры, перенос заряда, диоксид титана.

References

1 Ghosh R., Paria Ch., & Paria S. (2012). Core/Shell Nanoparticles: Classes, Properties, Synthesis Mechanisms, Characterization, and Applications. *Chemical Reviews*, 112, 2373–2433.

2 Ryzhonkov, D.I., Levina, V.V., & Dzidziguri, E.L. (2010) *Nanomaterialy [Nanomaterials]*. Moscow: BINOM; Laboratoriia znanii [in Russian].

3 Zimon, A.D., & Pavlov, A.N. (2012) *Kolloidnaia himiia nanochastits [Colloid chemistry of nanoparticles]*. Moscow: Nauchnyi mir [in Russian].

4 Yin X., Que W., & Liao Y. (2012). Ag/TiO_2 nanocomposites with improved photocatalytic properties prepared by a low temperature process in polyethylene glycol. Colloids *and surf. A: Physicochem. eng. Aspects*, 410, 153–158.

5 Qi J., Dang X., Hammond P.T., & Belcher A.M. (2011). Highly efficient plasmon–enhanced dye–sensitized solar cells through metal@oxide core–shell Nanostructure. *ACS Nano*, 5, 9, 7108–7116.

6 Zhang R., Zhou Y., & Peng L. (2016). Influence of SiO2 shell thickness on power conversion efficiency in plasmonic polymer solar cells with Au nanorod@SiO_2 core–shell structures. *Scientific Reports*, 6, 25036, 1–9

7 Clavero C. (2014). Plasmon-induced hot-electron generation at nanoparticle/metal-oxide interfaces for photovoltaic and photocatalytic devices. *Nature Photonics*, 8, 95–103.

8 Calandra P., Ruggirello A., Pistone A., & Liveri V.T. (2010). Structural and optical properties of novel surfactant coated TiO2–Ag based nanoparticles. *J. Clust. Sci*, 21, 767–778.

9 Afanasyev, D.A., Ibrayev, N.Kh., Serikov, T.M., & Zeinidenov, A.K. (2016) Effect of the titanium dioxide shell on the plasmon properties of silver nanoparticles. *Russian Journal of Physical Chemistry* 90, 4, 833–837.

10 Afanasyev, D.A., Ibrayev, N.Kh., & Kasymov, M.E. (2018). Synthesis of aluminum-aluminium oxide nanostructures by laser ablation. *Bulletin of the Karaganda University, Physics series,* 3, 91, 8–15.

11 Toporko, A.V., Tsvetkov, V.V., Yagodovskii, V.D., & Issa, A. (1995). Change of the properties of copper small particles during sulfur-containing ions adsorption from solutions. *Zhurnal fizicheskoi khimii,* 5, 69, 867–870.

12 Podlegaeva, N.L., Russakov, D.M., Sozinov, S.A., Morozova, T.V., Shvaiko, I.L. Zvidencova, N.S., & Kolesnikov, L.V. (2009). Issledovanie svoistv nanochastic serebra, poluchennykh vosstanovleniem iz rastvorov i termicheskim napyleniem v vakuume [Investigation of the properties of silver nanoparticles obtained by reduction from solutions and thermal spraying in vacuum]. *Vestnik Kemerovskoho hosudarstvennoho universiteta. Seriia Himiia – Bulletin of Kemerovo State Universit. Chemistry, Vol. 2,* 95–99 [in Russian].

13 Shklyarevskii, I.N., & Pakhmov P.L. (1973). Separation of the contribution of free and bound electrons into real and imaginary parts of the dielectric constant of gold. *Optika i Spektroskopiya,* 34, 1, P. 163–166.

14 Serpone N., Lawless D., & Khairutdinov R. (1995). Size Effects on the Photophysical Properties of Colloidal Anatase $Ti0_2$ Particles: Size Quantization or Direct Transitions in This Indirect Semiconductor. *J. Phys. Chem,* 99, 16646–16654.

15 Bulavchenko, A.I., Kolodin, A. N., Podlipskaya, T.Yu., Demidova, M.G., Maksimovskii, E.A., Beizel', N.F., Larionov, S.V., & Okotrub, A.V. (2015). Photon correlation spectroscopic and spectrophotometric studies of the formation of cadmium sulfide nanoparticles in ammonia-thiourea solutions. *Russian Journal of Physical Chemistry A*, 90, 5, 1034–1038.

16 Ping H., Xing–Hai Sh., & Hong–Cheng G. (2004). Photoluminescence phenomenon during the formation of silver nanoparticles. *Acta Phys. — Chim. Sin,* 20, 10, 1200–1203.

17 Kasap S.O. (2002). Principles of Electronic Materials and Devices, Third Edition. McGraw–Hill, 768 p.

18 Scanlon M.D., Peljo P., Méndez M.A., Smirnov E., & Girault H.H. (2015). Charging and discharging at the nanoscale: Fermi level equilibration of metallic nanoparticles. *Chem. Sci,* 6, 5, 2705–2720.

DOI 10.31489/2019Ph3/17-21

UDC 537.8: 537.5

E. Çopuroğlu[1], T. Mehmetoğlu[2]

[1]*Department of Physics, Faculty of Arts and Sciences, Gaziosmanpaşa University, Tokat, Turkey;*
[2]*Amasya University, Taşova Vocational School, Turkey*
(E-mail: ebrucopuroglu@gmail.com)

Analytical evaluation of the Uehling potential using binomial expansion theorems

In this paper, we have introduced a new method to study of Uehling potential using binomial expansion theorems. Note that, the Uehling potential is a powerful tool to determine the effect of vacuum polarization in atomic and muon-atomic systems. The correcting of vacuum-polarization for an electron in a nuclear Coulomb field can be defined more precisely by the use of Uehling potential. From this point of view, the determination of explicit and closed-form analytical expressions for Uehling potential is very important. Therefore, presented method is illustrated by analytically calculation of the Uehling potential with the simple binomial coefficients and exponential integral functions. As can be seen from table and figure, the newly derived analytical expression well avoids the computational difficulties. An evaluation analysis of the Uehling potential is reported for arbitrary values of parameters. Because of its simple form the suggested method can be generally applied to the quantum thermodynamical problems.

Keywords: Uehling potential, vacuum polarization, quantum electrodynamics, Bickley-Naylor functions, Exponential integral function.

Introduction

The interaction potential between two electric charges which contains an additional term responsible for the electric polarization of the vacuum was introduced by Uehling [1], and has seen a series of successful applications in quantum electrodynamics (QED) [2–10]. This formalism can be applied to the effect of vacuum polarization itself and for various electrons and atoms [11]. Note that the Uehling potential is the integral function, therefore, before applying to the physical problems it should be analytically evaluated. Unfortunately, there are limited numbers of studies in literature for the analytical evaluation methods of Uehling potential. In this sense, recently, Frolov [2, 11] has suggested an efficient and useful analytical approximation by using Bickley-Naylor functions and modified Bessel function of zero order. The Bickley-Naylor functions are one of the conceptual tools in the nuclear computational science [11–15]. Therefore, obtaining the efficient formulae for the any order Bickley-Naylor functions has significant role in physical applications of Uehling potential. For the analytical evaluation of the first and second order Bickley-Naylor functions author has proposed new formulae [12].

In the present article, by using binomial expansion theorems, we propose a new formula in terms of exponential integral functions occurring one infinite sum which enables fast and accurate evaluation of the Uehling potential. The new analytical approach for evaluating the Uehling potential is conceptually simpler than existing methods in the literature.

Definition and basic formulas

The interaction potential of two-point particles with including the vacuum polarization is described by [1, 2]:

$$\phi(r)=\frac{Qe}{r}\left[1+\frac{2\alpha}{3\pi}\int_1^\infty e^{-2\alpha^{-1}rt}\left(1+\frac{1}{2t^2}\right)\frac{\sqrt{t^2-1}}{t^2}dt\right]. \tag{1}$$

The Eq. (1) in the atomic units systems can be rewritten as:

$$\phi(r)=\frac{Q}{r}+\frac{2\alpha Q}{3\pi}\int_1^\infty e^{-2\alpha^{-1}rt}\left(1+\frac{1}{2t^2}\right)\frac{\sqrt{t^2-1}}{t^2}dt=\frac{Q}{r}+U(r), \tag{2}$$

where Q is electric charge, α is fine structure constant ($\alpha^{-1}\approx 137.03599911$) and $U(r)$ is Uehling potential determined as:

$$U(r)=\frac{2\alpha Q}{3\pi}I(r). \tag{3}$$

Here $I(r)$ is the Uehling function defined as:

$$I(r)=\int_1^{\infty}e^{-2\alpha^{-1}rt}\left(1+\frac{1}{2t^2}\right)\frac{\sqrt{t^2-1}}{t^2}dt. \tag{4}$$

In study [2] useful formulae have obtained for Uehling potential in following form:

$$U(a)=\frac{4Q}{3\pi a}\left[\left(1+\frac{a^2}{12}\right)Ki_0(a)-\frac{a}{12}Ki_1(a)-\left(\frac{a^2}{12}+\frac{5}{6}\right)Ki_2(a)\right], \tag{5}$$

$$U\left(a\right)=\frac{4Q}{3\pi a}\left[Ki_0(a)-\frac{1}{2}Ki_2(a)-\frac{1}{2}Ki_4(a)\right], \tag{6}$$

where $a=2\alpha^{-1}r$. Here $Ki_n(x)$ are the Bickley-Naylor functions determined as:

$$Ki_n(x)=\int_0^{\infty}\frac{\exp(-x\cosh t)}{\cosh^n t}dt. \tag{7}$$

Notice that in special case of $n=0$ Bickley-Naylor functions reduce to the Bessel functions $Ki_0\left(x\right)=K_0(x)$ and defined as:

$$Ki_0\left(x\right)=K_0(x)=\sum_{k=0}^{\infty}\left(\psi\left(k+1\right)+\ln 2-\ln x\right)\frac{x^k}{2^{2k}\left(k!\right)^2}, \tag{8}$$

where $\psi\left(k+1\right)$ is the Euler Function defined following as:

$$\psi\left(k+1\right)=-\gamma-\sum_{i=1}^{\infty}\frac{\left(-1\right)^i F_i\left(k\right)}{i}. \tag{9}$$

Here γ is the well known Euler's constant. For $n\geq 2$, Bickley-Naylor functions can be evaluated by the following recursive formula [13]:

$$nKi_{n+1}(x)=\left(n-1\right)Ki_{n-1}(x)-xKi_n(x)+xKi_{n-2}(x). \tag{10}$$

Note that for the calculation of Uehling potential by using Eq. (5), the $Ki_1(a)$ and $Ki_2(a)$ Bickley-Naylor functions must be determined. It is clear from the literature that there is not enough and efficient studies for the evaluation of these functions. Beside these insufficiencies recently the author [12] has given accurate formulae for the one and second order Bickley-Naylor functions in his study as following:

$$\begin{aligned}Ki_1\left(x\right)=&\frac{\pi}{2}+x\left[\gamma+\ln(x/2)\right]\sum_{k=0}^{\infty}\frac{\left(x/2\right)^{2k}}{\left(k!\right)^2\left(2k+1\right)}-x\sum_{k=0}^{\infty}\frac{\left(x/2\right)^{2k}}{\left(k!\right)^2\left(2k+1\right)^2}\\&-x\sum_{k=0}^{\infty}\frac{\left(x/2\right)^{2k}\Phi\left(k+1\right)}{\left(k!\right)^2\left(2k+1\right)},\end{aligned} \tag{11}$$

$$\begin{aligned}Ki_2\left(x\right)=&1-\frac{\pi}{2}x+\frac{x^2}{2}\left[\gamma+\ln(x/2)\right]\sum_{k=0}^{\infty}\frac{\left(x/2\right)^{2k}}{\left(k!\right)^2\left(k+1\right)!\left(2k+1\right)}+\frac{x^2}{4}\sum_{k=0}^{\infty}\frac{\left(4k+3\right)\left(x/2\right)^{2k}}{\left[\left(k+1\right)!\left(2k+1\right)\right]^2}\\&+\frac{x^2}{2}\sum_{k=0}^{\infty}\frac{\left(x/2\right)^{2k}\Phi\left(k+1\right)}{\left(k!\right)^2\left(k+1\right)!\left(2k+1\right)}.\end{aligned} \tag{12}$$

Here $\Phi\left(k+1\right)$ functions are determined as:

$$\Phi\left(k+1\right)=1+\frac{1}{2}+\frac{1}{3}+....+\frac{1}{k}. \tag{13}$$

The calculation tests show that it is necessary to give various accurate and efficient analytical formulae for the evaluation of Uehling potential. The objective of this paper is to derive basic analytical expression for the Uehling potential. For this purpose we use binomial expansion theorems for the evaluation of Uehling potential. The binomial expansion theorem can be demonstrated by [13, 15]:

$$(x \pm y)^n = \sum_{m=0}^{N} (\pm 1)^m \, f_m(n) \, x^{n-m} \, y^m, \tag{14}$$

here $f_m(n)$ are the binomial functions given as:

$$f_m(n) = \begin{cases} \dfrac{1}{m!} \displaystyle\prod_{i=0}^{m-1} (n-i) & \text{for integer } n \\ \dfrac{(-1)^m \, \Gamma(m-n)}{m! \Gamma(-n)} & \text{for noninteger } n \end{cases}. \tag{15}$$

With the help of binomial expansion theorem we can rewrite Eq. (4) given for the Uehling potential following as:

$$I(a) = \lim_{N \to \infty} \sum_{i=0}^{N} F_i(1/2)(-1)^i \left[E_{1+2i}(a) + \frac{1}{2} E_{3+2i}(a) \right]. \tag{16}$$

Here $E_n(t)$ is the exponential integral function determined by:

$$E_n(t) = \int_1^{\infty} \frac{e^{-ty}}{y^n} dy, \tag{17}$$

$$E_n(t) = t^{n-1} \Gamma(1-n, t). \tag{18}$$

In Eqs. (15) and (18), the $\Gamma(\alpha)$ and $\Gamma(\alpha, x)$ are well known complete and incomplete Gamma functions, respectively (see Ref. [13, 15] for exact definition).

Numerical Results and Discussion

In this paper, a new formula for the analytical calculation of the Uehling potential is presented. The proposed algorithm is based on the binomial expansion theorem and exponential integral functions. The analytical evaluation allows us to calculate Uehling potential by using simple mathematical expressions. The obtained formulae were performed by using Turbo Pascal programming language. The computational results of Uehling potential for various values of parameters have been demonstrated in Table and Figure.

T a b l e

Comparison of obtained results by considering Eq. (16) and Eq. (5) for calculating Uehling function (N=450)

r	Results of Eq. (16)	Results of Eq. (5)
1	2	3
0.01	8.115051	8.115036
00.2	7.422076	7.422061
0.2	5.122582	5.122568
0.5	4.211433	4.211418
1	3.526823	3.526809
1.5	3.129856	3.1298421
2	2.850633	2.8506191
5	1.984293	1.984275
8	1.562901	1.562887
10.5	1.330496	1.330483
15.7	1.007708	1.007696
20	0.828739	0.828728

1	2	3
25.2	0.670948	0.670938
30	0.561539	0.561530
35.9	0.458456	0.458447
40.8	0.3913553	0.391347
48.7	0.3077415	0.307734
55	0.256683	0.256677
60.9	0.218009	0.2180029
100	0.0820734	0.0820701
200	0.0098917	0.0098914

In Table, our results have been compared with literature [2] and it is shown that obtained results are satisfactory. In Fig. 1, we plot our analytical and literature results for Uehling potential as a function of interparticle distance r. The solid and dashed curves represent our and literature data, respectively.

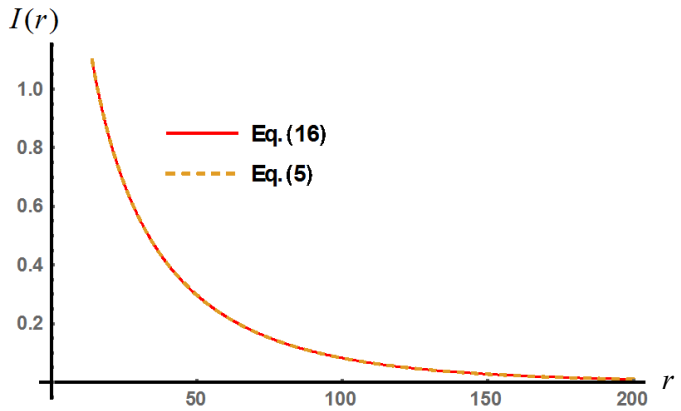

Figure. Using Eqs. (16) and (5), the values of Uehling function *I(r)* with respect to interparticle distance *r*

Table and Figure show that our analytical algorithm is reliable and fast in a wide range interparticle distance r . For instance, in the case of $r = 0.01$, the CPU times taken from the use of Eqs. (16) and (5) are 0.062 ms and 0.343 ms, respectively. As a result, we made the calculation time about 20 times as fast with compared to the literature. Thus, we have proposed an alternative method for the evaluation of Uehling potential which has significant role in atomic and muon-atomic systems, especially the interaction potential between two electric charges.

References

1 Uehling, E.A. (1935). Polarization effects in the positron theory. *Physical Review*, *48*(1), 55–62.

2 Frolov, A.M., & Wardlaw, D.M. (2012). Analytical formula for the Uehling potential. *The European Physical Journal B*, *85*(10), 348–350.

3 Dirac, P.A.M. (1930). The principles of quantum mechanics. *The Clarendon Press*.

4 Heisenberg, W. (1936). Euler H.*Z. Physik*, *38*, 314–319.

5 Pauli, W., & Villars, F. (1949). On the invariant regularization in relativistic quantum theory. *Reviews of Modern Physics*, *21*(3), 434–444.

6 Akhiezer, A.I., & Beresteskii, V.B. (1981). Quantum Electrodynamics, Nauka Science, Moscow.

7 Petelenz, P., & Smith Jr, V.H. (1987). Exact matrix elements of the Uehling potential in a basis of explicitly correlated two-particle functions. *Physical Review A*, *35*(10), 4055–4059.

8 Frolov, A.M., & Efros, V.D. (1984). Accurate solution method in the three-body problem and binding energies of mesic molecules. *JETP Lett*, *39*(9), 544–547.

9 Frolov, A.M., & Efros, V.D. (1985). An accurate method in the Coulomb three-body problem and muonic-molecule excited states, *J. Phys. B*, *18*, L265-L270.

10 Gocheva, A.D., Gusev, V.V., Melezhik, V.S., Ponomarev, L.I., Puzynin, I.V., Puzynina, T.P, & Vinitsky, S.I. (1985). High accuracy energy-level calculations of the rotational-vibrational weakly bound states of ddμ and dtμ mesic molecules. *Physics Letters B*, *153*(6), 349–352.

11 Frolov, A.M. (2012). On the properties of the Uehling potential. *arXiv preprint arXiv:1210.6737*.

12 Altaç, Z. (1996). Integrals involving Bickley and Bessel functions in radiative transfer, and generalized Exponential Integral functions. *ASME J. Heat Transfer*. 118 789–792.

13 Abramowitz, M., & Stegun, I.A. (1972). Confluent hypergeometric functions. *Ch*, *13*, 503–515.

14 Milgram, M.S. (1978). Analytic method for the numerical solution of the integral transport equation for a homogeneous cylinder. *Nuclear Science and Engineering*, *68*(3), 249–269.

15 Çopuroğlu, E., & Mehmetolu, T. (2015). Full analytical evaluation of the Einstein relation for disordered semiconductors. *IEEE Transactions on Electron Devices*, *62*(5), 1580–1583.

Э. Чопуроглу, Т. Мехметоглу

Биномиалдық жіктеу теоремасын қолдану арқылы Юлинг потенциалын аналитикалық жуықтап анықтау

Мақалада Юлинг потенциалын талдаудың биномиалдық жіктеу теоремасына негізделген жаңа әдісі ұсынылған. Атомдық және мюон-атомдық жүйелерге вакуумның поляризациясын анықтауда Юлинг потенциалының алатын орны ерекше екендігі белгілі. Юлинг потенциалының көмегімен ядроның кулон өрісіндегі электрондарға вакуумның поляризациясының әсерін дәл анықтауға болады. Осы тұрғыдан Юлинг потенциалының аналитикалық өрнегін білудің маңызы ерекше. Қарапайым биномиалдық және экспоненциал интегралық функцияларды пайдалана отырып, Юлинг потенциалының аналитикалық өрнегін есептеу мүмкіндігі көрсетілген. Келтірілген кестелерден, суреттерден жұмыста алынған аналитикалық өрнек есептеу, зерттеу барысын бірталай жеңілдететіндігін байқауға болады. Юлинг потенциалын есептеу параметрлердің кез келген мәндері үшін іске асырылған. Ұсынылып отырған әдісті кванттық-термодинамикалық есептерді-мәселелерді талдау үшін де пайдалануға болады.

Кілт сөздер: Юлинг потенциалы, вакуум поляризациясы, кванттық электродинамика, Бикли-Нейлор функциясы, экспоненциалды интегралдық функция.

Э. Чопуроглу, Т. Мехметоглу

Аналитическая оценка потенциала Юлинга с использованием теорем биномиального разложения

В статье введен новый метод изучения потенциала Юлинга с использованием теорем о биномиальном разложении. Отмечено, что потенциал Юлинга является мощным инструментом для определения влияния поляризации вакуума в атомных и мюон-атомных системах. Коррекция поляризации вакуума для электрона в ядерном кулоновском поле может быть более точно определена с помощью потенциала Юлинга. С этой точки зрения определение явных и замкнутых аналитических выражений для потенциала Юлинга очень важно. Представленный метод иллюстрируется аналитическим расчетом потенциала Юлинга с простыми биномиальными коэффициентами и экспоненциальными интегральными функциями. Как видно из таблицы и рисунка, полученное в статье аналитическое выражение позволяет избежать вычислительных трудностей. Оценочный анализ потенциала Юлинга приведен для произвольных значений параметров. Из-за своей простой формы предложенный метод может быть в целом применим к квантово-термодинамическим задачам.

Ключевые слова: потенциал Юлинга, поляризация вакуума, квантовая электродинамика, функции Бикли-Нейлора, экспоненциальная интегральная функция.

DOI 10.31489/2019Ph 3/22-26

UDC 530.182

B.B. Kutum, G.N. Shaikhova

L.N. Gumilyov Eurasian National University, Nur-Sultan, Kazakhstan
(E-mail: kuttykadam@mail.ru)

Q-soliton solution for two-dimensional q-Toda lattice

The Toda lattice is a non-linear evolution equation describing an infinite system of masses on a line that interacts through an exponential force. The paper analyzes the construction of soliton solution for the q-Toda lattice in the two-dimensional case. For this purpose, the equation of motion is taken and the transformation of the dependent variable is used to convert the nonlinear equation into a bilinear form, which is written as the Hirota polynomial. As one of the most effective methods for constructing multisoliton solutions of integrable nonlinear evolution equations, Hirota method is applicable to a wide class of equations, including nonlinear differential, nonlinear differential-difference equations. Using the Hirota method, the bilinear form was obtained for the two-dimensional q-Toda lattice on the basis of which the q-soliton solution was found. The dynamics of the q-soliton solution for two-dimensional q-Toda lattice is presented. Note that the soliton is conserved due to the equilibrium between the action of the nonlinear environment with dispersion. In addition, the soliton behaves like a particle: does not collapse when interacting with each other or other disturbances, while maintaining the structure and continues to move. This quality has the ability to use when transferring data or information over long distances with virtually no interference. In addition, the study of the Toda lattice and the application to it of different methods in different dimensions allows one to proceed to the understanding of such complex terms as matrix models that can be used to describe different physical systems.

Keywords: dispersion, soliton, Toda lattice, bilinear form, Hirota method.

Introduction

Waves described by different nonlinear differential equations, which consist of special pulses, have the property of preserving their original shape like stable particles. They are called solitary waves, single wave particles or solitons. Nonlinear lattices or lattices also contain solitons. When the energy is not very large, nonlinear lattices behave periodically, so stable pulses propagate in such nonlinear continuous systems. The fact of the existence of such lattices shows that there must be some non-linear lattice that allows strict periodic waves, and certain impulses will be stable. One such example is the Toda lattice equation. The Toda lattice is a non-linear evolution equation describing an infinite system of masses on a line that interacts through an exponential force. The Toda lattice is considered as a simple model of the nonlinear one-dimensional crystal in solid state physics. It is defined by a lattice of particles with the interaction of the nearest neighbor, described by the equations of motion [1].

To find the exact solutions for nonlinear differential equations, a huge number of methods are used, such as the Backlund transform [2], the Hirota method [3], the inverse scattering transform method [4], and others. One of the most effective methods for constructing soliton solutions of integrable nonlinear evolution equations is the direct Hirota method, which can be found in [3]. This method is applicable to a wide class of equations, including nonlinear differential, nonlinear differential-difference equations [5-7]. The initial step in this method is to use the transformation of the dependent variable to convert nonlinear partial differential equation into a quadratic form, the so-called bilinear form. The main idea of the method is to write the bilinear form as a Hirota polynomial - D. This compact form is called Hirota's bilinear form. It should be noted that nonlinear partial differential or differential-difference equations can have not only Hirota bilinear forms but also trilinear or multilinear forms [8]. It is assumed that all fully integrable nonlinear partial differential equations or difference equations can be written in Hirota bilinear form. On another hand, for an equation that admits Hirota's bilinear form, the existence of N-soliton solutions of any order is not guaranteed. The equations admitting Hirota's bilinear form and having N-soliton solutions are called integrable by Hirota [9].

In this paper, we present a two-dimensional q-Toda lattice. A one-dimensional case for this equation was studied in [10]. Using the Hirota bilinear method, we find the bilinear form for the two-dimensional q-Toda lattice. Dispersion relation and the q-soliton solution are obtained by bilinear form for the two-dimensional q-Toda lattice.

Two-dimensional q-Toda lattice

In the beginning, classical mechanics was studied specifically for one-dimensional lattices, where the particles forming them interact only with their nearest neighbors. If we restrict their consideration to homogeneous systems, then the mass of each particle is denoted by m, the displacement of the n −th particle y_n and the interaction potential between neighboring particles is $\varphi(y_{(n+1)} - y_n)$. Then the equation of motion takes the following form

$$m\frac{d^2y_n}{dt^2} = \varphi'\left(y_{(n+1)} - y_n\right) - \varphi'\left(y_n - y_{(n-1)}\right)(n = \ldots, -1, 0, 1, 2\ldots), \tag{1}$$

where φ' derivative φ. Thus,

$$f(r) = -\varphi'(r) = -\frac{d\varphi(r)}{dr}, \tag{2}$$

$f(r)$ is a force which the spring acts, stretched by the value of r_n

$$r_n = y_{n+1} - y_n \text{ or} \qquad r_n = y_n - y_{n-1} \tag{3}$$

(3) – this is a relative displacement. When the force $f(r)$ is proportional to the displacement r_n Hooke's law is satisfied. The Toda equation [10], describing the motion of the anharmonic lattice, has the form

$$m\frac{d^2y_n}{dt^2} = a[e^{br_n} - e^{-br_n}], \tag{4}$$

where a, b and m are real constants. Introducing the force of the n −th particle into the lattice, we obtain the following equation

$$V_n = a[e^{br_n} - e^{-br_n}], \tag{5}$$

as a rapidly decreasing function, equation (4) turns out to be

$$\frac{d^2}{dt^2}ln(1 + V_n) = V_{(n+1)} + V_{(n-1)} - 2V_n. \tag{6}$$

The two-dimensional q-Toda lattice has the following form

$$\frac{d^2}{dxdt}ln(1 + V(x, y, t)) = \Delta_x^2 V(x, y, t) = V(x, qy, t) + V\left(x, \frac{y}{q}, t\right) - 2V(x, y, t). \tag{7}$$

Present the transformation of the dependent variable as

$$V(x, y, t) = \frac{d^2}{dxdt}\ln\big(f(x, y, t)\big). \tag{8}$$

Substituting (8) into (7) and integrating the obtained expression twice, we get

$$\frac{f_{xt}f - f_t f_x}{f^2} = \frac{f(x,qy,t)f\left(x,\frac{y}{q},t\right)}{f^2} - 1. \tag{9}$$

Equation (9) can be rewritten in the Hirota bilinear form, namely in terms of the Hirota D-operator, as

$$\left[D_x D_t - \left(e^{hyD_y} + e^{-hyD_y} - 2\right)\right]\{f(x, y, t) \cdot f(x, y, t)\} = 0, \tag{10}$$

which follows from (9) by multiplying by $2f^2(x, y, t)$, where we use the q-exponential identity [10]. For functions $f(y), g(y)$ the q-exponential unit [10] will be

$$e^{hyD_y}f(y)g(y) = f(qy)g\left(\frac{y}{q}\right) = E_q f(y)E_q^{-1}g(y), \ y \in R. \tag{11}$$

The last equation is satisfied if we have the usual relation between two quantum parameters h and q for $q = e^h$. To find the soliton solutions of the Toda lattice, we apply the expansion of perturbations around the formal perturbation parameter ε in the form

$$f(x, y, t) = 1 + \epsilon f^{(1)}(x, y, t) + \varepsilon^2 f^{(2)}(x, y, t) + \cdots. \tag{12}$$

Substituting (12) into (10) we obtain the equation

$$\begin{gathered} P(D)\{f(x, y, t) \cdot f(x, y, t)\} = P(D)[\{1 \cdot 1\} + \varepsilon\{1 \cdot f^{(1)} + f^{(1)} \cdot 1\} \\ +\varepsilon^2\{1 \cdot f^{(2)} + f^{(2)} \cdot 1 + f^{(1)} \cdot f^{(1)}\} + \varepsilon^3\{1 \cdot f^{(3)} + f^{(3)} \cdot 1 + f^{(1)} \cdot f^{(2)} + f^{(2)} \cdot f^{(1)}\} \\ +\varepsilon^4\{1 \cdot f^{(4)} + f^{(4)} \cdot 1 + f^{(1)} \cdot f^{(3)} + f^{(3)} \cdot f^{(1)} + f^{(2)} \cdot f^{(2)}\} + \cdots], \end{gathered} \tag{13}$$

where $P(D) = D_x D_t - \left(e^{hyD_y} + e^{-hyD_y} - 2\right)$. We collect the coefficients with respect to ε^i, $\forall i \geq 0$ of equation (13). The coefficient of the first term ε^0 disappears trivially, and from the coefficient ε^1 we have

$$P(D)\left\{1 \cdot f^{(1)} + f^{(1)} \cdot 1\right\} = 2P(\partial) = 2\left[\partial_x \partial_y - \left(e^{hyD_y} + e^{-hyD_y} - 2\right)\right] f^{(1)} = 0. \quad (14)$$

The equation (14) is a direct result of the property of the Hirota operator D [9] because $P(D)$ has an even order. The next important step in the calculation is to find solution for equation (14).

The general trend for soliton solutions is exponential, but the exponential function $f^{(1)}$ does not satisfy equation (14). Due to the nature of the q-numbers, the solution to equation (14) should have a power function for the analog of the q-discrete spatial variable. Therefore, you can choose the original solution (14) as

$$f^{(1)}(x, y, t) = y^{\alpha} e^{\beta t + \gamma x + \eta}, \quad (15)$$

where, $\alpha, \beta, \eta -$ arbitrary constants.

A solution with the usual behavior of soliton and having power analogs for q-discrete variables is called a q-soliton solution. If we substitute (15) in (14), we obtain the relation between the parameters

$$\beta\gamma = q^{\alpha} + q^{-\alpha} - 2, \quad (16)$$

which is called the dispersion relation.

The coefficient ε^2 obtained from (13) gives the following

$$P(D)\left\{1 \cdot f^{(2)} + f^{(2)} \cdot 1 + f^{(1)} \cdot f^{(1)}\right\} = 2P(\partial) f^{(2)} + P(D)\left\{f^{(1)} \cdot f^{(1)}\right\}.$$

That gives

$$\left[D_x D_t - \left(e^{hyD_y} + e^{-hyD_y} - 2\right)\right]\left\{f^{(1)}(x, y, t) \cdot f^{(1)}(x, y, t)\right\} = -2\left[\partial_x \partial_t - \left(e^{hy\partial_y} + e^{-hy\partial_y} - 2\right)\right] f^{(2)}(x, y, t). \quad (17)$$

Since $f^{(1)}$ given in (14) satisfies to form (17), we can assume that all members of higher order are zero, i.e. $f^{(j)} = 0, j \geq 2$. Further, as a generalization, this fact can be assumed in the derivation of the i-q-soliton solution, $f^{(j)} = 0$ for all $j \geq i + 1$. When $\varepsilon = 1$, one-q-soliton solution is constructed by substituting equations (15) and (16) into (17) and taking into account that $f(x, y, t) = 1 + f^{(1)}(x, y, t)$ then

$$V(x, y, t) = \frac{d^2}{dxdt} \ln f(x, y, t) = \frac{y^{\alpha} \beta\gamma e^{\beta t + \gamma x + \eta}}{\left(1 + y^{\alpha} e^{\beta t + \gamma x + \eta}\right)^2}, \quad (18)$$

which is the one-q-soliton solution of the two-dimensional q-Toda lattice. The dynamics of the one-q-soliton solution is presented in Figure.

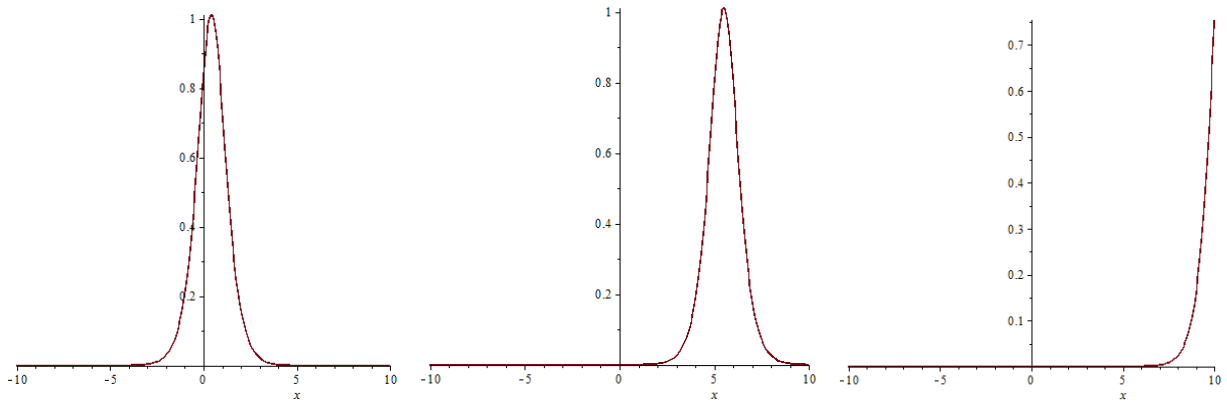

Figure. Dynamics of a one-q-soliton solution for the two-dimensional q-Toda lattice with parameters: γ=2, α=-5, η=0, q=1.25, (a) t=-5, (b) t=0, (c) t=5.

Figure shows the dynamics of the obtained solution (18) depending on t. So with different values of t, the wave's shape is saved. This proves there is a soliton in a two-dimensional q-Toda lattice, which means that energy transfer is possible. The Toda lattice is unique because it has a wide range from the harmonic to the anharmonic limit and has the so-called N-soliton solutions. As presented above, soliton is a structurally unchanged solitary wave in a nonlinear environment. When interacting with each other or other disturbances,

solitons behave like particles, therefore they are called particle-like. Due to the balance between the action of nonlinearity and dispersion, they save their structure, not collapsing in a collision.

Conclusion

Thus, we present the q-Toda lattice in the two-dimensional case. Using the Hirota bilinear method, we find the bilinear form for the two-dimensional q-Toda lattice and obtain the dispersion relation and the one-q-soliton solution. This algorithm can be applied to obtain N-soliton solutions. The soliton is conserved due to the equilibrium between the action of a nonlinear environment with dispersion. In addition, the soliton behaves as a particle (particle-like): it does not collapse when interacting with each other or other disturbances while maintaining the structure and continues to move. This quality has the ability to use when transferring data or information over long distances with virtually no interference. The study of the Toda lattice in various dimensions allows one to go on to understand such complex terms as matrix models that can be used to describe different physical systems.

The article is performed as part of the financial support of the scientific and technical program (F. 0811, No. 0118RK00935) of the MES of the Republic of Kazakhstan.

References

1 Тода М. Теория нелинейных решеток / М. Тода. — М.: Высш. шк., 1984. — 262 с.

2 Vegal, L.C. Bäcklund transformation and solitonic solutions for a parametric coupled Korteweg-de Vries system / L.C. Vega1, A. Restuccia, A. Sotomayor // Journal of Physics: Conference Series. — 2014. — 490. — 012024.

3 Hirota, R. The direct method in soliton theory / Cambridge university press. — 2004. — 198 p.

4 Gardner, C.S., Method for solving the Korteweg-de Vries equation / C.S. Gardner, J.M. Greene, M.D. Kruskal, R.M. Miura // Physical Review Letters. — 1967. — 19. — P. 1095–1097.

5 Hirota, R. Exact solution of the Korteweg-de Vries equation for multiple collisions of solitons / R. Hirota // Physical Review Letters. — 1971. — 27. — P. 1192–1194.

6 Hirota, R. Exact solution of the Sine-Gordon equation for multiple collisions of solitons / R. Hirota // Journal of the Physical Society of Japan. — 1972. — 33. — P. 1459–1463.

7 Hirota, R. Exact envelope-soliton solutions of a nonlinear wave equation / R. Hirota // Journal of Mathematical Physics. — 1973. — 14. — P. 805–809.

8 Мухамедина К.Т. Екікомпонентті Хирота теңдеуінің солитондық шешімдері [Soliton solutions of two-component Hirota equation] / К.Т. Мухамедина, А.М. Сыздыкова, Г.Н. Шайхова // Қарағанд. ун-нің хабаршысы. Математика Сер. — 2015. — 4. — P. 103–107.

9 Grammaticos, B. Multilinear operators: the natural extension of Hirota's bilinear formalism / B. Grammaticos, A. Ramani, J. Hietarinta // Physics Letters A. — 1994. — 190. — P.65–70.

10 Silindir, B. Soliton solutions of q-Toda lattice by Hirota direct method / Advances in Difference Equations. — 2012. — 121.

Б.Б. Кутум, Г.Н. Шайхова

Екіөлшемді q-Тода тізбегінің q-солитондық шешімі

Тода тізбегі экспоненциалдық күш арқылы өзара әрекеттесетін, сызықтағы шексіз массалар жүйесін сипаттайтын сызықты емес эволюциялық теңдеу болып табылады. Авторлар q-Тода тізбегінің екіөлшемді кеңістіктегі солитондық шешімін құрастыруды талдады. Мақсатқа қолжеткізу үшін қозғалыс теңдеуі алынып, Хирота полиномы ретінде жазылған бисызықты түрге келтіру үшін сызықты емес теңдеуді тәуелді айнымалыны түрлендіру қолданды. Интегралданатын сызықты емес эволюциялық теңдеулердің көп солитонды шешімдерін құрастырудың тиімді әдістерінің бірі ретінде берілген әдісті көптеген теңдеулерге, олардың ішінде сызықты емес дифференциал, сызықты емес дифференциал-айырымдық теңдеулерге қолдануға болады. Хирота әдісін қолдана отырып, екіөлшемді q-Тода тізбегінің бисызықты түрі алынып, оның негізінде q-солитондық шешімі есептелді. Екіөлшемді q-Тода тізбегінің q-солитондық шешімнің динамикасы ұсынылды. Атап айтқанда, солитон сызықты емес орта мен дисперсия арасындағы әрекетінің тепе-теңдігі арқасында сақталады. Сонымен қатар солитон өзін бөлшек ретінде ұстайды: бір-бірімен немесе басқа ауытқулармен өзара әрекеттесу кезінде қирамай, құрылымын сақтап, қозғалысын жалғастырады. Осындай қасиетті мәліметті немесе ақпаратты алысқа дерлік кедергісіз жіберу кезінде қолдануға мүмкіндік туғызады. Бұдан басқа, Тода тізбегін және оған түрлі өлшемділіктегі әртүрлі әдістердің қолдануын зерттеу

әркелкі физикалық жүйелерді сипаттау мақсатында қолдануға болатын, матрицалық модельдер сияқты күрделі терминдерді түсінуге мүмкіндік туғызады.

Кілт сөздер: дисперсия, солитон, Тода тізбегі, бисызықты форма, Хирота әдісі.

Б.Б. Кутум, Г.Н. Шайхова

Q-солитонное решение двумерной цепочки q-Тоды

Цепочка Тоды является нелинейным эволюционным уравнением, описывающим бесконечную систему масс на линии, которые взаимодействуют через экспоненциальную силу. В работе проведен анализ построения солитонного решения цепочки q-Тоды в двумерном пространстве. Для этой цели взято уравнение движения и использовано преобразование зависимой переменной для преобразования нелинейного уравнения в билинейную форму, которая записана как полином оператора Хироты. Как один из наиболее эффективных методов построения многосолитонных решений интегрируемых нелинейных эволюционных уравнений, данный метод применим к широкому классу уравнений, включая нелинейные дифференциальные, нелинейные дифференциально-разностные уравнения. Применяя метод Хироты, была получена билинейная форма для двумерной цепочки q-Тоды на основе, которой найдено q-солитонное решение. Представлена динамика q-солитонного решения двумерной цепочки q-Тоды. Отметим, что солитон сохраняется благодаря равновесию между действием нелинейной среды с дисперсией. Помимо этого солитон ведет себя как частица: не разрушается при взаимодействии друг с другом или другими возмущениями, при этом сохраняет структуру и продолжает движение. Такое качество имеет возможность использования при передаче данных или информации на дальние расстояния практически без помех. Кроме того, исследование цепочки Тоды и применение к ней разных методов в различных размерностях позволяет перейти к пониманию таких сложных терминов, как матричные модели, которые можно применить для описания разных физических систем.

Ключевые слова: дисперсия, солитон, цепочка Тоды, билинейная форма, метод Хироты.

References

1 Toda, M. (1984). *Teoriia nelineinykh reshetok [Nonlinear lattice theory]*. Moscow: Vysshaia shkola [in Russian].

2 Vegal, L.C., Restuccia, A., & Sotomayor, A. (2014). Bäcklund transformation and solitonic solutions for a parametric coupled Korteweg-de Vries system. *Journal of Physics: Conference Series*, 490, 012024.

3 Hirota, R. (2004). *The direct method in soliton theory.* Cambridge university press.

4 Gardner, C.S., Greene, J.M., Kruskal, M.D., & Miura, R.M. (1967). Method for solving the Korteweg-de Vries equation. *Physical Review Letters, 19,* 1095–1097.

5 Hirota, R. (1971). Exact solution of the Korteweg-de Vries equation for multiple collisions of solitons. *Physical Review Letters, 27,* 1192–1194.

6 Hirota, R. (1972). Exact solution of the Sine-Gordon equation for multiple collisions of solitons. *Journal of the Physical Society of Japan, 33,* 1459–1463.

7 Hirota, R. (1973). Exact envelope-soliton solutions of a nonlinear wave equation. *Journal of Mathematical Physics, 14,* 805–809.

8 Mukhanmedina, K.T., Syzdykova, A.M., & Shaikhova, G.N. (2015). Ekikomponentti Hirota tendeuinin solitondyk sheshimderi [Soliton solutions of two-component Hirota equation]. *Karahandy universitetinin khabarshysy. Matematika Seriiasy – Bulletin of the Karaganda University. Series Mathematics, 4,* 103–107 [in Kazakh].

9 Grammaticos, B., Ramani, A., & Hietarinta J. (1994). Multilinear operators: the natural extension of Hirota's bilinear formalism. *Physics Letters A, 190,* 65–70.

10 Silindir, B. (2012). Soliton solutions of q-Toda lattice by Hirota direct method. Advances in Difference Equations, 121.

DOI 10.31489/2019Ph 3/27-33

UDC 620.9:662.6; 621.1

A.D. Mekhtiyev, P.M. Kim, V.V. Yugay, A.D. Alkina

Karaganda State Technical University, Kazakhstan
(E-mail: Barton.kz@mail.ru)

Electrovacuum heating elements

Improving the efficiency of heat supply systems for buildings and structures in the current trends in the global development of energy saving cannot be fully realized without the introduction of high-tech and low-energy-intensive electrical equipment. The heat supply of remote objects for various purposes is accompanied by significant losses, since the coolant has to cover considerable distances, in some cases the connection of the object to the heating plant is impossible due to technical problems or considerable material costs for the installation of pipelines. One solution could be the introduction of a low-pressure steam electric heater. This is a new generation electric heater with a fundamentally new design of the heating element. It combines the efficiency of an electric spiral and the comfortable warmth of a traditional heating radiator.

Keywords: radiator, electric heater, energy saving, heating system, heating device, heating.

Throughout the developmental stages of his development, man sought ways to heat his home. It all started with a fire, then the stoves and fireplaces were invented. With the development of technology, previous methods were replaced by autonomous heating systems with boilers operating on various types of fuel and thermal power plants capable of heating cities. But despite the presence of a centralized heating system, a person is not always satisfied with the ambient air temperature in a residential area, such a situation may occur during the interseasonal heating time when the outdoor temperature is still cool and the central heating system is not functioning or has already ceased to function due to the end your season work. A similar situation arises in the southern countries, where there is practically no cold winter and snow, but there are small periods of time when a heat source is needed to heat the dwelling. To solve this problem, you can use a solid fuel and gas stove, but it is not always acceptable for urban conditions besides the fire hazard of a heat source with open fire, it also produces harmful emissions of exhaust gases in the course of its work, which harm the environment of the city and create local areas of concentration of flue gas. The search for the most ecologically clean source of heat prompted engineers to use electric current and create an electric heater, a kind of autonomously working heat source connected to the electrical network. Compact thermal device is capable of producing enough warm to heat a home.In the 30s of the last century in Geneva, the French engineer Jacques Noir [1] developed and launched into production an electric heater, the basis of its design was an electric spiral, which was blown by the air flow created by a fan. Subsequently, he created his own company «Noir». At the same time, oil radiators were developed, the heating element was immersed in oil, placed in a sealed metal case from which heat is transferred to the surrounding air. In the process of heating, the oil transfers the resulting heat to the environment. Each type of heat equipment has certain disadvantages and advantages that have already been described many times in the literature, as well as electric heaters have come a long way to improve and modernize their design [2]. In 1972, the company «Noir» products came to the market with electric heaters equipped with a thermostat, it was possible to regulate the temperature of the supplied air. In 1988, the company «Noir» created

a convector, which was later taken as a basis by many manufacturers. The production of a convection-type heater has opened up new possibilities for heating devices: safety, operation of the device without noise, energy saving. In 2000, a new type of heater called the «Kalida», equipped with a climate control system, entered the market. Currently in the world there are a huge number of different types of heaters and manufacturers of this electrical equipment. The analysis of world production of electric heaters is very significant and is presented by various companies in Europe, Asia and America, for example: De'Longhi, General Climate, Polaris, EWT, Hansa, Timberk, Supra Wika, Fluke, Noir, Hyundai, Resanta, NOVEL, ZASS, Kaiser, Ballu, Siemens, EVUB [3]. Electrical oil with a spiral heating element, convectors, split-systems, as well as infrared heaters are produced. At the moment, the export of electric heaters in Kazakhstan is 100 %, the vast majority is collected in factories in China. Our task is to develop a new generation electric heater equipped with all modern electronic monitoring and control systems, which will make it possible to achieve maximum comfort of use and efficiency of the thermal device.

We have developed a low-pressure energy-saving steam electric heater (LSEH), which can be a substitute for a traditional oil cooler, as well as to compete with existing electric heaters. LSEH combines the advantages of electric spiral, converters and oily electric heaters into a single whole. For example, oily electric heater contains oil that is dangerous in the fire relationship, it heats up for a long time, the metal body heats up strongly, and the oil is subject to degradation. In addition to the thermostat, more expensive branded models have a timer and protection that turns it off from the network when tipping to the floor, which makes its use more convenient and safer. Heaters with an electric helix also have several disadvantages, for example, emit unpleasant odors when burning dust and create noise during their work. There is also an analogue of LSEH developed by VEST, but which has a number of serious differences, its cost is several times higher than the electric heater proposed by us, so it cannot be considered in future as a competitor in the market [4].

After analyzing the sources [5], we developed a LSEH, which does not have the above disadvantages of the above-mentioned electric heaters, has high efficiency and creates comfortable heat. This is a fully automated electric heater with the «Climate Control» system and the possibility of coordination with the «Smart Home» system; it is controlled by using a remote control or a smartphone. The achieved technical indicators of the electric heater make it possible to ensure its service life for more than 20 years with a constant efficiency of 90 %.

We have developed and created an experimental laboratory sample of LSEH, consisting of separate sections with a capacity of from 50 to 100 watts. The block-modular layout of the electric heater allows the owner to change its power, if it is necessary, independently, without resorting to the services of skilled workers. Sections are connected in parallel using electrical connections. The LSEH section is made of duralumin alloy, inside which is placed a vacuum electric heater. One section can effectively heat up to 3 m^2 of living space at a ceiling height of 2.5 meters. The appearance of the prototype laboratory sample and the device of the electrovacuum heater is shown in Figure 1. The LSEH can be floor mounted or mounted on the wall, like a classic radiator, only instead of pipes you need to connect an electrical wire to it, which simplifies its installation [6].

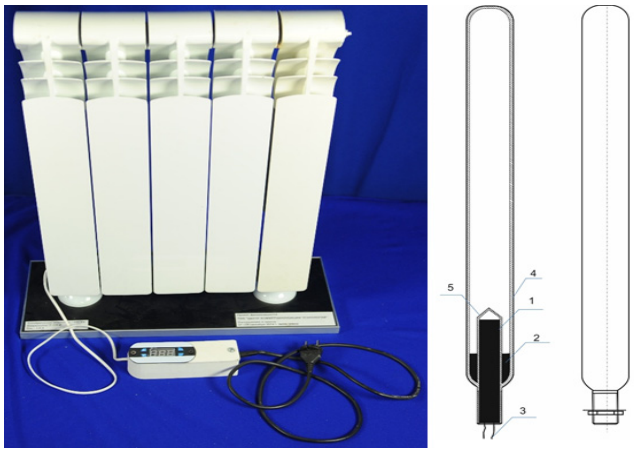

Figure 1. The appearance of the experimental laboratory sample
and the device of the electrovacuum heater LSEH

The basis of the LSEH is an electrovacuum heater, which operates as follows: an electric spiral heater 1 provides for rapid heating of the heat-transfer fluid 2 (distilled water); electric current is supplied to the coil by means of electrical wires 3. When the heat-carrier evaporates, the steam reaches the upper part of the body 4, where it gives off heat received from the heater. Cooling off steam condenses and flows along the walls of the body to the bottom again heats up and evaporates. The principle of its operation is based on the well-known effect of the phase transition of a heat pipe. The electric heating element is placed in the housing 5 and does not come into contact with the coolant [7]. The recommended pressure inside the electrovacuum heater should be within 4.053 kPa (0.04 bar). Heat particles move inside the body at the speed of sound due to which the LSEH section weighing about 230 grams is heated to 700 °C in less than 5 minutes, unlike the traditional oily electric heater more than 5 times faster. But there is one problem in the design that had to be solved in order to achieve reliable performance of the LSEH, this is to ensure high tightness of the body of the electrovacuum heating element, since when the pressure rises above 0.1 Atm, the effect of high-grade heating is lost, there were also problems with the set of the required temperature. The principle of operation is discussed in detail in the source [8], and also the novelty of the electrovacuum heating element is given.

During the work on the design of LSEH, we have developed a 3D model (Fig. 2). 3D model allows to execute drawings for its production, as well as to learn more about the device electric heater [9].

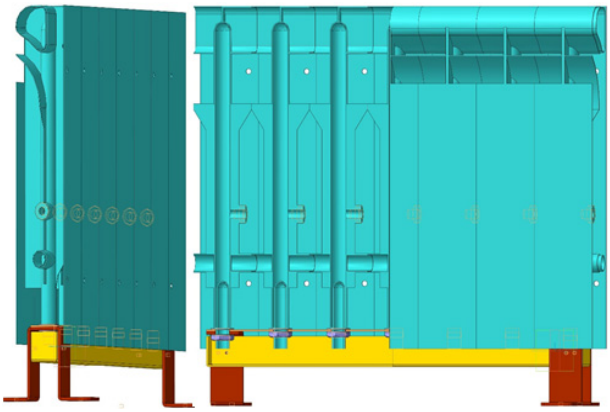

Figure 2. 3D model of LSEH

In the process of creating LSEH, we carried out a series of laboratory experiments aimed at improving the design of an electrovacuum heater, which were made in the form of copper tubes with diameter of 20, 28, 32, weight from 270 to 530 grams, length from 250 to 450 mm, heater power — 60, 80 and 100 watts. The pressure inside the tube is 4–10 kPa (0.04–0.1 atm). Temperature is 0 °C. In total, we manufactured and tested 40 electric vacuum heaters. Some results are presented in the dependency graphs in Figures 4 and 5. Temperature was measured using a Fluke 51 contact thermometer with laboratory accuracy (0.05 % + 0.3 °C) and a measurement limit of up to 900 °C (1600° F). Vacuum pump DUO 6/M SERIES PFEIFFER VACUUM with an integrated vacuum meter was used to create the vacuum [10].

The required number of repetitions of experiments [11] is determined on the basis of the coefficient Kvar and the required degree of accuracy.

The value of the coefficient of variation is determined by the formula:

$$K_{\text{var}} = \frac{100 \cdot \delta}{\chi}, \%, \tag{1}$$

where δ — mean square deviation;

χ — arithmetic average.

The value of the mean square deviationis calculated by the formula:

$$\delta = \sqrt{\frac{\Sigma \delta_i^2}{N - n}}, \tag{2}$$

where δ_i – deviations of individual results from group means;

N — the total number of experiments;

n — the number of experimental groups [12].

To establish the required number of experiments a valid value of K_{add} in percent is given. Knowing the coefficient of variation K_{var} for a given test method, it is possible with a reliability of 0.95 to determine the required number of experiments. According to the results of numerous experimental data, K_{add} = 12 % is taken (K_{var} = 11.5 %). This coefficient corresponds to (with a confidence probability of 0.95) the required number of experiments equal to 4. During the processing of the exertional data, data processing using the means of the Microsoft Excel spreadsheet processor, quadratic interpolation of the function (solid line) and the rms (root mean square) approximation (dashed line) were used, as well as performed regression analysis.

Figure 3 shows a plot of temperature change versus heating time for tubes with volume of 10 and 15 ml. The tube of the electrovacuum heater with the parameters copper — 28 mm in diameter, weight — 355 g, length — 310 mm, heater power — 80 W was investigated. The volume of coolant is 10 and 15 ml. The pressure inside the tube is 5.066 kPa (0.05 atm).

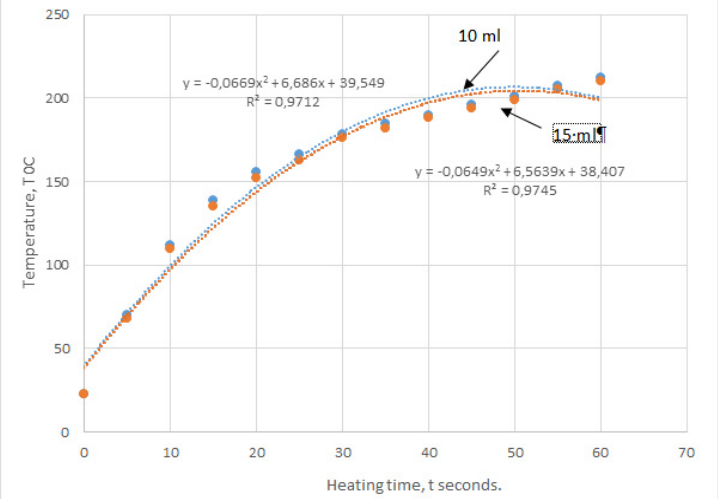

Figure 3. Graph of temperature change versus heating time for tubes with a volume of 10 and 15 ml

Figure 4 shows a plot of temperature versus coolant volume from 5 to 15 ml. The tube of an electrovacuum heater with a tube with parameters copper 20 mm in diameter, weight — 368 g, length — 305 mm, heater power — 80 W was investigated. The volume of coolant is 10 and 15 ml. The pressure inside the tube is 4,053 kPa (0.04 atm). Presumably, in the process of switching to a pressure of 0.01 atm (1.01 kPa), the efficiency of the electrovacuum heater, as well as the heat pipe, can be increased by 15–20 %, because the friction energy losses in a more discharged atmosphere decrease, the transmission rate can reach sound. If the pressure in the heat pipe is lower, then the heat transfer process is more efficient and the efficiency is higher. In the process of increasing the pressure in the internal cavity of an electrovacuum heater (above 0.1 atm), the effect of high-grade heating is completely lost and there are problems with a set of the required temperature.

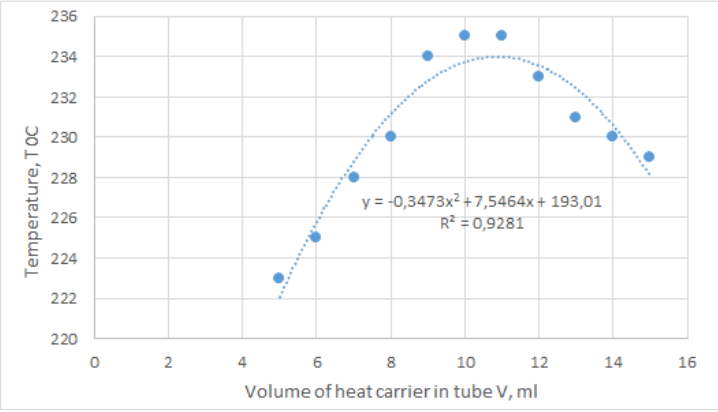

Figure 4. A plot of temperature change versus coolant volume from 5 to 15 ml

We have carried out experiments related to the determination of the mass of an 80W electric vacuum heater. The volume of coolant is 10 and 15 ml. The pressure inside the tube is 5.066 kPa (0.05 atm). As the mass increases, the surface temperature of the heater decreases. The tests were carried out with 5 samples of different mass when heated from 1300 to 2160 with a mass of, respectively, from 230 to 530 grams. The dependence of the temperature change of the surface of the housing of the electrovacuum heater on its mass is established, the graph is shown in Figure 5. The LSEH has automatic power adjustment depending on the ambient temperature in the room, therefore, if necessary, the electrovacuum heater has a significant dynamic range margin for adjustment.

It should be noted that modern electric heaters have low maintainability, this leads to the fact that the consumer is not able to perform repairs on his own and is forced to contact specialized organizations that perform repairs, on the one hand it's right that the manufacturer excludes the possibility of self-repair at home, but workshops cannot always help in the repair, a couple just do not have the necessary spare parts. Sections LSEH have a unified design and allow you to repair by yourself.

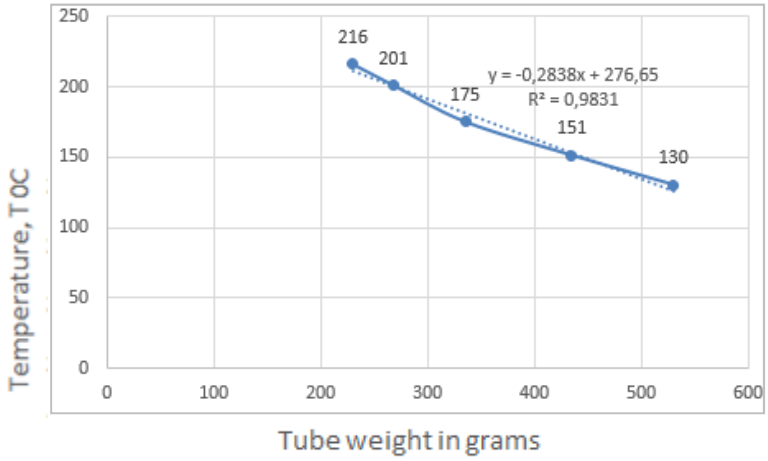

Figure 5. Dependence of the surface temperature of the case of an electrovacuum heater on its mass

A low-pressure energy-saving steam electric heater is an economical replacement for a traditional oil radiator; it can compete with existing electric heaters. The technological advantage is the high efficiency of heat transfer inside the system without loss. The main economic advantage of LSEH is lower power consumption; it is up to 1.3 times less than an oily electric heater, high reliability and a long service life. LSEH is absolutely safe in terms of an explosion or a fire in the event of a leak or falling onto the floor. Water is used in the place of expensive synthetic oil, which significantly reduces the cost and facilitates the design of the electric heater. Low material costs for installation and operation of the heating system are not achievable by competitors, 100 % automation with the possibility of coordination with the «Smart Home» system. The use of LSEH technology can have a multiplier effect for creating heating radiators with a liquid heat carrier; this will allow reducing their metal consumption and cost, without loss of consumer qualities. There is an opportunity to use our technology in systems «warm floor».

Список литература

1 Сайт журнала «История бытовой техники» [Электронный ресурс]. — Режим доступа: http://tehnikaland.ru /klimaticheskaya-tehnika/istoriya-izobreteniya-obogrevatelya.html

2 Сайт журнала «OBI» [Электронный ресурс]. — Режим доступа: https://diy.obi.ru/articles/ obogrevateli-plusi-i-minysi-19964/

3 Козлов С.В. Современные высокоэффективные автономные энергосберегающие системы отопления / С.В. Козлов // Новости теплоснабжения — 2007. — № 8. — С. 84–86.

4 Сайт журнала «Onliner» [Электронный ресурс]. — Режим доступа: https://people.onliner.by/2015/09/25/heater

5 Сайт журнала «Электронагреватели парокапельного типа» [Электронный ресурс]. — Режим доступа: http://vestkz.ru/opisanie.htm

6 Температуры касаемых поверхностей. Эргономические данные для установления предельных величин горячих поверхностей: ГОСТ 51337–99. — М., 2000 — 16 с.

7 Братенков В.Н. Теплоснабжение малых населенных пунктов / В.Н. Братенков, П.А. Хаванов, Л.Я. Вэскер. — М.: Стройиздат, 1988. — 223 с.

8 Дмитриев А.Н. Энергосбережение в реконструируемых зданиях / А.Н. Дмитриев, П.В. Монастырев, С.Б. Сборщиков. — М.: Изд-во АСВ, 2008. — 208 с.

9 Радиатор отопления: Патент на полезную модель № 2816. — Зарегистрирован в Государственном реестре полезных моделей Республики Казахстан, 24.04.2018 г.

10 Радиатор отопления: Патент на изобретение № 32156 — Зарегистрирован в Государственном реестре изобретении Республики Казахстан, 16.05.2017 г.

11 Аметистов Е. В. Основы теории теплообмена / Е.В. Аметистов. — М.: Изд. МЭИ, 2000. — 242 с.

12 Безродный М.К. Процессы переноса в двухфазных термосифонных системах: моногр. / М.К. Безродный, И.Л. Пиоро, Т.О. Костюк. — Киев: Факт, 2003. — С. 55–57.

А.Д. Мехтиев, П.М. Ким, В.В. Югай, А.Д. Алькина

Электрвакуум жылыту элементтері

Ғимараттар мен құрылыстардың жылу мен жабдықтау жүйелерінің энергия үнемдеудің жаһандық дамуының ағымдағы үрдістеріндегі тиімділігін жоғарылату жоғары технологиялық және төменқуатты тұтынатын электржабдықтарын енгізбестен толығымен іске асырыла алмайды. Әртүрлі мақсаттар үшін қашықтағы объектілерді жылумен жабдықтау маңызды шығындармен қатар жүреді, себебі салқындатқыш қашықтықты айтарлықтай қамтуы тиіс, ал кейбір жағдайларда құбырларды орнатуға техникалық қиындықтар немесе елеулі материалдық шығындар салдарынан нысанды жылыту қондырғысы қосылмайды. Бір шешім ретінде төменқысымды буэлектрлі жылытқышты енгізу болып табылады. Бұл қыздыру элементінің түбегейлі жаңа дизайны мен жаңа буын электржылытқышы. Ол электрлік спиралдың тиімділігін және дәстүрлі жылурадиаторының ыңғайлы жылуын біріктіреді.

Кілт сөздер: радиатор, электржылытқышы, энергияүнемдеу, жылыту жүйесі, жылыту құрылғысы, жылыту.

А.Д. Мехтиев, П.М. Ким, В.В. Югай, А.Д. Алькина

Электровакуумные нагревательные элементы

Повышение эффективности систем теплоснабжения зданий и сооружений в современных тенденциях общемирового развития энергосбережения не может быть реализовано в полной мере без внедрения высокотехнологичного и низкоэнергоемкого электрооборудования. Теплоснабжение удаленных объектов различного назначения сопровождается значительными потерями, так как теплоносителю приходиться преодолевать значительные расстояния, в некоторых случаях подключение объекта к теплоцентрали невозможно в силу технических проблем или значительных материальных затрат на монтаж трубопроводов. Одним из решений может быть внедрение парового электрообогревателя низкого давления. Это электрообогреватель нового поколения с принципиально новой конструкцией нагревательного элемента. В нем сочетаются эффективность электрической спирали и комфортное тепло традиционного радиатора отопления.

Ключевые слова: радиатор, электрообогреватель, энергосбережение, система теплоснабжения, тепловой прибор, отопление.

References

1 Sait zhurnala «Istoriia bytovoi tekhniki» [Site of journal «History of household appliances»]. *tehnikaland.ru.* Retrieved from http://tehnikaland.ru/klimaticheskaya-tehnika/istoriya-izobreteniya-obogrevatelya.html [in Russian].

2 Sait zhurnala «OBI» [Site of journal «OBI»]. *diy.obi.ru.* Retrieved from https://diy.obi.ru/articles/obogrevateli-plusi-i-minysi-19964/ [in Russian].

3 Kozlov, S.V. (2007). Sovremennye vysokoeffektivnye avtonomnye enerhosberehaiushchie sistemy otopleniia [Modern high-efficiency Autonomous energy-saving heating systems]. *Novosti teplosnabzheniia – News of heat supply* 8, 84–86 [in Russian].

4 Sait zhurnala «Onliner» [Site of journal «Onliner»]. *people.onliner.by.* Retrieved from https://people.onliner.by /2015/09/25/heater [in Russian].

5 Sait zhurnala «Elektronahrevateli parokaptelnoho tipa» [Site of journal «Electric heaters of steam-drop type»]. *vestkz.ru.* Retrieved from http://vestkz.ru/opisanie.htm [in Russian].

6 Temperatury kasaemykh poverkhnostei. Erhonomicheskie dannye dlia ustanovleniia predelnykh velichin horiachikh poverkhnostei (2000) [The temperatures of the surfaces to be touched. Ergonomic data for setting the limit values of hot surfaces]. HOST 51337-99. Moscow [in Russian].

7 Bratenkov, V.N., Havanov, P.A., & Vesker, L.Ya. (1988). *Teplosnabzhenie malykh naselennykh punktov [Heat supply to small settlements]*. Moscow: Stroiizdat [in Russian].

8 Dmitriev, A.N., Monastyrev, P.V., & Sborshchikov, S.B. (2008). *Enerhosberezhenie v rekonstruiruemykh zdaniiakh [Energy savings in reconstructed buildings]*. Moscow: Izdatelstvo ASV [in Russian].

9 Radiator otopleniia [Heating radiator]. (2018). *Patent na poleznuyu model No. 2816 – Zarehistrirovan v Hosudarstvennom reestre poleznykh modelei Respubliki Kazakhstan*, 24.04.2018 [in Russian].

10 Radiator otopleniia [Heating radiator]. (2018). *Patent na izobretenie No. 32156 – Zarehistrirovan v Hosudarstvennom reestre izobretenii Respubliki Kazahstan*, 16.05.2017 [in Russian].

11 Ametistov, E.V. (2000). *Osnovy teorii teploobmena [Fundamentals of heat transfer theory]*. Moscow.: Izdatelstvo MEI [in Russian].

12 Bezrodnyi, M.K. (2003). *Protsessy perenosa v dvukhfaznykh termosifonnykh sistemakh [Transfer processes in two-phase thermosyphon systems]*. Kiev: Fakt [in Russian].

ТЕХНИКАЛЫҚ ФИЗИКА
ТЕХНИЧЕСКАЯ ФИЗИКА
TECHNICAL PHYSICS

DOI 10.31489/2019Ph 3/34-42

UDC 620 (075.8)

I. Klinovitskaya[1], S. Plotnikov[1], D. Kalygulov[1], P. Lay[2]

[1]D. Serikbayev East Kazakhstan Technical University, The Faculty of Energy, Ust-Kamenogorsk, Kazakhstan;
[2]ECM Technologies, 46 rue Jean Vaujany – Technisud, F-38029 Grenoble, France
(E-mail: iklinovitskaya@inbox.ru)

The investigation of the properties of solar cells based on Kazakhstan silicon

The study of the properties of solar cells is a relevant topic since the development of solar energy corresponds to the global trend and the course of the Government of the Republic of Kazakhstan on the transition to a «green» economy. Various properties of solar cells such as resistivity and surface resistance, carrier lifetime, reflectivity, quantum efficiency, directly affect the efficiency of solar cells. This paper is devoted to obtaining and comprehensive study of solar cells manufactured on the basis of the Kazakhstani silicon of «solar» quality. The study applied: a method of microwave detected photoconductive decay (μ-PCD), four probe methods for measuring resistance, methods for spectrometric analysis of reflection, transmission and photoluminescence coefficients, scanning electron microscopy, and methods for analyzing current-voltage characteristics. The mastered methods of solar cells production are described. A modification of the standard Back Surface Field (BSF) cell line to the Passivated Emitter and Rear Cell (PERC) line has been proposed.

Keywords: photoelectric converters, solar cells, silicon, Al-BSF structure, PERC structure, solar energy.

Introduction

As it is known [1], the world population is projected to grow from 7.6 billion (2018) to 9.2 billion by 2040. In response to a burgeoning population global energy use is forecast to increase by 28 % [2]. But in recent decades, energy consumption per capita has increased tenfold. As a result, the active production of energy from traditional types of hydrocarbon fuels (oil, coal, gas) led to a reduction in their reserves and to environmental pollution at the same time. All this has led to the need to find alternative unconventional approaches to energy generation. These sources include the energy of the sun.

As part of the transition to the «green» economy, in 2010, Kazakhstan began to implement a project for the production of photovoltaic modules based on the Sarykol quartz deposit. A consortium of French enterprises led by the Commissariat for Atomic Energy and Alternative Energy Sources of France took part in the «solar» project. The base material silicon is produced by carbothermic technology at the enterprise of the «Metallurgical Combine KazSilicon» LLP in the Ushtobe city, the production of solar cells and the assembly of modules is carried out at the factories of the «Kazakhstan Solar Silicon» LLP and the «Astana Solar» LLP, in the cities of Ust-Kamenogorsk and Astana, respectively.

In this paper, the implemented technology for the production of solar cells at «Kazakhstan Solar Silicon» LLP is considered. However, the production technology of solar cells based on multicrystalline silicon is constantly evolving and continuously improving. So, the natural progress from the Al-BSF structure production technology is the PERC structure [3].

The purpose of this work is to study and analyze the properties of photoelectric converters. Based on the obtained results of a comprehensive study, we conclude that it is possible to modify the existing line in order to increase the efficiency of solar cells.

Materials and methods

The material for the study is solar grade multi crystalline silicon (SOG mc-Si) wafer, with a thickness of 180-200 microns. Silicon wafers passed all stages of technological operations, such as: texturing, emitter creation by phosphorus diffusion method, removal of phosphorosilicate glass, antireflection coating deposition, metallization (creating a contact grid and current collecting busbars), and firing. As a result of a series of physicochemical processes, solar cells were obtained.

The solution of hydrochloric and nitric acids (HCl / HNO_3) was used to texturize the silicon wafer surface, as a result of which wells were formed on the surface, regardless of the orientation of the crystals. For etching a layer of porous silicon, silicon wafers were treated in a solution of potassium hydroxide (KOH), and then with the purpose of etching metals – in a solution of hydrofluoric and hydrochloric acids (HF / HCl). The X-Rite SP62 spherical reflectometer was used to measure reflectivity. This system measures the spectrum of the light source incident on the surface and the spectrum of light reflected from the surface, then compares the measured spectra. An analysis of the surface morphology of silicon wafer before and after texturing was performed by scanning electron microscopy using a JSM-6390LV microscope.

The emitter was formed using the diffusion method on Lydop equipment of Semco Engineering at the next stage. Phosphorus doping was carried out at a pressure slightly below atmospheric and at temperatures of 830–860 °C. The phosphorus oxychloride $POCl_3$ was used as a source of phosphorus, which is fed into the reactor along with nitrogen. The emitter, formed at a depth of 0.3-0.5 μm, has two functions: the formation of a p/n junction with the base and the transfer of electrons to metal contacts. For the analysis of the surface resistance of the formed emitter, CMT SR2000N device for measuring the surface and specific resistance by the 4-probe method was used. In order to evaluate the effect of gettering and measuring the lifetime of minority charge carriers, we used the method of measuring photoconductivity decay in the microwave range (μ-PCD) using the WT-2000 PVN Semilab measuring system at a laser wavelength of 904 nm.

Plasma-enhanced chemical vapor deposition (PECVD) was used for antireflection coating (ARC) depositing. The deposition of silicon nitride film was carried out in a vacuum chamber at a temperature of 350-450 °C in the presence of silane (SiH_4) and ammonia (NH_3). The thickness of the obtained antireflection coating, measured using Semilab LE-200PV ellipsometer by polarization-optical method, was 75 nm.

Metallic contacts and busbars were screen printed on Dubuit equipment. For the front side busbars and grids, silver-containing conductor paste with a specific resistance of less than 2 mΩ /sq and viscosity of 16-23 Pa*s was used, and for rear current-collecting busbars – silver paste with a resistance of 5 mΩ / sq and viscosity of 89 Pa*s. For the BSF creation, which plays the role of not only the rear solid contact but also a passivating layer, aluminium paste was used, with a resistance of 0.05 Ω /sq and a viscosity of 50 – 70 Pa*s.

Results and discussion

Figure 1 shows the obtained images of the silicon wafer surface before texturing (Fig. 1a), and after (Fig. 1b).

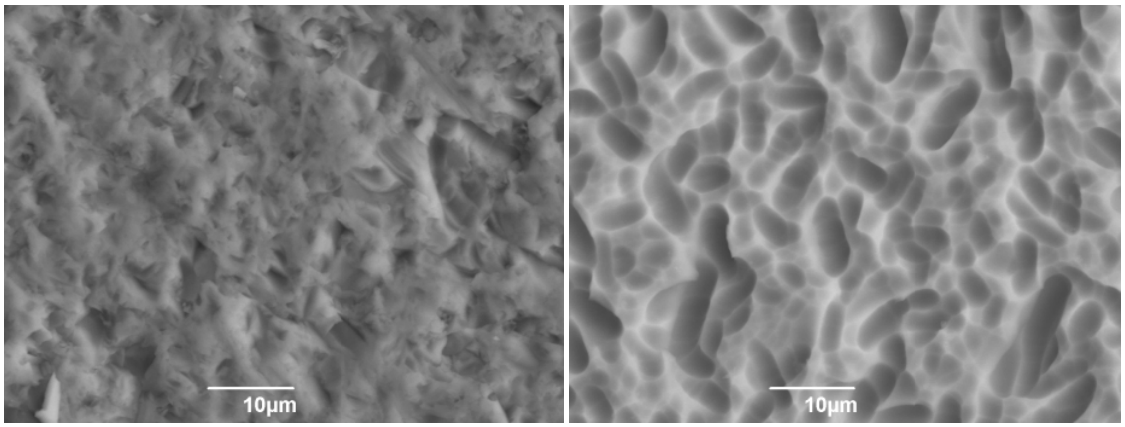

a) b)

Figure 1. Scanning electron microscope (SEM) image of the wafersurface: a) before texturing; b) after texturing

As Figure 1a shows, the surface of the source wafer is severely damaged. There is a huge number of cavities, microcracks and hills on it – this is the disturbed layer that was formed during the wafer production

(cutting ingots into wafers). Such surface is simply destructive for solar cells due to the extremely high surface recombination rate. After texturing and etching, the wells formed on the surface of the wafer (Fig. 1b), which leads to a significant decrease in reflectivity (Fig. 2).

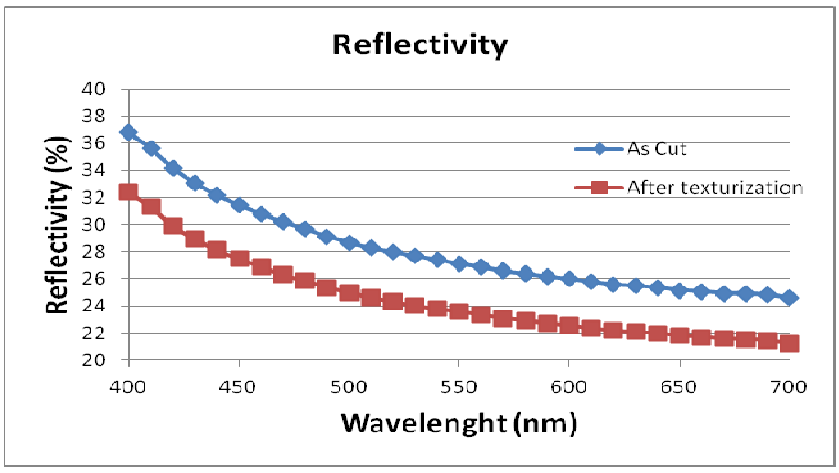

Figure 2. The reflectivity before and after texturing, obtained by spherical spectrometry on X-Rite SP62 reflectometer

CMT SR2000N device for measuring the sheet resistance and resistivity by the 4-probe method was used to determine the sheet resistance (Rsh).

The resistivity was determined by the formula [4]:

$$Rho = Rsh \bullet t, \quad (1)$$

where, Rho — resistivity, Ω*sm;

Rsh — sheet resistance Ω/sq;

t — silicon wafer thickness, sm.

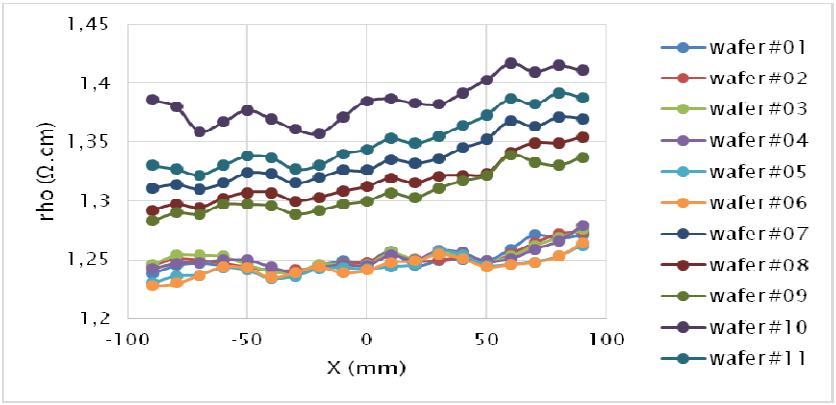

Figure 3. Silicon wafer resistivity obtained by the 4-probe method

Figure 3 shows the uneven distribution of resistivity across a sample of the wafer that can negatively affect the solar cell performance. The uniformity of the distribution of the average value of r_{ho} is 5.46 %.

A method for measuring the photoconductivity decay in the microwave range (μ-PCD) on the WT-2000 PVN measuring system was used to map the distribution of the lifetime of minority charge carriers (Fig. 4), and also their average values were obtained.

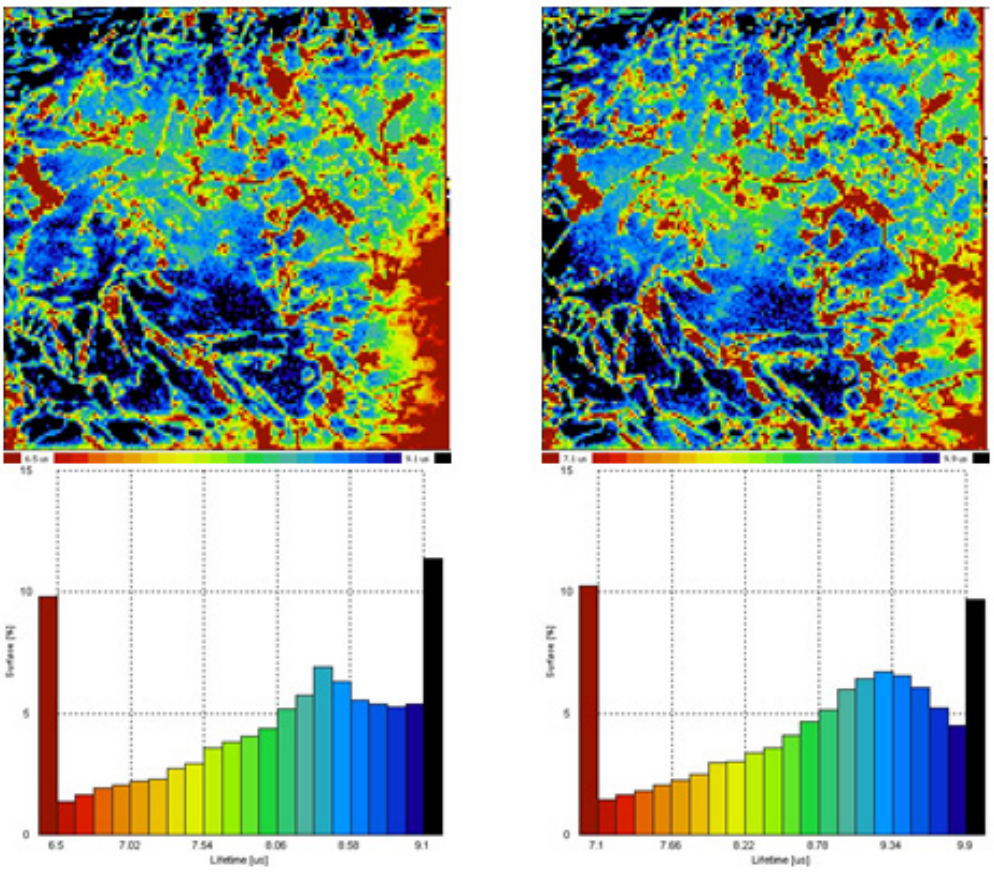

Figure 4. Maps of the lifetime of minority charge carriers distribution in wafer

The study showed that the lifetime of free charge carriers increased from 2 μs (before the diffusion process) to 11.6 μs (with a formed emitter after diffusion) with a uniformity coefficient of 1.5 %. As can be seen in Figure 4, the lifetime is distributed more evenly, with the exception of the boundary zones, where an accumulation of lattice defects and recombination zones formed during the crystallization process occurred.

It is known [5–8] that the surface of a multicrystalline silicon wafer is the maximum possible disorder in the symmetry of the crystal lattice, as a result of which the surface recombination of charge carriers increases. Surface recombination can greatly affect the short circuit current and the open-circuit voltage. Surface recombination has a particularly detrimental effect on the short-circuit current, since the front surface is also the region with the highest carrier generation in the solar cell. The reduction in high surface recombination is usually achieved by reducing the number of dangling bonds on the surface by passivation. In this work, the surface was passivated using non-stoichiometric films with a large amount of hydrogen (SixNy: H) applied by the PECVD method. An ellipsometer Semilab LE 200PV was used to measure the thickness and refractive index of the films obtained. The refractive index was 2.05-2.06, and the thickness of the films obtained was in the range from 73 to 78 nm.

The study of the properties and parameters of silicon wafers and solar cells by the method of spectrometric analysis of photoluminescence on a Luminescence ImaGing System – Model LIS-R1 measuring system was conducted at the National Institute for Solar Energy of France, INES. Photoluminescent Imaging (PL-images) of silicon wafers (Fig. 5) and solar cells (Fig. 7) were obtained.

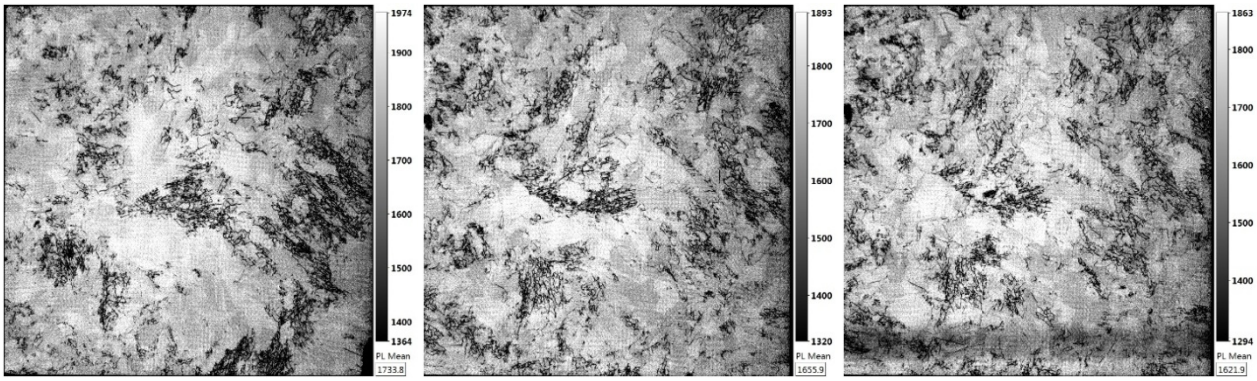

Figure 5. PL-images of wafer (samples 1, 7, 10) obtained on the Luminescence ImaGing System - Model LIS

The dark zones presented in the PL images of silicon wafers (Fig. 5) can be the sites of dislocation accumulations that occur during the crystallization of silicon ingots. These defects adversely affect the performance of solar cells.

The reflectivity is one of the main parameters affecting the efficiency of the finished solar cells. Figure 6 presents the results of measurements of the reflectivity of the samples under study by the method of spectrometric analysis of the reflection and transmission coefficients. For the analysis ready-made solar cells coated with anti-reflective coating were selected.

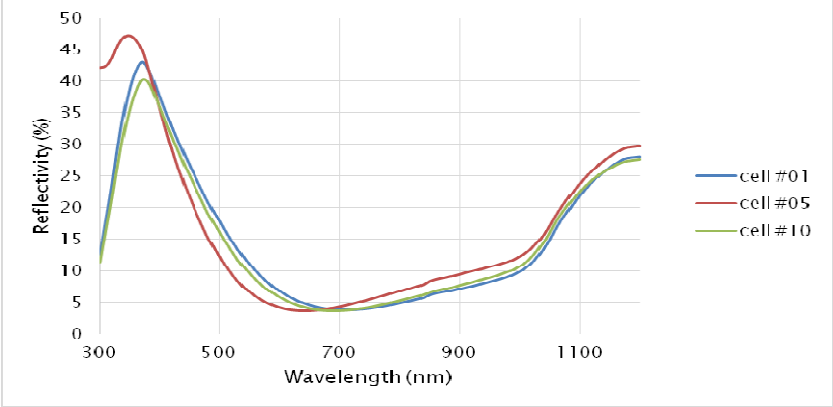

Figure 6. The reflectivity of solar cells at different wavelengths

The graph of the dependence of reflectivity on the wavelength of the incident radiation shows that the solar cells under study have the lowest reflectivity at 660-680 nm, which increases dramatically at a wavelength of more than 700 nm. This, of course, limits the possibility of charge separation in the spectrum and leads to a decrease in efficiency.

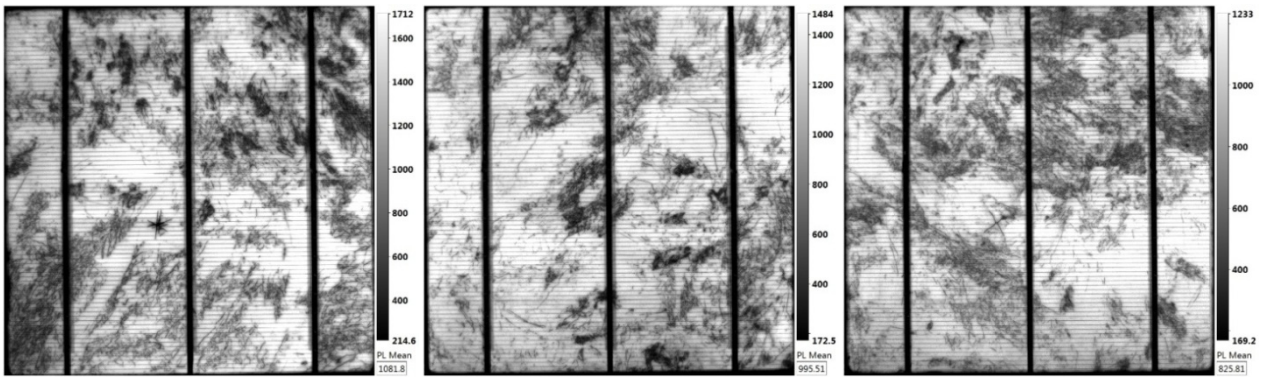

Figure 7. PL-images of solar cells (samples 1, 7, 10) obtained on the Luminescence ImaGing System - Model LIS-R1

Analysis of the obtained PL-images of solar cells (Fig. 7) proved the assumption that the dark zones are the result of the accumulation of defects arising in the process of crystallization and do not arise as a result of the physicochemical operations of the production of solar cells.

To measure the electrical parameters (short circuit current *Isc*, open circuit voltage *Uoc*, filling factor *FF*, maximum power *Pmpp*, efficiency *Eff*), the Solar simulator ORIEL Sol3A CLASS AAA was used. The measurement results are presented in Table.

Table

Electrical Parameters

Internal ID	Voc, [mV]	Isc [mA]	FF [%]	Pmpp [mW]	Eff [%]
cell #02	612,622	31,062	76,105	3788,435	15,567
cell #03	610,715	31,674	76,47	3863,883	15,877
cell #04	607,994	31,706	77,273	3869,516	15,9
cell #05	606,694	31,496	77,546	3846,173	15,804
cell #06	609,721	31,793	77,601	3882,786	15,955
cell #07	609,757	31,81	76,91	3877,285	15,932
cell #09	612,052	31,751	77,436	3881,803	15,951
cell #10	612,596	31,253	75,047	3809,801	15,655
average	**609,7397**	**31,5882**	**76,9674**	**3855,216**	**15,8415**

Thus, the studied samples of photovoltaic devices of Kazakhstan production showed efficiency in the range from 15.6 ÷ 15.9 %. As noted in [9], the average efficiency of mc-Sisolar cells manufactured in the world reaches 19 % in industrial conditions, and in laboratory conditions – about 25 %, therefore, the increase in efficiency of solar cells produced at «Kazakhstan Solar Silicon» LLP is an actual task.

While in the past, most of the research aimed at increasing the efficiency of solar cells was carried out on the front (sunny) side of the cell, recently the photovoltaic industry has shifted its focus to the rear (back) side. Or to be precise, today it is a lot about passivating the rear surface of a solar cell and accordingly modifying the metallization scheme. These rather simple changes adapted to standard solar cell processing entitle the produced silicon slices for a new name – PERC, which stands for Passivated Emitter and Rear Cell. Also, global trends and the power of energy produced in 2016-2020 are shifting towards PERC technology. As it was noted in [10], about 50 % of all the produced «solar» energy by 2020 will be accounted for by the PERC. Therefore, the transition from the standard Al-BSF technology (implemented at «Kazakhstan Solar Silicon» LLP) to PERC technology is a win-win proposition for the development of solar energy in the Republic of Kazakhstan.

The PERC structure is a natural progression from the standard Back Surface Field (BSF) cell architecture. The electrical and optical losses, resulting in reduced efficiency of solar cells, as described above, can be greatly reduced by applying an additional dielectric passivation layer on the rear side. Although the transition to the PERC structure only requires that a few pieces of equipment are added to the standard production line. PERC is gradually becoming the most cost-efficient choice for mass production of cells, and offers a good approach to surpass the 20 % cell efficiency level in mass production.

It is known [11] that record-breaking efficiency values of 22.04 % (for mc-Si PERC solar cells, Jinco) and 23.95 % (for mono-Si PERC solar cells) were not obtained on an industrial scale. However, the graph [11] reflects the potential and progress of this technology, both in the multi and in the mono production.

Processing PERC involves depositing a rear surface passivation film, which is subsequently opened to give way for formation of a rear contact – these are two important additional steps over Kazakhstan solar cell processing (Fig. 8). In addition, the chemical wet-bench based edge isolation step is tweaked for rear polishing. That means texturing accomplished on both sides of the wafer is removed only on the rear side by etching off the pyramid structure. The degree of polishing changes from case to case. Thus, a passivation film deposition system and a film opening system – mainly accomplished with PECVD and lasers – are additional tool sets typically hooked up to standard cell processing lines.

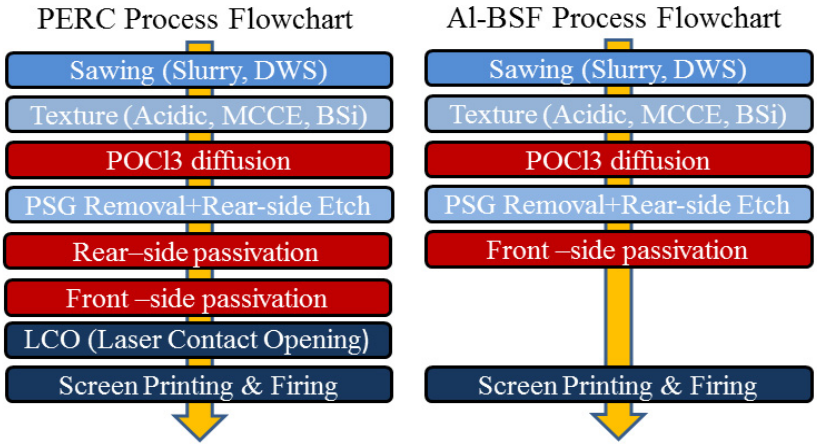

Figure 8. PERC and Al-BSF Process Flowchart

At «Kazakhstan Solar Silicon» LLP, equipment for antireflection coating (silicon nitride) deposition TWYN PECVD is presented. The PECVD process consists in the decomposition of a chemical element under the influence of plasma and temperature into individual elements in the reactor, which then settle to the surface of the wafer and enter into a chemical reaction. As a result, the thinnest film (up to 80 nm) of silicon nitride, which has the required properties, is «grown» on the front surface of the wafer. In [3], it is shown that the PECVD equipment can be modified to apply a rear passivation layer (AlOx + SixNy), while the general principle of deposition remains the same. The easiest way to open the back passivating layer is to use laser technology. Today, the photovoltaic industry has a large number of laser solutions offered by companies such as InnoLas Solutions, Rofin, 3D-Micromac, Schmid or Manz.

Conclusions

Thus, at «Kazakhstan Solar Silicon» LLP it is possible to upgrade Al-BSF standard solar cell production line to a new PERC line, which will allow the enterprise to increase the efficiency of the produced solar cells and be competitive in the global market.

References

1 Department of Economic and Social Affairs, Population Division. World population prospects: the 2018 revision. — New York: United Nations. [Electronic resource]. — Access mode: https://www.un.org/development/desa/publications/2018-revision-of-world-urbanization-prospects.html

2 US Energy Information Administration. International energy outlook 2018 [Electronic resource] — Access mode: https://www.eia.gov/outlooks/ieo/

3 Shravan Chunduri. PERC Solar Cell Technology 2018 [Electronic resource] — Access mode: http://taiyangnews.info/reports/perc-solar-cell-technology-report-2018/

4 Поклонский Н.А. Четырехзондовый метод измерения электрического сопротивления полупроводниковых материалов / Н.А. Поклонский, С.С. Белявский, С.А. Вырко, Т.М. Лапчук // Учеб.-метод. пос. по спецпрактикуму «Физика полупроводниковых материалов и приборов». — Мн.: БГУ, 1998. — С. 7.

5 Jan Schmidt Surface passivation of crystalline silicon solar cells: Present and future / Schmidt Jan, Robby Peibst, Rolf Brendela // Solar Energy Materials and Solar Cells. — 2018. — Vol. 187. — P. 39–54.

6 Kim J.E. Characterization of SiNx: H thin film as a hydrogen passivation layer for silicon solar cells with passivated contacts / J.E. Kim, Se JinPark S.J., Yeon Hyun J.Y., Park H., Bae S., Hyunho K-s. J., et al // Thin Solid Films. — 2019. — Vol. 675. — P. 109–114.

7 José A. Silva Feasibility of Antireflection and Passivation Coatings by Atmospheric Pressure PECVD / Silva José A, Anatolii Lukianov, Remy Bazinette, Danièle Blanc-Pélissier, Julien Vallade, Sylvain Pouliquen, Laura Gaudy, Mustapha Lemiti, Françoise Massines // Energy Procedia. — 2014. — Vol. 55. — P. 741–749.

8 Blacka L.E. Explorative studies of novel silicon surface passivation materials: Considerations and lessons learned / L.E. Blacka, B.W.H. van de Loo, B.Macco, J. Melskens, W.J.H. Berghuis, W.M.M. Kessels // Solar Energy Materials and Solar Cells. — 2018. — Vol. 188. — P. 182–189.

9 Плотников С.В. Исследование технологии производства фотоэлектрических преобразователей / С.В. Плотников, Д.А. Калыгулов, И.А. Клиновицкая // Вестн. ВКГТУ им. Д. Серикбаева. — 2017. — № 4 (78). — С. 67–73.

10 Trend Force. Trend Force Reports PERC Cell's Global Production Capacity to Reach 25GW in 2017, Resulting in Doubling of Total Annual Output [Electronic resource] — Access mode: https://press.trendforce.com/press/20170119–2737.html

11 Shravan Chunduri Taiyang News PERC Solar Cell Technology 2018 [Electronic resource] — Access mode: http://taiyangnews.info/reports/perc-solar-cell-technology-report-2018/

И. Клиновицкая, С. Плотников, Д. Калыгулов, Ф. Лэ

Қазақстандық кремний негізінде фотоэлектрлік түрлендіргіштердің қасиеттерін зерттеу

Күнсәулелік энергетикасын дамыту жалпыәлемдік тренд пен Қазақстан Республикасы Үкіметінің «жасыл» экономикаға көшу жөніндегі бағытқа сәйкес келетіндіктен, фотоэлектрлік түрлендіргіштердің (ФЭТ) қасиеттерін зерттеу өзекті тақырып болып табылады. Меншікті және беттік кедергі, қуаттасушының қызмет ету уақыты, шағылыстыру қабілеті, кванттық тиімділік секілді ФЭТ-нің әртүрлі қасиеттері ФЭТ алынатын тиімділігіне тікелей әсер етеді. Осы жұмыс «күнсәулелік» сапалы қазақстандық кремний негізінде әзірленетін фотоэлектрлік түрлендіргіштерді алу мен оны кешенді зерттеуге арналған. Зерттеуде қысқатолқынды диапазонда (μ-PCD) фотоөткізгіштіктің ыдырауын өлшеу әдісі, беттік және меншікті кедергіні өлшеудің 4 нүктелі әдісі, шағылу, өткізу және фотолюминесценция коэффициенттерін спектрометрлік талдау әдістері, электрондық микроскопия әдістері, сондай-ақ вольтамперлік сипаттамаларын талдау әдістері қолданылған. ФЭТ өндірісінің меңгеріп алынған әдістері сипатталған. Al-BSF стандартты желісін PERC желісіне дейін модификациялау ұсынылды.

Кілт сөздер: фотоэлектрлік түрлендіргіштер, күнсәулелік элементтер, кремний, Al-BSF құрылымы, PERC құрылымы, күнсәулелік энергетика.

И. Клиновицкая, С. Плотников, Д. Калыгулов, Ф. Лэ

Исследование свойств фотоэлектрических преобразователей на основе казахстанского кремния

Исследование свойств фотоэлектрических преобразователей (ФЭП) является актуальной темой, поскольку развитие солнечной энергетики соответствует общемировому тренду и взятому курсу Правительства Республики Казахстан по переходу на «зеленую» экономику. Различные свойства ФЭП, такие как удельное и поверхностное сопротивление, время жизни носителей заряда, отражательная способность, квантовая эффективность непосредственно влияют на эффективность получаемых ФЭП. Настоящая работа посвящена получению и комплексному исследованию фотоэлектрических преобразователей, изготавливаемых на основе казахстанского кремния «солнечного» качества. В исследовании применены метод измерения распада фотопроводимости в микроволновом диапазоне (μ-PCD), 4-зондовый метод измерения поверхностного и удельного сопротивления, методы спектрометрического анализа коэффициентов отражения, пропускания и фотолюминесценции, метод растровой электронной микроскопии, а также методы анализа вольтамперных характеристик. Описаны освоенные методы производства ФЭП. Предложена модификация стандартной линии Al-BSF до линии PERC.

Ключевые слова: фотоэлектрические преобразователи, солнечные элементы, кремний, Al-BSF структура, PERC структура, солнечная энергетика.

References

1 Department of Economic and Social Affairs, Population Division. (2018). *World population prospects: the 2018 revision.* New York: United Nations. Retrieved from https://www.un.org/development/desa/publications/2018-revision-of-world-urbanization-prospects.html

2 US Energy Information Administration. (2018). *International energy outlook 2018.* Retrieved from https://www.eia.gov/outlooks/ieo/

3 Shravan Chunduri (2018). *PERC Solar Cell Technology 2018.* Retrieved from http://taiyangnews.info/reports/perc-solar-cell-technology-report-2018/

4 Poklonsky, N.A., Belyavsky, S.S., Vyrko, S.A., & Lapchuk, T.M. (1998). *Chetyrekhzondovyi metod izmereniia elektricheskoho soprotivleniia poluprovodnikovykh materialov* [*Four-probe method for measuring the electrical resistance of semiconductor materials*]. Minsk: Belarusian State University [in Russian].

5 Schmidt, J., Peibst, R., & Brendela, R. (2018). Surface passivation of crystalline silicon solar cells: Present and future. *Solar Energy Materials and Solar Cells*, *Vol. 187,* 39–54. DOI: https://doi.org/10.1016/j.solmat.2018.06.047

6 Kim, J.E., Se JinPark, S.J., Yeon Hyun, J.Y., Park, H., Bae, S., & Hyunho, K-s., J., et al. (2019). *Characterization of SiNx: H thin film as a hydrogen passivation layer for silicon solar cells with passivated contacts. Thin Solid Films, Vol. 675,* 109–114. DOI: https://doi.org/10.1016/j.tsf.2019.02.016

7 Silva, J.A., Lukianov, A., Bazinette, R., Blanc-Pélissier, D., Vallade, J., & Pouliquen, S., et al. (2014). *Feasibility of Antireflection and Passivation Coatings by Atmospheric Pressure PECVD. Energy Procedia, Vol. 55,* 741–749. DOI: https://doi.org/10.1016/j.egypro.2014.08.054

8 Blacka L.E., van de Loo B.W.H., Macco B., Melskens J., Berghuis W.J.H., & Kessels W.M.M. (2018). Explorative studies of novel silicon surface passivation materials: Considerations and lessons learned. Solar Energy Materials and Solar Cells, Vol. 188, 182–189. DOI: https://doi.org/10.1016/j.solmat.2018.07.003

9 Plotnikov, S.V., Kalygulov, D.A., & Klinovitskaya, I.A. (2017). Issledovanie proizvodstva fotoelektricheskiкh preobrazovatelei [Research of the production technology of photovoltaic cells]. Vestnik VKHTU – Bulletin of EKSTU, 4 (78), 67-73 [in Russian].

10 Trend Force. (2017). Trend Force Reports PERC Cell's Global Production Capacity to Reach 25GW in 2017, Resulting in Doubling of Total Annual Output. press.trendforce.com. Retrieved from https://press.trendforce.com/press/20170119-2737.html

11 Shravan Chunduri. (2018). Taiyang News PERC Solar Cell Technology 2018. *taiyangnews.info.* Retrieved from http://taiyangnews.info/reports/perc-solar-cell-technology-report-2018/

DOI 10.31489/2019Ph 3/43-51

UDC 621.382

V.V. Kukharchuk[1], V.Y. Kucheruk[1], S.Sh. Katsyv[1],
V.F. Hraniak[1], D.Zh. Karabekova[2], A.K. Khassenov[2]

[1]Vinnitsa National Technical University, Ukraine;
[2]Ye.A. Buketov Karaganda State University, Kazakhstan
(E-mail: titanxp2000@ukr.net)

Conditions for «deterministic chaos» phenomenon occurrence in a non-linear rl-diode electric circuit of sinusoid current

In this work, the phenomenon of «deterministic chaos» in a nonlinear RL-diode electrical circuit of a sinusoidal current was investigated. The diode is represented by an equivalent circuit, which in the general case includes a nonlinear resistor and two nonlinear capacitances – barrier and diffusion. With certain ratios of the frequency of the current and the parameters of the circuit, the transition process for the period of oscillation of the input voltage hasn't time to finish. In this case, at the beginning of each period there is a residual voltage on the capacitances, that is, each new cycle of the transition process has non-zero initial conditions. It is noted that the residual voltage in each period is different; therefore, the current in the circuit in each period is also different. Thus, in this case, a continuous transition occurs, the parameters of which are chaotic. The simulation of the phenomenon of «deterministic chaos» was carried out in the environment of the MicroCap circuit simulation program. During the simulation for each type of diode, the set of circuit parameters f, R, L (frequency, load resistance, inductance) was divided into two subsets – a subset for which the transition process during the oscillation period of the input voltage has time to finish (the residual voltage on the capacitance is almost zero) and the mode of operation of the circuit can be considered deterministic, and a subset for which the transient process during the oscillation period of the input voltage doesn't attenuate (the residual voltage on the capacitance is significantly different from zero) and the mode of operation of the circuit can be considered chaotic. As a result, the recommended sets of parameters of the circuit for designing the generators of chaotic oscillations were determined.

Key words: deterministic chaos, barrier capacitance, diffusion capacitance, residual stress, initial conditions, oscillation generator.

Introduction

When creating parametric resistive transducers that would allow for required metrological characteristics (particularly, resolution), one should quite frequently transform extremely insignificant changes in output resistance, for instance, during tensiometric measurements.

This in turn results in random interferences' amplification at a desired signal, as a consequence of which a random measurement error grows [1, 2]. That is why raising the sensitivity of resistive transducers while ensuring a low level of random noises comprises a crucial task.

One of the methods to solve this task consists in the use of *RL*-diode generators of chaotic oscillations [3–6].

The paper [7] presented the analysis of the reasons for chaotic oscillations in *RL*-diode circuits with required calculations carried out.

The objective of this paper is to devise the algorithm for determination of circuit parameters in order to devise the generators of chaotic oscillations.

Results of previous studies

It was noted above that detailed analysis of the reasons for chaotic oscillations' emergence in *RL*-diode circuits was carried out in paper [7]. In this sub-section, we are only setting forth the basic concepts of this analysis.

The simplest diagram chaotic oscillations' generator is presented by a quadrupole, at the output of which a resistor is switched on (Fig. 1).

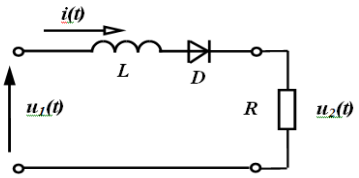

Figure 1. The simplest diagram of chaotic oscillations' generator

According to [8], the diode equivalent circuit in a small signal mode (in the most common case) is shown in Figure 2.

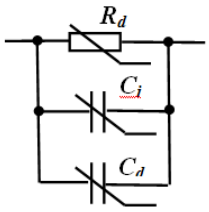

Figure 2. Diode equivalent circuit in a small signal mode

According to this circuit, a diode represents a parallel connection between non-linear resistor R_d and two non-linear capacities – a barrier C_j and a diffusion C_d one.

The barrier capacity is determined using the formula:

$$C_j = \frac{C_{j0}}{\left(1-\frac{U}{U_D}\right)^n}, \quad (1)$$

where C_{j0} – barrier capacity at the diode's zero voltage; U – the diode's current voltage; U_D – the diode's diffusion voltage; n – the technological coefficient ranging within $(\frac{1}{3}..\frac{2}{3})$.

The diffusion capacity is determined as:

$$C_d = \frac{\tau_B I_S}{mU_T} e^{\frac{U}{mU_T}}, \quad (2)$$

where I_S – the diode's thermal current; τ_B – the lifetime of minority charge carriers; U – the diode's current voltage; U_T – the diode's thermal stress; m – emission factor.

Please note that in the direct voltage mode, given that $U \geq U_D$ the barrier capacity may be disregarded. In the back voltage mode, the diffusion capacity may be disregarded.

The equivalent circuit of the simplest generator of chaotic oscillations is shown in Figure 3.

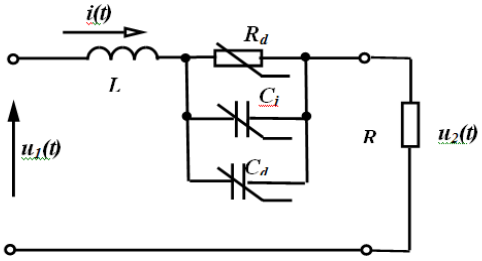

Figure 3. Equivalent circuit of chaotic oscillations' generator

This circuit contains three non-linear elements at once: resistor R_d, barrier capacity C_j and diffusion capacity C_d. Please note that both resistor resistance and capacities depend on the diode voltage.

It's as if the current flowing through resistor R_d is $i_1(t)$, the one flowing along capacity C_j being $i_2(t)$, and the one flowing along capacity C_d is $i_3(t)$. Since the voltage at the capacities and at resistor R_d is the same, we designate it as $u_C(t)$.

Let us compose an equation system under Kirchhoff's laws for the equivalent circuit (Fig. 3).

$$\begin{aligned} & i(t) = i_1(t) + i_2(t) + i_3(t) \\ & L\frac{di(t)}{dt} + Ri(t) + R_d(u_C(t))i_1(t) = u_1(t) \\ & R_d(u_C(t))i_1(t) = u_C(t) \\ & i_2(t) = C_j(u_C(t))\frac{du_C(t)}{dt} \\ & i_3(t) = C_d(u_C(t))\frac{du_C(t)}{dt} \end{aligned} \tag{3}$$

Since $i_1(t) = \dfrac{u_C(t)}{R_d(u_C(t))}$ and $i(t) = \dfrac{u_C(t)}{R_d(u_C(t))} + C_j(u_C(t))\dfrac{du_C(t)}{dt} + C_d(u_C(t))\dfrac{du_C(t)}{dt}$, the series of algebraic transformations may be followed by the record:

$$\begin{aligned} & \left(LC_j(u_C(t)) + LC_d(u_C(t))\right)\frac{d^2u_C(t)}{dt^2} + \\ & + \left(\frac{L}{R_d(u_C(t))} + RC_j(u_C(t)) + RC_d(u_C(t))\right)\frac{du_C(t)}{dt} + \\ & + \left(\frac{R}{R_d(u_C(t))} + 1\right)u_C(t) = u_1(t). \end{aligned} \tag{4}$$

The resultant expression for non-linear second-order differential equation, to which the circuit operation mode corresponds (Fig. 3), with due account for expressions (1) and (2), looks as follows

$$\begin{aligned} & \left(L\frac{C_{j0}}{\left(1 - \dfrac{u_C(t)}{U_D}\right)^n} + L\frac{\tau_B I_S}{mU_T}e^{\frac{u_C(t)}{mU_T}}\right)\frac{d^2u_C(t)}{dt^2} + \\ & + \left(\frac{L}{R_d(u_C(t))} + R\frac{C_{j0}}{\left(1 - \dfrac{u_C(t)}{U_D}\right)^n} + R\frac{\tau_B I_S}{mU_T}e^{\frac{u_C(t)}{mU_T}}\right)\frac{du_C(t)}{dt} + \\ & + \left(\frac{R}{R_d(u_C(t))} + 1\right)u_C(t) = u_1(t). \end{aligned} \tag{5}$$

Let us solve this differential equation using the operator method in general terms.

The operator equation of Kirchhoff's law II for this circuit looks as follows:

$$I(s)\left(R + sL + \frac{R_d(u_C)\dfrac{1}{sC_j(u_C)}\dfrac{1}{sC_d(u_C)}}{R_d(u_C)\dfrac{1}{sC_j(u_C)} + R_d(u_C)\dfrac{1}{sC_d(u_C)} + \dfrac{1}{sC_j(u_C)}\dfrac{1}{sC_d(u_C)}}\right) = E(s). \tag{6}$$

Then the operator presentation of circuit voltage is defined as follows:

$$I(s)=\frac{E(s)}{\left(R+sL+\frac{R_d(u_C)\frac{1}{sC_j(u_C)}\frac{1}{sC_d(u_C)}}{R_d(u_C)\frac{1}{sC_j(u_C)}+R_d(u_C)\frac{1}{sC_d(u_C)}+\frac{1}{sC_j(u_C)}\frac{1}{sC_d(u_C)}}\right)}. \quad (7)$$

It is evident that, as a consequence of a considerable non-linearity of this expression, it is impossible to obtain the original of circuit current $i(t)$ in general terms.

Considering the fact that diode parameters do significantly differ from direct and inverse voltage, it would be advisable to analyze the circuit mode using a modified method of lump-linear approximation using transient characteristics and Duhamel's integral.

Iteration algorithm of calculation may be formulated as follows:

1. Let us divide the curve of input sinusoid voltage into equal time intervals, and match each of them with particular sections of BAX diode (i.e. $R_d(u_C)$ and particular values $C_j(u_C)$ and $C_d(u_C)$.

2. For each linearized section of BAX and $C_j(u_C)$ and $C_d(u_C)$ values, the operator presentation of the circuit's transient characteristics in relation to its current is defined as follows:

$$h_i(s)=\frac{1}{s\left(R+sL+\frac{R_d(u_C)\frac{1}{sC_j(u_C)}\frac{1}{sC_d(u_C)}}{R_d(u_C)\frac{1}{sC_j(u_C)}+R_d(u_C)\frac{1}{sC_d(u_C)}+\frac{1}{sC_j(u_C)}\frac{1}{sC_d(u_C)}}\right)}= \quad (8)$$

$$=\frac{sR_d(u_C)C_d(u_C)+sR_d(u_C)C_j(u_C)+1}{s\left(sR_d(u_C)C_d(u_C)R+sR_d(u_C)C_j(u_C)R+R+s^2LR_d(u_C)C_d(u_C)+s^2LR_d(u_C)C_j(u_C)+sL+R_d(u_C)\right)}.$$

3. Let us find out the original of transient characteristic $h_i(t)$ using the decomposition theorem, for which purpose the denominator's root should be determined in the first place:

$$s\left[s^2\left(LR_d(u_C)C_d(u_C)+LR_d(u_C)C_j(u_C)\right)+s\left(R_d(u_C)C_d(u_C)R+R_d(u_C)C_j(u_C)R+L\right)+R+R_d(u_C)\right]=0. \quad (9)$$

Equation (9) has three roots:

$$s_1=0,\ s_{2,3}=\frac{-b\pm\sqrt{b^2-4ac}}{2a},$$

where – $a=\left(LR_d(u_C)C_d(u_C)+LR_d(u_C)C_j(u_C)\right),\ b=\left(R_d(u_C)C_d(u_C)R+R_d(u_C)C_j(u_C)R+L\right),\ c=R+R_d(u_C)$.

Denominator derivative:

$$\left[s^3\left(LR_d(u_C)C_d(u_C)+LR_d(u_C)C_j(u_C)\right)+s^2\left(R_d(u_C)C_d(u_C)R+R_d(u_C)C_j(u_C)R+L\right)+s\left(R+R_d(u_C)\right)\right]=$$
$$3s^2\left(LR_d(u_C)C_d(u_C)+LR_d(u_C)C_j(u_C)\right)+2s\left(R_d(u_C)C_d(u_C)R+R_d(u_C)C_j(u_C)R+L\right)+\left(R+R_d(u_C)\right).$$

Therefore, the original of the transient characteristic:

$$h_i(t)=\frac{1}{R+R_d(u_C)}+$$
$$+\frac{s_2R_d(u_C)C_d(u_C)+s_2R_d(u_C)C_j(u_C)+1}{3s_2^2\left(LR_d(u_C)C_d(u_C)+LR_d(u_C)C_j(u_C)\right)+2s_2\left(R_d(u_C)C_d(u_C)R+R_d(u_C)C_j(u_C)R+L\right)+\left(R+R_d(u_C)\right)}e^{s_2t}+ \quad (10)$$
$$\frac{s_3R_d(u_C)C_d(u_C)+s_3R_d(u_C)C_j(u_C)+1}{3s_3^2\left(LR_d(u_C)C_d(u_C)+LR_d(u_C)C_j(u_C)\right)+2s_3\left(R_d(u_C)C_d(u_C)R+R_d(u_C)C_j(u_C)R+L\right)+\left(R+R_d(u_C)\right)}e^{s_3t}.$$

4. Let us find out the value of current at the end of each time interval with the aid of Duhamel's integral using the formula:

$$i(t_k) = i(t_{k-1}) + \int_{t_{k-1}}^{t_k} \frac{de(\tau)}{d\tau} h_k(t-\tau)d\tau. \quad (11)$$

5. Let us determine the diode voltage using the approximation formula:

$$u_{dk} = u(t_{k-1}) - \left(L\frac{i(t_k) - i(t_{k-1})}{t_k - t_{k-1}} + i(t_k)R \right), \quad (12)$$

after which $R_d(u_C), C_d(u_C), C_j(u_C)$ parameters should be updated.

6. Let us go back to the algorithm's station 2 and repeat the calculation until u_{dk} value has almost no difference from the previous iteration.

Based on the above algorithm, paper [7] presented a cycle of numeric calculations in MathCAD environment. These calculations proved that, under particular correlations of frequency and circuit parameters, the period of input voltage fluctuations will not be enough for the transient process to come to its end, that is why residual voltage is available at capacities in the beginning of each period, meaning that each new cycle of transient process has non-zero initial conditions. Such being the case, an undamped transient process takes place, with the parameters of this process being of chaotic nature.

It has also been established that transition from a deterministic process to a chaotic one takes place gradually rather than in a leap, meaning that, with the input voltage frequency growth, the residual voltage at capacities will increase quite slowly.

Hence, the triggering event for a chaotic transient process may be formulated as follows:

– in the beginning of each (except for the first one) oscillation cycle, non-zero voltage is present at capacities;

– in the beginning of any two different oscillation cycles, capacity voltages differ from one another.

At the same time, numeric calculations (even in MathCAD environment) are quite a labor-consuming procedure.

Since this paper's objective is determination of the circuit's total recommended parameters for designing of chaotic oscillations' generators, which requires a large volume of calculations, a much quicker simulation of «deterministic chaos» was carried out in the circuit (Fig. 3) using MicroCap general-circuit simulation software.

Results of «deterministic chaos» simulation in a non-linear rl-diode electric circuit of sinusoid current

Such presentation of circuit model (Fig. 3) is shown in Fig. 4.

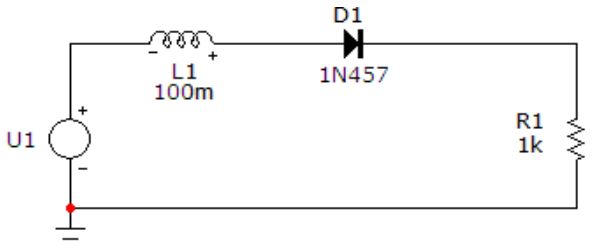

Figure 4. Model of chaotic oscillations' generator

Let us simulate the dependence between the output and input voltage, i.e. in MicroCap environment we obtain $u_2(t) = \psi(u_1(t))$ function for different values of output voltage frequency f with circuit parameters $L1 = 100$ mH, $R1 = 1$ kOhm and diode type 1N457. Please note that $u_2(t) = Ri(t)$.

The diagrams of this dependency are shown in Figures 5–7.

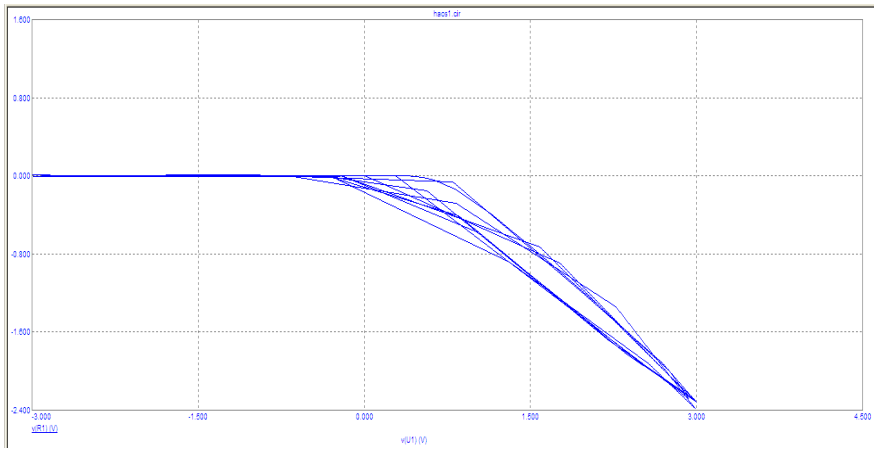

Figure 5. Diagram of function $u_2(t)=\psi(u_1(t))$ at 100 Hz frequency

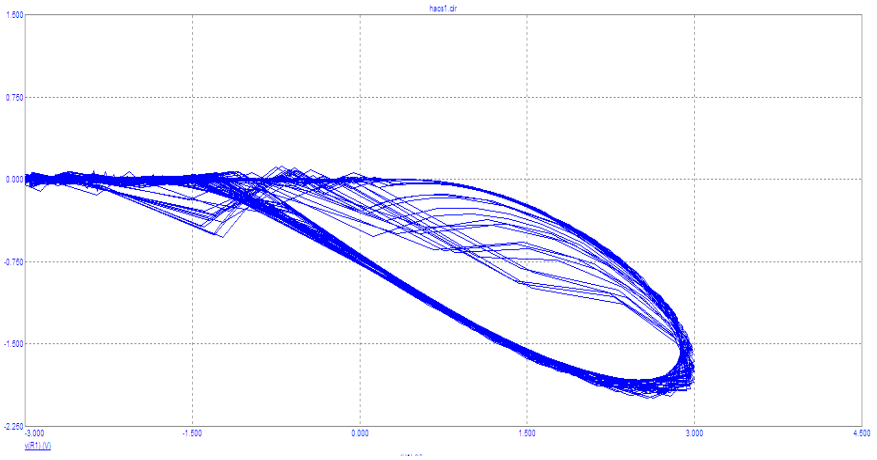

Figure 6. Diagram of function $u_2(t)=\psi(u_1(t))$ at 1 kHz frequency

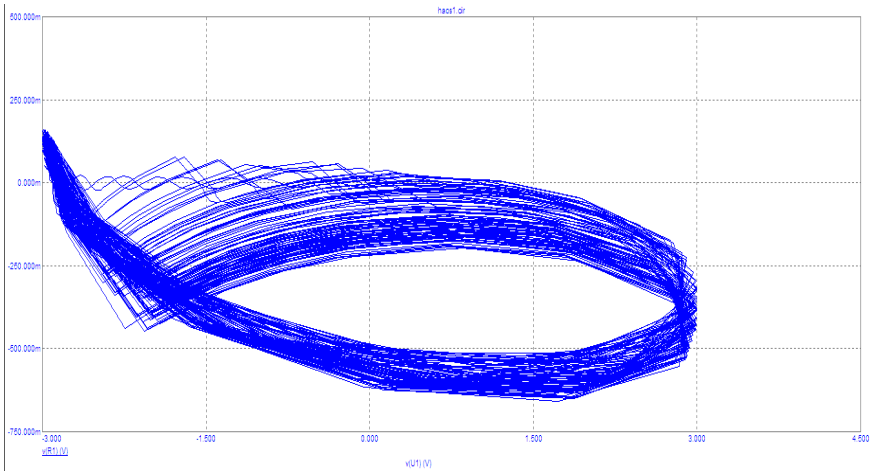

Figure 7. Diagram of function $u_2(t)=\psi(u_1(t))$ at 10 kHz frequency

It follows from diagram (Fig. 5) that, with the input voltage frequency of 100 Hz, the circuit's transient process almost fades, and function $u_2(t)=\psi(u_1(t))$ may be deemed deterministic.

With the input voltage frequency of 1 kHz (Fig. 6), the circuit's transient process stops fading, and function $u_2(t)=\psi(u_1(t))$ behaves in a chaotic manner. At the same time, the amplitude of chaotic oscillations is insignificant.

Much better result was obtained with the frequency of 10 kHz (Fig. 7), where the amplitude of chaotic oscillations is already significant.

Simulated in the paper were numerous options of circuits of chaotic oscillations' generator with various types of diodes and circuit parameters' values.

At first, simulations were made for generator operation modes with widespread diode types and equal circuit parameters ($L1 = 100$ mH, $R1 = 1$ kOhm) with recommended generator frequencies determined, under which the amplitude of chaotic oscillations is significant (Fig. 7). Simulation results are summarized in Table 1.

Table 1

Dependence between the generator's recommended frequency and diode types

Diode types	1N456 – 1N486	1N625 – 1N629	1N658 – 1N661	1N746 – 1N749	1N750 – 1N754	1N755 – 1N759
Recommended frequency, kHz	10	25	140	100	120	150

It follows from Table 1 that, with equal circuit parameters, significant amplitude of chaotic oscillations may be reached at the lowest frequency of 10 kHz for diode types 1N456 – 1N486 only.

Hereinafter, these diodes and this frequency underwent studies, during which determined were the ranges of the generator's optimal parameters that ensure an acceptable amplitude of chaotic oscillations. Study results are summarized in Table 2.

Table 2

Optimal generator parameters

Inductance L1, mH	10 – 100	150 – 300	350 – 500
Resistor R1, kOhm	0,01 – 0,4	0,6 – 2	2 – 4

Conclusions

1. This is a non-linear RL-diode electric circuit of sinusoid current, where an unfading transient process takes place, which, under given relationship between the input voltage frequency and circuit parameters may be deemed having a chaotic nature.

2. The transition from a deterministic process to a chaotic one takes place gradually rather than in a leap, that is why chaotic oscillations' generators require a significant amplitude (for a number of technical purposes, the amplitude of a chaotic component must exceed a deterministic one).

3. When designing such generators, it is advisable to use diodes of 1N456 – 1N486 types, since they ensure the lowest frequency (about 10 kHz), at which acceptable amplitude of chaotic oscillations is present.

References

1 Belik M. Usage of data acquisition device NI PCI-6221 for power engineering applications // Proceedings of the 2018 19th International Scientific Conferenceon Electric Power Engineering (EPE). — Piscataway: IEEE, 2018. — P. 410–414.

2 Belik M. Automated Data Acquisition For Electrical Power Engineering // Proceedings of the 14th International Scientific Conference EEE «Energy-Ecology-Economy 2018», 2018. — P. 124–128.

3 Kolpakova L.V. Chaotic-oscillator measuring devices / L.V.Kolpakova // Measuring and computing equipment in technological processes, 2011. — No. 2. P. — 101–104.

4 Kucheruk V. Generator oscylacji chaotycznych o układzie RL-dioda jako przetwornik rezystancja-napięcie / V. Kucheruk, Z.L. Warsza, V. Sevastyanow, W. Mankowska // Przegląd elektrotechniczny. — ISSN 0033–2097. — R. 89 NR 10/2013.

5 Alam J. Chasing Chaos with an RL-Diode Circuit / J. Alam, S. Anwar LUMS School of Science and Engineering. — 2010. — March 24.

6 Azzonz A. Orbitsofthe RL-Diode / A. Azzonz, M. Hasler // Circuits and Systems. — 1990. — No. 11. — Vol. 37. — P. 1330–1338.

7 Volodymyr Kucheruk. Deterministic chaos in RL-diode circuits and its application in metrology / Volodymyr Kucheruk // Proc. SPIE 10031, Photonics Applicationsin Astronomy, Communications, Industry, and High-Energy Physics Experiments. — 2016. — No. 9.

8 Уве Хэндфорд. Аналоговая электроника. Основы, расчет, моделирование. — М.: Техносфера, 2008. — 472 с.

В.В. Кухарчук, В.Ю.Кучерук, С.Ш. Кацыв,
В.Ф. Граняк, Д.Ж. Карабекова, А.К. Хасенов

Синусоидалды токтың сызықты емес диодэлектрлік тізбегінде «детерминирленген хаос» құбылысының пайда болу шарттары

Мақалада синусоидалды токтың сызықты емес RL-диодты электр тізбегіндегі «детерминирленген хаос» құбылысы зерттелді. Диод алмастыру схемасымен берілген, ол жалпы жағдайда сызықты емес резистор және барьерлік және диффузиялық – екісызықты емес сыйымдылықты қамтиды. Ток жиілігінің және тізбек параметрлерінің белгілі бір арақатынасы кезінде кіріс кернеуінің тербеліс кезеңінде өтпелі процестің аяқталуы іске аспайды. Бұл жағдайда әрбір кезеңнің басында сыйымдылықтарда қалдық кернеу болады, яғни өтпелі процестің әрбір жаңа циклінің нөлдік емес бастапқы жағдайлары бар. Әр кезеңдегі қалдық кернеу әртүрлі, сондықтан әр кезеңдегі тізбектегі ток та басқа. Осылайша, бұл жағдайда параметрлері хаостық сипатта болатын өшпейтін өтпелі процесс болады. «Детерминирленген хаос» құбылысын модельдеу MicroCap схемотехникалық модельдеу бағдарламасының ортасында жүргізілді. Диодтың әрбір түрі үшін модельдеу кезінде F, R, L (жиілік, жүктеме кедергісі, индуктивтілік) тізбектерінің көптеген параметрлері екі ішкі жиынға бөлінді – кіріс кернеуінің тербеліс кезеңінде өтпелі процесс аяқталатын ішкі жинақта (яғни сыйымдылықтардағы қалдық кернеу іс жүзінде нөлдік болып табылады), ал тізбектің жұмыс режимі детерминирленген деп санауға болады және ішкі жинаққа ол үшін өтпелі процесс кіріс кернеуінің тербеліс кезеңінде өшпейді (яғни сыйымдылықтардағы қалдық кернеу нөлден айтарлықтай өзгеше) және тізбектің жұмыс режимін хаостық деп санауға болады. Осылайша, хаостық тербеліс генераторларын құрастыру үшін тізбек параметрлерінің ұсынылған жиынтығы анықталды.

Кілт сөздер: детерминирленген хаос, барьерлік сыйымдылық, диффузиялық сыйымдылық, қалдық кернеу, бастапқы шарттар, тербеліс генераторы.

В.В. Кухарчук, В.Ю. Кучерук, С.Ш. Кацыв,
В.Ф. Граняк, Д.Ж. Карабекова, А.К. Хасенов

Условия возникновения явления «детерминированный хаос» в нелинейной диодэлектрической цепи синусоидального тока

В статье исследовалось явление «детерминированный хаос» в нелинейной RL-диодной электрической цепи синусоидального тока. Диод представлен схемой замещения, которая в общем случае включает в себя нелинейный резистор и две нелинейные ёмкости – барьерную и диффузионную. При определенных соотношениях частоты тока и параметров цепи переходный процесс за период колебаний входного напряжения не успевает закончиться. В этом случае в начале каждого периода на ёмкостях присутствует остаточное напряжение, то есть каждый новый цикл переходного процесса имеет ненулевые начальные условия. Отметим, что остаточное напряжение в каждом периоде разное, поэтому ток в цепи в каждом периоде также разный. Таким образом, в этом случае происходит незатухающий переходный процесс, параметры которого носят хаотический характер. Моделирование явления «детерминированный хаос» проводилось в среде программы схемотехнического моделирования MicroCap. Во время моделирования для каждого типа диода множество параметров цепи f, R, L (частота, сопротивление нагрузки, индуктивность) разделялось на два подмножества – на подмножество, для которого переходный процесс за период колебаний входного напряжения успевает закончиться (т.е. остаточное напряжение на ёмкостях является практически нулевым), а режим работы цепи можно считать детерминированным, и на подмножество, для которого переходный процесс за период колебаний входного напряжения не затухает (т.е. остаточное напряжение на ёмкостях существенно отличается от нуля) и режим работы цепи можно считать хаотическим. Таким образом, были определены рекомендованные совокупности параметров цепи для конструирования генераторов хаотических колебаний.

Ключевые слова: детерминированный хаос, барьерная емкость, диффузионная емкость, остаточные напряжения, начальные условия, генератор колебаний.

References

1 Belik, M. (2018). Usage of data acquisition device NI PCI-6221 for power engineering applications. *Proceedings of the 2018 19th International Scientific Conferenceon Electric Power Engineering (EPE)*. (pp. 410–414). Piscataway: IEEE.

2 Belik, M. (2018). Automated Data Acquisition For Electrical Power Engineering. *Proceedings of the 14th International Scientific Conference EEE «Energy-Ecology-Economy*. (pp. 124–128).

3 Kolpakova, L.V. (2011). Chaotic-oscillator measuring devices. *Measuring and computing equipment in technological processes, No. 2,* 101–104.

4 Kucheruk, V., Warsza, Z.L., Sevastyanow, V., & Mankowska, W. (2013). Generator oscylacji chaotycznych o układzie RL-dioda jako przetwornik rezystancja-napięcie. *Przegląd elektrotechniczny*, ISSN 0033–2097, R. 89 NR 10.

5 Alam, J.L., & Anwar, S. (2010). Chasing Chaos with an RL-Diode Circuit. LUMS School of Science and Engineering.

6 Azzonz, A., & Hasler, M. (1990). Orbitsofthe RL-Diode. *Circuits and Systems, Vol. 37, No. 11,* 1330–1338.

7 Volodymyr, Kucheruk, et al., (2016). Deterministic chaos in RL-diode circuits and its application in metrology. *Proc. SPIE 10031, Photonics Applicationsin Astronomy, Communications, Industry, and High-Energy Physics Experiments, No. 9.*

8 Uve, Naundford (2008). *Analogovaia elektronika. Osnovy, raschet, modelirovanie [Analog electronics. Basics, calculation, modeling]*. Moscow: Technosfera [in Russian].

DOI 10.31489/2019Ph 3/52-58
UDC 539.219.3

E.P. Shevchuk[1], D.K. Nurumkanov[1], B.M. Muratbekov[1], B. Ahmetzhanov[1], V.A. Plotnikov[2]

[1]S. Amanzholov East Kazakhstan State University, Ust-Kamenogorsk, Kazakhstan;
[2]Altay State University, Barnaul, Russia
(E-mail: evgeniya-shevchu@mail.ru)

Surface modification of steel 20 by the method of chemical-thermal treatment by annealing in a muffle furnace

The article is devoted to the current problem related to the hardening of the surface layers of metal materials, including steel parts. The authors of the article describe the methods of chemical and thermal treatment of surface layers of materials to effectively improve the durability of machine parts and tools operating under various conditions of wear, at high temperature and force effects. The method of saturation of samples of iron plates by means of coating them with boron-containing mixtures in different volume proportions and their subsequent annealing in a muffle furnace is considered. The results of studies of the microhardness and thickness of the diffusion layer are given.

Keywords: steel 20, saturating mixture, boration, diffusion layer, microhardness, chemical-thermal treatment, muffle furnace.

Introduction

At the present stage of development of technology it is an urgent task of developing methods of strengthening the surface layers of metal materials, including steel parts with qualitatively new high properties that reduce the metal content of products and provide resource saving. Changing and complicating the operating conditions of machines, components and assemblies requires constant improvement of materials and modernization of manufacturing technologies.

Much attention is paid to the development of surface hardening technologies. This is due to a new approach to assessing the role of the material in ensuring the structural strength of products, according to which it is the state of the surface layers of materials largely determines the performance properties of parts.

Scientific and technical progress in such industries as engineering, transport, machine-tool industry and other high-tech sectors of the economy is largely associated with the improvement of the materials used in the direction of obtaining a set of performance properties.

Fundamentally new high physical, mechanical and operational properties of products can be achieved by purposeful modification of the surface by doping with various elements or their compositions using highly concentrated energy sources, including metallization, i.e. diffusion saturation of metals during furnace heating. The advantage of this method is the possibility of non-contact heating of the surface of the processed material. It is carried out at high temperatures (up to 1420°C) while the thickness of the modified layer does not exceed 100 microns and the concentration of alloying elements in it, and therefore the hardness decreases sharply from the surface deep into the material.

Chemical-thermal treatment, changing the composition, structure, and, consequently, the properties of the surface layers of materials, is an effective way to increase the durability of machine parts and tools operating under different wear conditions, at high temperature and force effects [1, 2].

In this regard, relevant are: the study of processes occurring in the near-surface layer of carbon steels, when alloying using furnace heating. Development of new combined technologies that can not only significantly improve the physical, mechanical and operational properties of machine parts and tools by activating the maximum possible number of reinforcing mechanisms, but also to replace expensive alloy steel at a cheaper and affordable, to save energy and consumables, reduce the duration of processes and improve processing efficiency compared to traditional methods of hardening of structural and tool steels.

The aim of the work was to study the surface of ST20 after chemical and thermal treatment.

The use of the SNOL 30/1300 muffle laboratory furnace made it possible to ensure uniform and rapid heating of samples from 50°C to 1300°C.

Research methods

To study the kinetics of the growth of boride layers on the surface of the samples of iron plates, saturation was carried out with the help of coating and circular heating in the furnace. Boron paste contained a mixture of iron and boron powders in different volume proportions (25 % Fe-75 % H_3BO_3, 50 % Fe-50 % H_3BO_3, 75 % Fe-25 % H_3BO_3), ammonium hydroxide, activated carbon and liquid glass [3; 387]. Previously, a similar coating composition was not applied when hardening the surface layers of steels of this class by boriding. What is a novelty in research?

Surface boration was carried out at a temperature of ≈1000 °C for 5 minutes.

Weight and volume of reagents: all data are obtained in accordance with the surface area of the treated surface of the iron plate.

Liquid glass – Na_2SiO_3 (concentrate) – 1 ml;

20 % p-p of liquid glass – 1 ml;

Ammonium hydroxide – NH_4OH – 1 ml.

Chemical processes in boration: liquid glass when mixed with a mixture of boric acid and iron powders forms a gel-like mass.

At a temperature of 50 °C, the NH4OH activator decomposes into ammonia in the form of gas and water ($NH_4OH \rightarrow NH_3\uparrow + H_2O \rightarrow N\uparrow + H_2O\uparrow + O_2\uparrow$), at 235 °C , boric acid decomposes into boron oxide and water ($2H_3BO_3 \rightarrow B_2O_3 + 3H_2O$). The introduction of an activator in the form of ammonium hydroxide and carbon into the coating makes it possible to ensure its reliable adhesion of the saturating charge to the hardened surface.

Boron oxide reacts with the coal and produces pure boron, and carbon monoxide ($2B_2O_3 + 3C \rightarrow 4C + 3CO_2$). In the temperature range from 500 °C to 1000 °C ammonia decomposes into nitrogen and hydrogen in the form of gas and acts as a boron carrier in the depth of the surface layer of the iron plate, forming a vast diffusion zone of iron borides. Water under high temperature is transferred into oxygen and hydrogen gas and evaporates ($2H_3BO_3 + 2Fe + 2NH_4OH + 2C \rightarrow Fe_2B + IN + 2N\uparrow + 8H_2\uparrow + 2O_2\uparrow + 2CO_2\uparrow$).

The released hydrogen acts as a boron carrier in the depth of the structure of the surface layer of the steel plate in the form of $B_{10}H_{14}$ [4].

The iron powder in the coating is partially oxidized by oxygen released during the interaction between the components of the coating, another part of the iron atoms diffuses into the surface of the samples in the form of separate iron borides.

The presence of iron powder in the coating helps to protect the active components of the coating from oxidation at high temperature heating.

Some iron particles in the process of high-temperature heating oxidized isolated during the interaction between the components of the oxygen coating, and part of them diffuses into the surface of the samples in the form of individual particles of iron and iron borides. Iron oxides remain in the scale zone and are removed during the preparation of samples for basic research by grinding.

Thermodynamically, iron borides are unstable, at 1650 °C they begin to decompose. The lower iron boride Fe_2B decomposes into iron and FeB: $FeB \rightarrow Fe_2B \rightarrow$ (α-phase + B) → base metal [5; 427].

Research result

The analysis of the layers obtained on steel plates shows the dependence of the diffusion zone thickness on the volume content of boric acid in the mixtures of the initial powder.

The results of determination of microhardness:

N microhardness was determined on the device PMT-3 [6].

When the load on the indenter P=100 g (0.98 N) and the holding time at this load 10 seconds. A regular four-sided diamond pyramid with an angle at the top of 1360 was used as an indenter for microhardness measurements, similar to the Vickers hardness test method. Microhardness of Hμ was determined in accordance with the requirements of GOST 9450-60 and the recommendations given in [7], using the formula (1):

$$H_\mu = \frac{1854\,P}{d_{\text{print}}{}^2}[kg \cdot s/mm^2] = \frac{18{,}2 \cdot 10^3}{d_{\text{print}}{}^2}[\text{MN}/m^2 = \text{MPa}], \quad (1)$$

where the load is P (g), and the diagonal of the print – d_{print} (μm).

Tests on the microhardness of the initial material ST20 were carried out. The microhardness of the starting material Hμ=2584 MPa, the microhardness of the material after thermal exposure is Hμ=2207 MPa.

After the thermal effect on the coated samples, the microhardness of each of them was determined and compared with the initial data. Microhardness was determined from three positions: along the edge of the treated layer, horizontally and vertically.

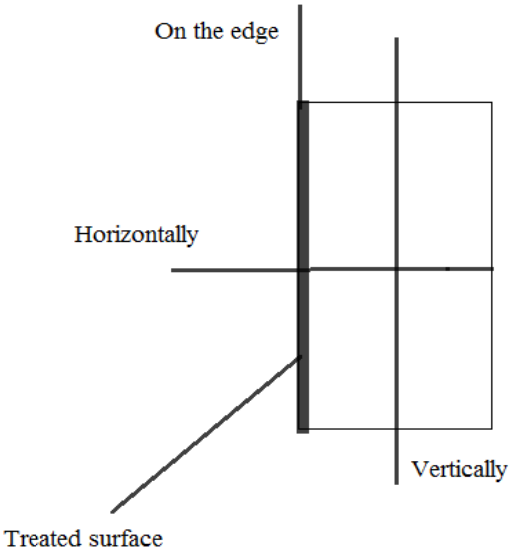

Figure 1. Direction of the measurement of microhardness

The microhardness of the first sample treated with a coating of 50 % H_3BO_3 and 50 % Fe was: horizontal Hμ=2144 MPa, vertical Hμ=2211 MPa, and on the edge Hμ=2202 MPa. There is no significant change from the original sample (Fig. 2).

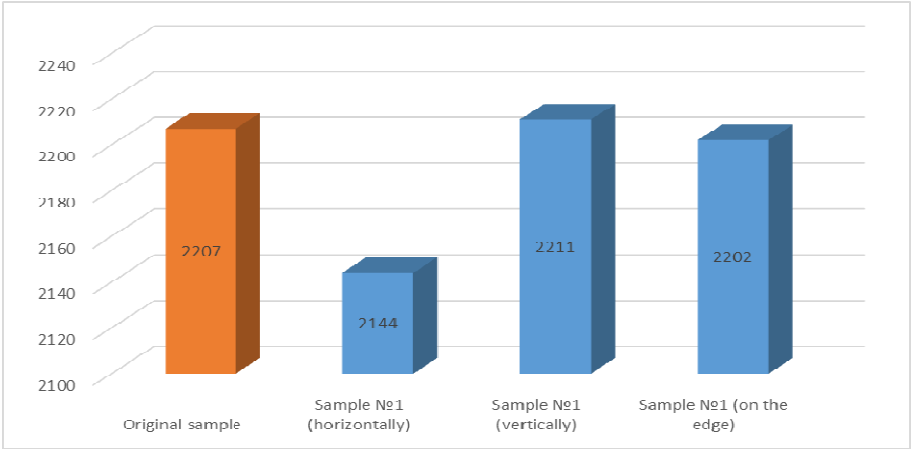

Figure 2. Microhardness of the treated sample 50 % H_3BO_3 and 50 % Fe without liquid glass

The surface of the 2nd sample is treated with a mixture of 25 % Fe-75 % H_3BO_3 with 20 % liquid glass solution. The microhardness of this sample was: horizontally Hμ=2373 MPa, vertically Hμ=2261 MPa, and at the edge Hμ=2409 MPa. Compared with the initial sample, no significant change was observed, the microhardness increased by 17 % (Fig. 3).

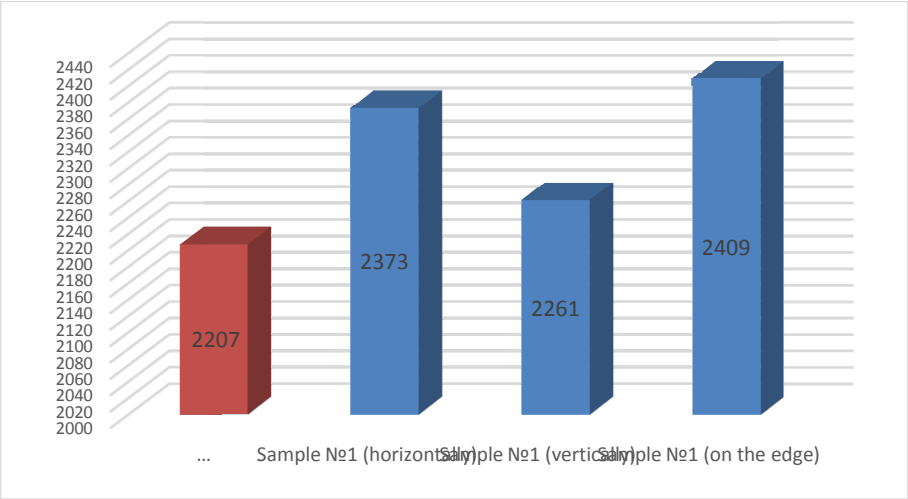

Figure 3. Microhardness of the treated sample 50 % H_3BO_3 and 50 % Fe with liquid glass

The surface of the third and fourth samples is treated with a mixture consisting of 75 % H_3BO_3 and 25 % Fe (by volume) and without 20 % liquid glass solution, and without it, respectively.

Microhardness in samples treated with 75 % H_3BO_3 and 25 % Fe without liquid glass has increased significantly. Here, the microhardness of the sample was: horizontally Hμ=2741 MPa, vertically Hμ=2647 MPa, and at the edge Hμ=2899 MPa. Compared with the original sample microhardness: horizontally increased by 20 %.

Microhardness of the surface layer of the sample treated with the same mixture, but with the addition of 20 % solution of liquid glass showed the best results compared to the microhardness of the starting material and other processed samples. Here, the microhardness was: horizontally Hμ=2919 MPa, vertically Hμ=2642 MPa, and on the edge Hμ=2535 MPa. After this treatment, the horizontal microhardness increased by 25 %.

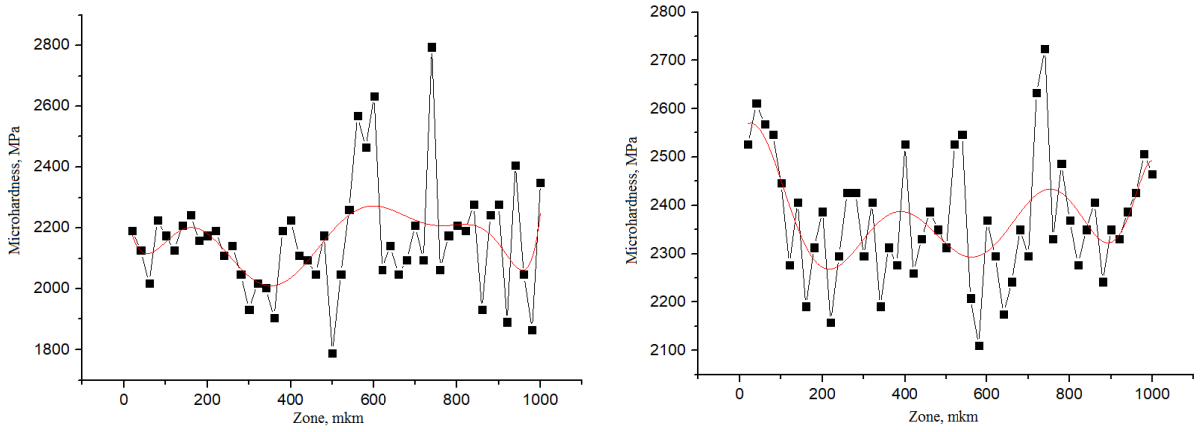

Figure 4. Distribution of microhardness in the borated surface of steel 20 sample: a – sample 1 and b – sample 2

From the data of Figure 4 on the distribution of microhardness in the cross section of samples 1 and 2, no significant change in microhardness compared to the microhardness of the substrate was revealed.

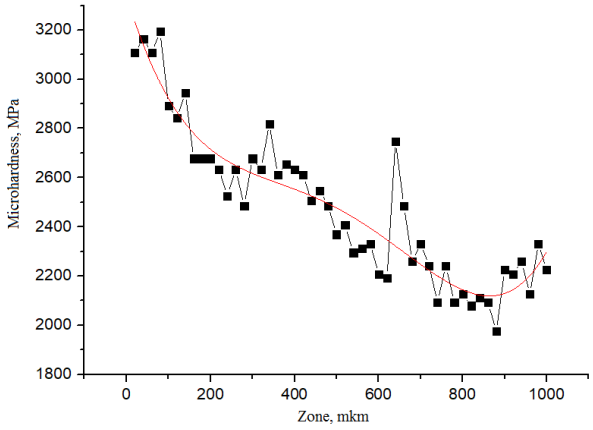

Figure 5. Distribution of microhardness in borated surface of steel 20 of sample 3

From Figure 5 it can be seen that the microhardness of the surface layer has increased significantly, and the diffusion distribution of boron in the diffusion zone is gradually reduced. At a depth of 595 μm, the microhardness of the test sample reaches the microhardness of the annealed substrate.

For most engineering calculations, there is a diffusion layer formula from the boration time [8].

$$h^2 = D\tau, \tag{2}$$

where h is the thickness of the diffuse coating, m; D is the diffusion coefficient, m/s, τ is the duration of the process, s.

Hence, the diffusion coefficient is D = 1.2·10-9 m^2/s. This indicates an abnormally high mass transfer of boron, since it is orders of magnitude higher than the diffusion coefficient of boron at 9500 °C, equal to 1.82·10-11 m^2/s [9].

X-ray structural analysis (Fig. 6, Table 1) showed the formation of two-phase α-Fe compositions with a volume-centered cubic lattice and B with an orthorhombic cubic lattice. Sample 3 is in a three-phase state: α-Fe with a bulk-centered cubic lattice, B with an orthorhombic cubic lattice, and FeB with a rhomboeder cubic lattice.

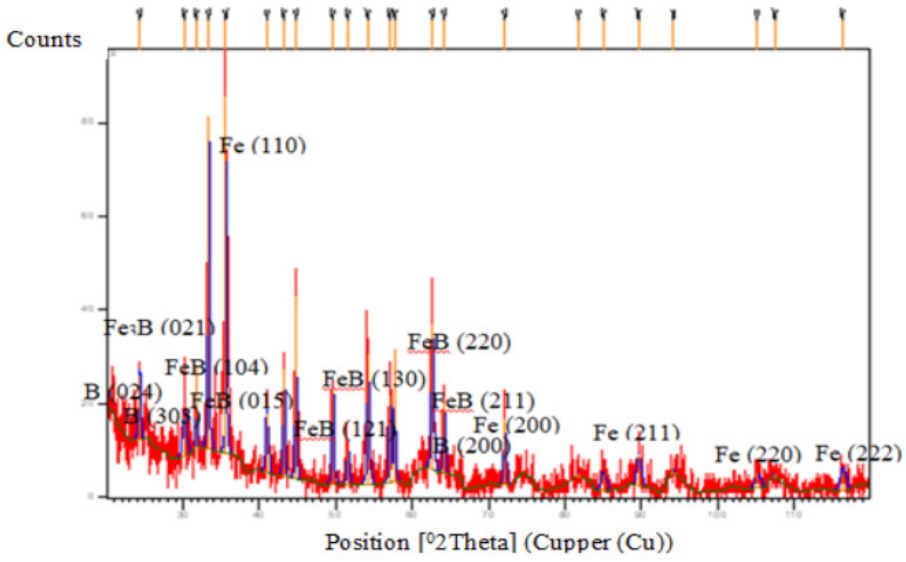

Figure 6. Structural phase state of sample 3

T a b l e

State of the surface layer of sample 3

Chemical element	hkl	Crystal lattice
B	024	Rhombogedric
B	303	Rhombogedric
Fe_3B	021	Volume-centered cubic
FeB	104	Orthorhombic
FeB	015	Orthorhombic
Fe	110	Cubic
FeB	121	Orthorhombic
FeB	130	Orthorhombic
FeB	220	Orthorhombic
FeB	211	Orthorhombic
B	200	Rhombogedric
Fe	200	Cubic
Fe	211	Cubic
Fe	220	Cubic
Fe	222	Cubic

Conclusion

Analysis of the calculations of the microhardness of the surface layers of the samples after annealing in a muffle furnace at a temperature of 1000 °C for 5 minutes showed that the microhardness increased.

Microhardness in samples treated with 75 % H_3BO_3 and 25 % Fe composition without liquid glass increased.

The experimental studies allow us to draw conclusions about the prospects of using this coating to produce iron borides on the surface layers of steel 20. The use of various components of the mixture affects the change in microhardness, microstructure of the surface layer of steel 20.

According to the results of the diffusion layer and the diffusion coefficient, it can be assumed that the growth of the boride layer is abnormal.

Studies aimed at studying the comparison of the effects of various components of the paste, allow us to draw conclusions about the prospects of using this coating to obtain iron borides on its surface layers. The use of various components of the mixture also affects the change in the microhardness, microstructure of the surface layer of St20, as well as on the convenience of applying the coating and its cheapness.

References

1 Лахтин Ю.М. Химико-термическая обработка металлов: учеб. пос. / Ю.М. Лахтин, Б.Н. Арзамасов. — М.: Металлургия, 1985. — 256 с.

2 Ворошнин Л.Г. Борирование стали: учеб. пос. / Л.Г. Ворошнин, Л.С Ляхович. — М.: Металлургия, 1978. — 239 с.

3 Шевчук Е.П. Исследование боридных слоев стали 20 после химико-термической обработки в индукционной печи / Е.П. Шевчук, В.А. Плотников, Б.К. Ахметжанов // Фундаментальные проблемы современного материаловедения. — 2018. — Т. 15, № 3. — С. 386–391.

4 Екимов Е.А. Получение микрокристаллов бора пиролизом декаборана $B_{10}H_{14}$ при высоких давлениях и температурах / Е.А. Екимов, И.П. Зибров, А.В. Зотеев // Неорганические материалы. — 2011. — Т. 47, № 11. — С. 1311–1316.

5 Шевчук Е.П. Формирование обширной диффузионной зоны при борировании стали 20 / Е.П. Шевчук, В.А. Плотников, А.В. Джес // Фундаментальные проблемы современного материаловедения. — 2018. — Т. 15, № 3. — С. 424–428.

6 Золоторевский В.С. Механические испытания и свойства металлов: учеб. / В.С. Золоторевский. — М.: Металлургия, 1974. — 304 с.

7 Харитонов Л.Г. Определение микротвердости: учеб. пос. / Л.Г. Харитонов. — М.: Металлургия, 1967. — 46 с.

8 Ворошнин Л.Г. Многокомпонентные диффузионные покрытия: учеб. пос. / Л.Г. Ворошнин. — Минск: Наука и техника, 1981. — 296 с.

9 Павлов П.В. Физика твердого тела: учеб. / П.В. Павлов, А.Ф. Хохлов. — М.: Высш. шк., 2000. — 494 с.

Е.П. Шевчук, Д.К. Нурумканов, Б.М. Муратбеков, Б. Ахметжанов, В.А. Плотников

Муфельді пеште жану арқылы химиялық термиялық өңдеу әдісімен 20 болаттың бетін модификациялау

Мақала металл бөлшектердің, соның ішінде болат бөлшектерінің беткі қабаттарының беріктігін қатайтумен байланысты өзекті мәселеге арналған. Мақаланың авторлары жоғары температура әсеріндегі әртүрлі тозу жағдайында жұмыс істейтін машина бөлшектері мен құралдарының беріктігін арттыру үшін материалдардың беткі қабаттарының химиялық-термиялық өңдеу әдістерін сипаттайды. Темір пластиналардың үлгілерін әртүрлі көлемдегі пропорцияларда құрамында бор бар қоспалармен жабу арқылы және олардың кейінгі муфельдік пеште жағу әдісі қарастырылды. Диффузия қабатының микроқаттылығы мен қалыңдығын зерттеу нәтижелері көрсетілген.

Кілт сөздер: болат 20, қанықтыру қоспасы, бор қосу, диффузиялық қабат, микроқаттылық, химия-термиялық өңдеу, муфельдік пеш.

Е.П. Шевчук, Д.К. Нурумканов, Б.М. Муратбеков, Б. Ахметжанов, В.А. Плотников

Модификация поверхности стали 20 методом химико-термической обработки путем отжига в муфельной печи

Статья посвящена актуальной на сегодняшний день проблеме, связанной с упрочнением поверхностных слоев металлических материалов, в том числе стальных деталей. Авторы описывают методы химико-термической обработки поверхностных слоев материалов для эффективного повышения долговечности деталей машин и инструментов, работающих в условиях различного износа, при высоких температурно-силовых воздействиях. Рассмотрен способ насыщения образцов железных пластинок с помощью обмазки их борсодержащими смесями в разных объемных пропорциях и последующим их отжигом в муфельной печи. Приведены результаты исследований микротвёрдости и толщины диффузионного слоя.

Ключевые слова: сталь 20, насыщающая смесь, борирование, диффузионный слой, микротвердость, химико-термическая обработка, муфельная печь.

References

1 Lakhtin, Yu.M., & Arzamasov, B.N. (1985). *Khimiko-termicheskaia obrabotka metallov [Chemical and thermal treatment of metals]*. Moscow: Metallurhiia [in Russian].

2 Voroshnin, L.G., & Lyakhovich L.S. (1978). *Borirovanie stali [Steel boration]*. Moscow: Metallurhiia [in Russian].

3 Shevchuk, E.P., Plotnikov, V.A., & Akhmetzhanov, B.K. (2018). Issledovanie boridnykh sloev stali 20 posle khimiko-termicheskoi obrabotki v induktsionnoi pechi [Study of boride layers of steel 20 after chemical and thermal treatment in an induction furnace]. *Fundamentalnye problemy sovremennoho materialovedeniia – Fundamental problems of modern materials science, 15, 3,* 386–391 [in Russian].

4 Ekimov, E.A., Zibrov I.P., & Zoteyev, A.V. (2011). Poluchenie mikrokristallov bora pirolizom dekaborana $B_{10}H_{14}$ pri vysokikh davleniiakh i temperaturakh [Obtaining of boron microcrystals by decemborane pyrolysis $B_{10}H_{14}$ at high pressures and temperatures]. *Neorhanicheskie materialy – Inorganic materials, 47.11,* 1311–1316 [in Russian].

5 Shevchuk, E.P., Plotnikov, V.A., & Dzhes, A.V. (2018). Formirovanie obshirnoi diffuzionnoi zony pri borirovanii stali 20 [Formation of a large diffusion zone in steel boration 20]. *Fundamentalnye problemy sovremennoho materialovedeniia – Fundamental problems of modern materials science, 15, 3,* 424–428 [in Russian].

6 Zolotorevskiy, V.S. (1974). *Mekhanicheskie ispytaniia i svoistva metallov [Mechanical tests and properties of metals]*. Moscow: Metallurhiia [in Russian].

7 Kharitonov, L.G. (1967). *Opredelenie mikrotverdosti [Determination of microhardness]*. Moscow: Metallurhiia [in Russian].

8 Voroshnin, L.G. (1981). *Mnohokomponentnye diffuzionnye pokrytiia [Multicomponent diffusion coatings]*. Minsk: Nauka i tekhnika [in Russian].

9 Pavlov, P.V., & Khokhlov, A.F. (2000). *Fizika tverdoho tela [Physics of the solid state]*. Moscow: Vysshaia shkola [in Russian].

DOI 10.31489/2019Ph 3/59-63

UDC 53.083.2

V.F. Stepanenko[1], K.Sh. Zhumadilov[2], M. Hoshi[3], Y.T. Zhunussov[4], S. Endo[3], M. Ohtaki[3], K. Otani[3], N. Fujimoto[3], K. Shichijo[5], N. Kawano[3], A. Sakaguchi[6], N.Z. Chaizhunusova[4], D.M. Shabdarbaeva[4], A. Baurzhan[4], V.S. Gnyrya[7], A.S. Azimkhanov[7], A.D. Kaprin[1], S.A. Ivanov[1], E. Yaskova[1], I. Belukha[1], T. Kolyzhenkov[1], A.D. Petukhov[1], V. Bogacheva[1]

[1]A. Tsyb MRRC – National Medical Research Center of Radiology, Ministry of Health, Obninsk, Russia;
[2]L.N. Gumilyov Eurasian National University, Nur-Sultan, Kazakhstan;
[3]Hiroshima University, 734-8553, Japan;
[4]Semey State Medical University, Kazakhstan;
[5]Nagasaki University, 1-12-4, Sakamoto, 852-8523, Japan;
[6]Graduate School of Pure and Applied Sciences, University of Tsukuba;
[7]National Nuclear Center of the Republic of Kazakhstan, Kurchatov, Kazakhstan
(E-mail: zhumadilovk@gmail.com)

Preliminary assessment of dose distribution on the spatial micro level for internal exposure of alveolar epithelium of rats by ^{56}Mn

Special dosimetry study of experimental rats exposure by sprayed ^{56}Mn powder was conducted during experiments in order to study internal irradiation effects. All experiments were performed in Kurchatov's reactor complex «Baikal-1» (Kurchatov city, East-Kazakhstan region) after neutron activation of stable Mn powder. This study was performed by group of scientists from Japan, Kazakhstan, and Russian Federation. The results of estimated doses in lungs alveolar epithelium of rats are shown in this paper. Absorbed dose on the «surface» of epitelium is equal to 160 Gy and absorbed dose in the «bottom» of epithelium for minimal thickness of epithelium cells is 8.9 Gy and for maximal thickness of epithelium cells equal to 0.4 Gy.

Keywords: internal exposure, Kurchatov, MCNP, rats, organs, powder of ^{56}Mn, epithelium layer.

Introduction

It was important to study effect of radiation, due to effect of possible influence to human, and effect of possible internal exposure because of close location to Semipalatinsk Nuclear Test Site and post effect of irradiation due to Hiroshima and Nagasaki atomic bombing, Chernobyl, and Fukushima-1 accidents [1–4].

At neutron irradiation, including such kind of extraordinary tragedy as A-bombing of Hiroshima and Nagasaki, the ^{56}Mn ($T_{1/2}$=2.58 hour) was one of the dominant neutron activated irradiators during the first hours following the neutron irradiation. Modeling of irradiation by residual radioactivity from activated dust using neutron-activated ^{56}Mn in a form of powder sprayed over experimental rats was conducted recently [5]. Activation of MnO_2 (manganese dioxide) powder was performed using the IVG.1M nuclear reactor («Baikal-1» experimental facility, Kurchatov city, Kazakhstan).

According to V. Stepanenko, et al. [6, 7], mean organ doses of internal irradiation of rats by ^{56}Mn powder are the following: 1.65, 1.33, 0.24, 0.1, 0.076 Gy, in large intestine, small intestines, stomach, lungs, and skin respectively.

The essential pathological effects were found in gastrointestinal tract [8, 9]. On the other hand, despite relatively low dose in the lungs (0.1 Gy), the hemorrhage and emphysema were found in this organ as well [8]. It is very difficult to interpret this fact, as far as these effects are observed at much larger doses of external irradiation.

As a result, due to ideas of Prof. M. Hoshi [5] and Prof. M. Ohtaki [10, 11], it was decided to estimate not only mean organ doses of internal irradiation, but distribution of dose on microlevel of biological tissue, particularly on the level of alveolus of lungs. Short range irradiation from ^{56}Mn (Auger electrons, low energy X-rays) can be a reason of much larger doses in microstructures of lungs.

Material and Methods

Monte Carlo code (MCNP-4C) with corresponding Library of cross sections for electrons and quanta was used for calculation of absorbed doses in biological tissue around $^{56}Mn0_2$ microparticles (density of manganese dioxide is 5.03 g/cm^3). Mean diameter of $^{56}Mn0_2$ microparticles is equal to 4 μm. The corresponding data of ^{56}Mn's Auger electrons, X-rays, beta particles < and gamma-rays are resented in Tables 1–3 and in Figure 1.

Irradiation of ^{56}Mn

Table 1

^{56}Mn: AUGER ELECTRONS

Type	Energy keV	Electrons/decay	R99, (loss of 99 % of initial energy at R99 – radius of tissue sphere around isotropic microsource), cm
KLL	5.51	1	8.8 E-6
KLX	6.28	0.274	1.1 E-4
KXY	7.01	0.0187	1.3 E-4
L	0.57	3.07	2.1 E-6

Table 2

^{56}Mn: X-RAYS

Type	Energy keV	Photons/decay	R99, (loss of 99 % of initial energy at R99 – radius of tissue sphere around isotropic microsource), cm
Kα2	6.39	0.51	
Kα1	6.40	1	about 1 E-2 cm
Kβ1	7.06		
Kβ5	7.10	0.21(total for all Kβ)	

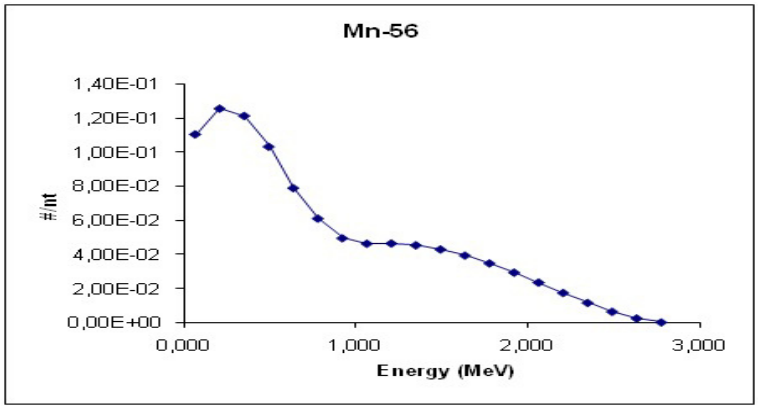

Figure 1. Beta particles of ^{56}Mn: intensity is 100 %, average energy is 829.21 keV (mean R99 is about 1.8 cm), and maximal energy is 2848.00 keV (maximal R99 is about 6 cm)

Table 3

^{56}Mn: MAIN GAMMA-RAYS

Type	Energy keV	Photons/decay	R99, (loss of 99 % of initial energy at R99 – radius of tissue sphere around isotropic microsource), cm
Gamma-1	846.8	0.989	about 80 cm
Gamma-2	1811	0.272	> 100 cm
Gamma-3	2113	0.143	> 100 cm
Gamma-4	7.10	0.173	> 100 cm

Geometry of calculation

Alveoli of lungs are the final destination for inhaled air and for microparticles entering into the lungs with air. Each alveolus is lined with squamous epithelial cells (from 0.05 mkm to 0.3 μm thick). Surfactant (which is over epithelial cells) is about 0.01 μm thickness. So, if 56Mn microparticle is attached to epithelium, the minimal distance to the «surface» of epithelium layer will be 1×10-6 cm and maximal distance to the «bottom» of epithelium layer will be 6×10-6 (in a case minimal thickness of epithelium cell) or 5×10-5 cm (in a case maximal thickness of epithelium cells) (Fig. 2). Absorbed doses were calculated in spherical layers of biological tissue around ^{56}Mn microparticle.

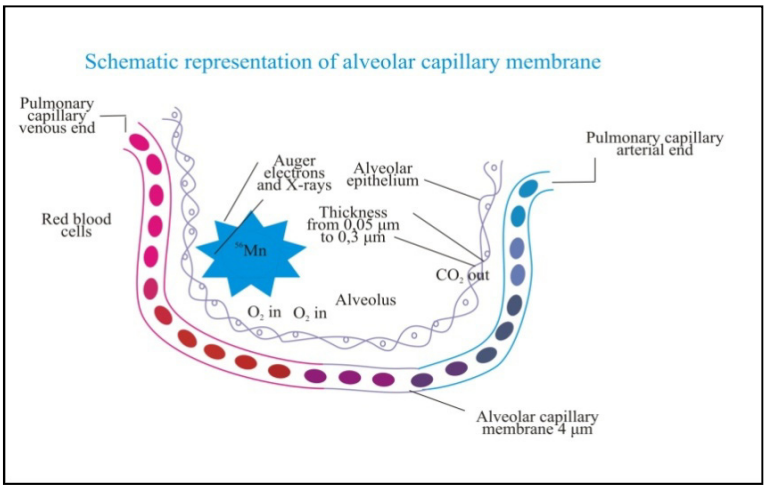

Figure 2. Schematic representation of lung's alveoli with $^{56}MnO_2$ microparticle.

Results and Discussion

It was estimated, that mean initial activity of one $^{56}MnO_2$ microparticle is equal to 0.196 Bq (with total activity of 0.1 g, MnO_2 equal to 2.74×10^8 Bq, according to Hoshi, et al. [5]. Period of ^{56}Mn physical half decay is equal to $T_{1/2}$ = 2.58 hours = $9.288\text{x}10^3$ seconds. Total number of ^{56}Mn decays up to whole decay in one ^{56}Mn microparticle with estimated activity 0.196 Bq is equal to: N=0.196 Bq×$9.288\text{x}10^3$ seconds/0,693 = 2.627×10^3 decays. Dose per one decay from Auger electrons, low energy X-rays, and beta particles of ^{56}Mn is presented in Figure 3. This figure shows results of calculations of spatial dose distribution around ^{56}Mn placed into biological tissue.

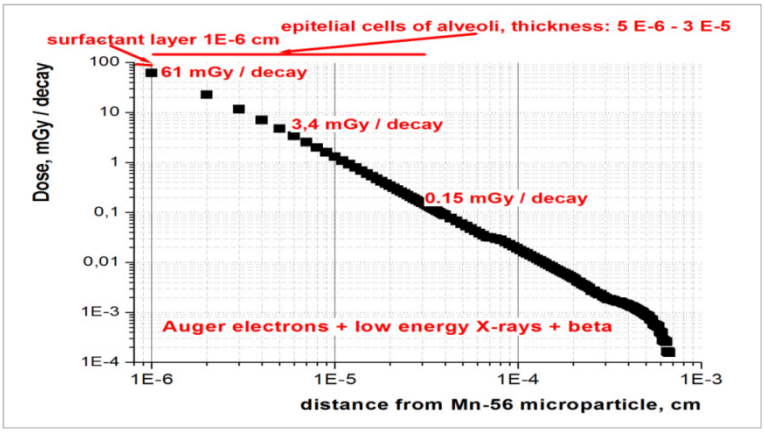

Figure 3. Results of calculations of spatial dose distribution around ^{56}Mn microparticle placed into biological tissue.

So, as result, these estimations shows the following doses per decay: 61 mGy/decay at distance 1×10^{-6} cm from microparticle («surface» of alveolar epithelium layer); 3.4 mGy/decay at distance 6×10^{-6} from microparticle («bottom» of alveolar epithelium layer, in a case of minimal thickness of epithelium cell); 0.15 mGy/decay at distance 3×10^{-5} cm from microparticle («bottom» of alveolar epithelium layer, in a case of maximal thickness of epithelium cell). Highest dose is due to short distance to radioactive source.

Total absorbed dose (up to whole decay of ^{56}Mn) is equal to: 160 Gy («surface» of alveolar epithelium layer); 8.9 Gy («bottom» of alveolar epithelium layer, in a case minimal thickness of epithelium cells); 0.4 Gy («bottom» of alveolar epithelium (in a case maximal thickness of epithelium cells).

Conclusion

Absorbed dose (up to whole decay of ^{56}Mn) is equal to: 160 Gy («surface» of alveolar epithelium layer); 8.9 Gy («bottom» of alveolar epithelium layer, in a case minimal thickness of epithelium cells); 0.4 Gy («bottom» of alveolar epithelium (in a case maximal thickness of epithelium cells).

The study was carried out with the financial support of the Semey State Medical University, Ministry of Health of the Republic of Kazakhstan (research support in the Republic of Kazakhstan). The research of specialists from Japan was supported by JSPS KAKENHI grants No. 26257501 and No. 24310044, Japan. This study was supported by MRRC named after A.F. Tsyb (equipment and MC calculations).

References

1 Yamamoto, M., Takada, T., Nagao, S., Koike, T., Shimada, K., Hoshi, M., & et al. (2012). An early survey of the radioactive contamination of soil due to the Fukushima Dai-ichi nuclear power plant accident, with emphasis on plutonium analysis. *Geochem J., 46,* 341–353.

2 Zhumadilov, K., Ivannikov, A., Zharlyganova, D., Zhumadilov, Z., Stepanenko, V., Apsalikov, K., & et al. (2009). ESR dosimetry study on population of settlements nearby Ust-Kamenogorsk city, Kazakhstan. *Radiat. Environ. Biophys. 48,* 419–425.

3 Zhumadilov, K., Ivannikov, A., Stepanenko, V., Toyoda, S., Skvortsov, V., & Hoshi M. (2016). EPR Dosimetry study for population residing in the vicinity of fallout trace for nuclear test on 7 August 1962. *Radiat. Prot. Dosim. ISSN: 0144–8420. 172 (1–3),* 260–264.

4 Stepanenko, V.F., Hoshi M., Bailiff I.K., Ivannikov A.I., Toyoda S., Yamamoto M., & et al. (2006). Around Semipalatinsk nuclear test site: Progress of dose estimations relevant to the consequences of nuclear tests. *A summary of 3rd Dosimetry Workshop on the Semipalatinsk nuclear test site area, RIRBM, Hiroshima University, Hiroshima, 9–11 March, 2005. J. Radiat. Res. 47, Suppl. A,* A1-A13.

5 Hoshi, M., Ohtaki, M., Otani, K., Fujimoto, N., Shichijo, K., Endo, S., & et al. (2018). Our Semipalatinsk studies. -S1: Experimental and theoretical studies on biological effects of radioactive micro-particles, S2: Air dust sampling and measurements, S3: Dosimetry and risk studies in Semipalatinsk area. *21th Hiroshima International Symposium: Studies on health effects of exposure to radioactive micro-particles, January 23,* Hiroshima (Japan).

6 Stepanenko, V.F., Rakhypbekov, T.K., Kaprin, A.D., Ivanov, S.A., Otani, K., Endo, S., & et al. (2016). Irradiation of experimental animals by neutron activated dust: development and realization of the method — first results of international multicenter study. *Radiation and Risk, 25,* 111–125.

7 Stepanenko, V., Rakhypbekov, T., Otani, K., Endo, S., Satoh, K., Kawano, N, & et al. (2017). Internal exposure to neutron-activated ^{56}Mn dioxide powder in Wistar rats—Part 1: Dosimetry. *Radiat. Environ. Biophys. Vol. 56, Issue 1,* 47–54.

8 Shichijo, K., Fujimoto, N., Uzbekov, D., Kairkhanova, Y., Saimova, A., Chaizhunusova, N., & et al. (2017). Internal exposure to neutron-activated ^{56}Mn dioxide powder in Wistar rats – Part 2: pathological effects. *Radiat. Environ. Biophys. 1 March 2017, Vol. 56, Issue 1,* 55–61.

9 Shichijo, K., Fujimoto, N., Uzbekov, D., Kairkhanova, Y., Saimova, A., Chaizhunusova, N., & et al. (2017). Erratum to: Internal exposure to neutron-activated ^{56}Mn dioxide powder in Wistar rats — Part 2: pathological effects. *Radiat. Environ. Biophys. 2017, Vol. 56, Issue 1,* 203–204.

10 Ohtaki, M., Otani, K., Tonda, T., Sato, Y., Hara, N., Imori, S., & et al. (2014). Effect of distance from hypocenter at exposure on solid cancer mortality among Hiroshima atomic bomb survivors with very low initial radiation dose in the Dosimetry System 1986 (DS86). *Health Phys. V. 107, Suppl. 1,* 45.

11 Stepanenko, V., Hoshi, M., Endo, S., Ohtaki, M., Otani, K., Fujimoto, N., & et al. (2018). Calculations of dose distribution on the spatial microlevel around ^{56}Mn microparticles incorporated into biological tissue: preliminary results. *21th Hiroshima International Symposium: Studies on health effects of exposure to radioactive micro-particles, January 23,* Hiroshima (Japan).

В.Ф. Степаненко, К.Ш. Жумадилов, М. Хоши, Е.Т. Жунусов, С. Эндо, М. Отаки, К. Отани, Н. Фуджимото, К. Шичиджо, Н. Кавано, А. Сакагучи, Н.Ж. Чайжунусова, Д.М. Шабдарбаева, А. Бауыржан, В.С. Гныря, А.С. Азимханов, А.Д. Каприн, С.А. Иванов, Е. Яськова, И. Белуха, Т. Колыженков, А.Д. Петухов, В. Богачева

Егеуқұйрықтардың альвеолярлық эпителийіне ^{56}Mn ішкі әсері кезіндегі кеңістіктік микродеңгейде мөлшерінің таралуын алдын ала бағалау

Курчатов қаласындағы Байкал-1 реакторлық кешенінде (Курчатов қ., Шығыс Қазақстан облысы) радиациялық әсер эффектісін зерттеу бойынша эксперимент жүзінде ^{56}Mn ұнтағы тозаңының егеуқұйрықтарға әсерінің ішкі дозиметриялық зерттеуі жүргізілді. Бұл зерттеу Жапония, Қазақстан және Ресей Федерациясы ғалымдарының тобымен орындалды. Берілген жұмыста егеуқұйрықтар

өкпесінің альвеолярлық эпителийін сәулелендіру дозасын бағалау нәтижелері көрсетілген. Эпителий «бетінде» жұтылған доза 160 г тең, эпителий жасушаларының «төменгі» минималды қалыңдығында жұтылған доза 8,9 г құрайды, ал эпителий жасушаларының максималды қалыңдығы үшін — 0,4 г.

Кілт сөздер: ішкі сәулелену, Курчатов, MCNP, егеуқұйрықтар, мүшелер, ^{56}Mn ұнтағы, эпителий қабаты, өкпе альвеоласы.

В.Ф. Степаненко, К.Ш. Жумадилов, М. Хоши, Е.Т. Жунусов, С. Эндо, М. Отаки, К. Отани, Н. Фуджимото, К. Шичиджо, Н. Кавано, А. Сакагучи, Н.Ж. Чайжунусова, Д.М. Шабдарбаева, А. Бауыржан, В.С. Гныря, А.С. Азимханов, А. Д. Каприн, С.А. Иванов, Е. Яськова, И. Белуха, Т. Колыженков, А.Д. Петухов, В. Богачева

Предварительная оценка пространственного распределения дозы на микроуровне при внутреннем воздействии ^{56}Mn на альвеолярный эпителий крыс

С целью изучения эффектов внутреннего облучения проведено специальное дозиметрическое исследование воздействия на экспериментальных крыс распыленным порошком массой ^{56}Mn. Все эксперименты проводились на реакторном комплексе «Байкал-1» (г. Курчатов, Восточно-Казахстанская область) после нейтронной активации стабильного порошка Mn. Данное исследование было проведено группой ученых из Японии, Казахстана и Российской Федерации. В настоящей работе приведены результаты оценки доз облучения альвеолярного эпителия легких крыс. Поглощенная доза на «поверхности» эпителия равна 160 г, а поглощенная доза в «дне» эпителия для минимальной толщины клеток эпителия составляет 8,9 г, а для максимальной толщины клеток эпителия — 0,4 г.

Ключевые слова: внутреннее облучение, Курчатов, MCNP, крысы, органы, порошок ^{56}Mn, слой эпителия, альвеолы легких.

DOI 10.31489/2019Ph 3/64-70
UDC 621.391.26

M.Z. Yakubova[1], T.G. Serikov[2]

[1]*Almaty University of Power Engineering & Telecommunications, Kazakhstan;*
[2]*Karaganda State Technical University, Kazakhstan*
(E-mail: Tansaule_s@mail.ru)

For the security of telecommunication networks on the application program package OPNET Modeler v.14.5 and the use of the «NetDoctor» module

The work is focused on modeling in OPNET Modeler v.14.5 wireless subscriber access network for its analysis and research by using and applying the NetDoctor module to ensure the security of the built network. Wireless communication is used, as it is accepted, in networks, connecting and wired (cable) means, and give the opportunity to take a convenient, fast and economical solution of problems arising in the process of solution and modernization of cable networks. Wireless communications, therefore, should be considered not a complete alternative to cable networks, but only an alternative technology for the implementation of individual segments or even entire levels of the designed, extensible or modernizing computer network. Detection of used erroneous technologies in the process of building and modeling of telecommunication networks ensures the security of their functioning and predicts their reliable building structure at their design. In our work we use the NetDoctor module of the program package of OPNET Modeler v.14.5 to test the security of the built wireless network.

Keywords: OPNET Modeler v. 14.5, LAN, program package, networks, NetDoctor, traffic, wireless communication.

In foreign countries, wireless subscriber access networks (WSAN) are widely used by corporate networks located inside buildings, on the territory of industrial enterprises as well as for communication of remote offices among themselves. Typical customers of such solutions are hospitals, warehouses and trade organizations. This includes non-stationary networks deployed for an indefinite period of time activities such as exhibitions or scientific and other seminars. In Russia, WSAN work outside of buildings, providing high-speed data transfer services to users located at a distance of several kilometers and even tens of kilometers [1].

In Kazakhstan, the wireless local area network (WLAN) sometimes expresses the only economically viable solution – when the cable system is geographically impossible and lacking or of poor quality. In this regard, the research proposed in the work is *relevant.*

The novelty involves the developed modeling technique on the module APP OPNET Modeler structure of its building and its research.

Wireless communication is used, as it is accepted, in networks, connecting and wired (cable) means, and gives the opportunity to take a convenient, fast and economical solution of problems arising in the process of solution and modernization of cable networks. Wireless communications, therefore, should be considered not a complete alternative to cable networks, but only an alternative technology for the implementation of individual segments or even entire levels of the designed, extensible or modernizing computer network.

The analysis shows that the IEEE 802.11 standard compliant technologies for WLAN have the following four levels of security features: Physical, Service Set ID, MAC ID-Media access control ID, and encryption.

This technology is predetermined for the transmission of data in the frequency range 2.4 Ghz at the present phase is widely used in military communication to enhance the security of wireless transmission. In the area of DSSS schema, the flows that cause the data transfer are «deployed» over a 20-Mhz bandwidth within the ISM range using the Complementary code Keying's scheme. The user must establish a reliable frequency channel and apply the same CCK scheme to decode the received information. Then, the technology on the basis of DSSS provides the first line of protection against unclaimed access to the transmitted information. In addition, DSSS is a «silent» interface, so almost all listening devices will filter it out as «white noise».

The SSID allows you to distinguish the certain WLAN that can act in the same place or region. It is a unique network name included in the header of the IEEE 802.11 data and control packages. Wireless clients

and access points use it to filter and accept only those requests that are related to their SSID. Therefore, the user will not be able to refer to the access points unless it is given the correct SSID.

The probability of accepting or rejecting a request to a network may also depend on the value of the MAC ID being a unique number assigned to each network card during production. When a client PC tries to access a wireless network, the access point must first check the MAC address for the client. Similarly, the client PC must know the name of the access point.

For an invasion of the wireless network, it is enough to be in the radio network visibility zone with equipment of the same type on which the network is built. The access check by MAC addresses of devices and the same WEP is provided in WLAN for reducing of probability of unauthorized access. Because access check is performed by using an access point, so it is only possible with an infrastructure network topology. The inspection technology involves pre-compiling the MAC addresses tables of allowed clients at the access point, and provides the only transfer between fixed wireless adapters. The access control at the level of the radio network is not foreseen in the «ad-hoc» technology (each with each).

In order to enter the WLAN, the intruder must:

– have the equipment for WLAN compatible with the used in the network (in relation to the standard equipment-the appropriate technology of wireless networks – DSSS or FHSS);

– recognize the non-standard sequences of frequency jumps at application in FHSS equipment;

– know the network ID, scrambling the infrastructure and a single for the entire logical network (SSID);

– know (in the case of DSSS) which of the 14 possible frequencies the network operates in, or enable the automatic scanning mode;

– be included in the allowed MAC addresses table in the access point of the network infrastructure technology;

– know the 40-bit WEP cipher key if there is an encrypted transmission in the wireless network. It is almost impossible to solve all this, so the probability of unauthorized entry into the wireless network, in which the standard security measures are taken, can be considered as very low.

We will note the following advantages of WLAN compared to wire:

– Speed and simplicity of deployment and wireless network settings;

– Saving investments in the local network when changing the office;

– Flexibility: quick structure change, configuration modification and network scale;

– Mobility of users in the network distribution zone;

– WLAN functions where the cable is not functioning.

The most elementary way to organize workplaces in the WLAN is the «each with each» (ad-hoc) way. The Network Adapter is entered into each computer and the conditions of direct radio visibility with neighboring points are provided. This method can be used to rapidly deploy a network in small areas where wired networks cannot be deployed for technical reasons.

The Figure 1 shows the developed model of the WSAN on the APP OPNET Modeller V.14.5.

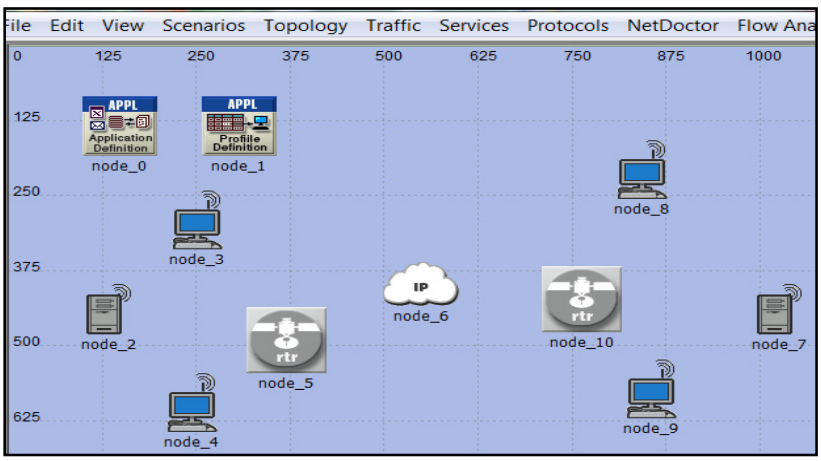

Figure 1. The window of the developed model WSAN on the RFP opnet Modeller V. 14.5

The model consists of the following devices which are wireless: servers, workstations, routers, IP clouds.

We will research the changes of traffic value when different codecs are used in modeling in such a network, for example, G711and G729 standardized in the 90s and used in wireless communications, PSTN networks and VoIP systems. The G.729 is based on an algorithm with a high degree of compression. In general, it allows to compress traffic more strongly, reaching an 8-fold result. Both methods have evolved over the past decades and have a number of versions in accordance with the ITU-T standard.

The research requires an experiment using the following APP OPNET Modeller V.14,5 technologies:

– selection and settings of network equipment;

– from the main menu of the package OPNET Modeller V. 14.5 «Traffic» selection of traffic: VoIP, IP.

As a result of the experiment we get the following data shown in Figure 2 when the codec G711 is used to modify the traffic in its transmission.

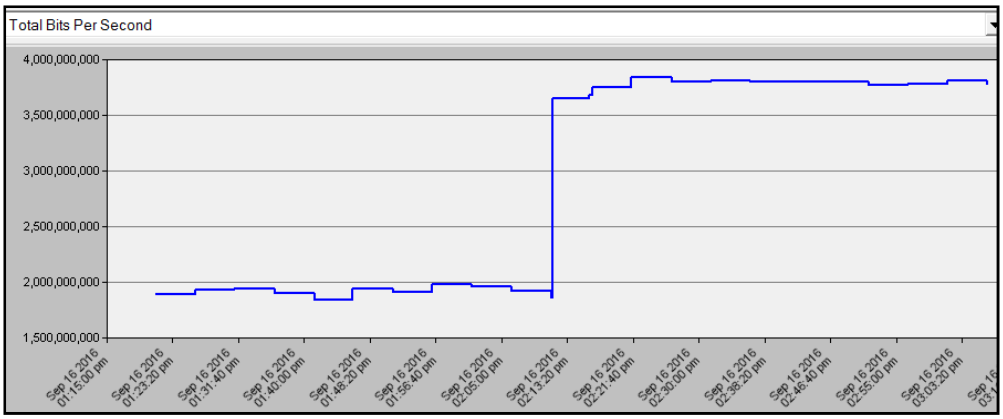

Figure 2. The result of the experiment on distribution of traffic for the model time using codec G711

The Figure 2 shows that at the beginning of the model time the traffic value has changed upward, then from the time of 02. 13.20 sharply increased to 3 800 000 000 bits and then changed very slightly. It can be said that starting from this time there is a steady traffic value in the channel.

We will consider how the traffic value changes by using the G729 codec to modify the traffic. We will use the G729 codec instead of the G711 codec before the modeling as shown in Figure 3.

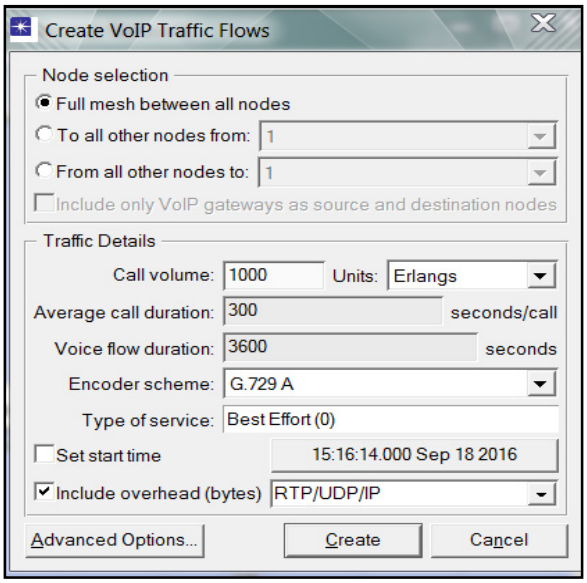

Figure 3. VoIP traffic creation using the G729 codec

The Figure 4 shows the modeling results with the use of the G729 codec from which you can see that from the time of 02. 21.40 there is an almost steady traffic value in the channel and the traffic value thus reaches 1 600 000 000 bits, i.e. by comparing the traffics values it turns out that the value of the transferred traffic using the G729 codec is less than with the G711 codec.

This is explained by the fact that the rate of traffic transmission using the G711 codec is more than G729 almost in 8 times.

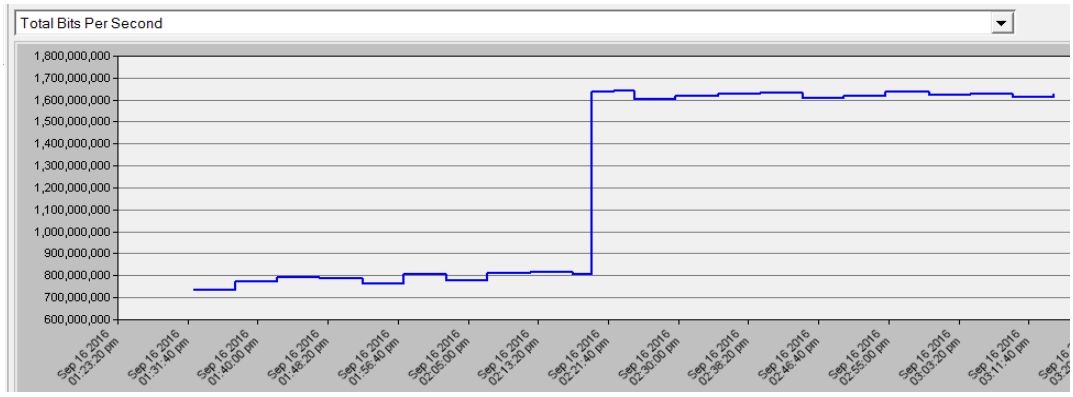

Figure 4. Traffic distribution for the model time using the G729 codec.

The used encrypting methods are used in communications and are standardized by the ITU-T Association. Both methods use 8000 cycles per second to read the signal using the Nyquist frequency theory, by consuming the bandwidth of 64 Kbit/sec for G.711 and 8 Kbit/sec for G.729.

The G.729 uses special compression methods to reduce the cost of the width of the information transmission, while G.711 will require low computational power compared to G.729, thanks to a simple encrypting methods. The analyzed encrypting and decrypting methods have their own extended versions with small variations. Despite the fact that G.729 provides a lower scope of information, it is necessary to pay attention to the issues of the license [1-4]. The G.729 includes program patents from several companies and is licensed on behalf of Sipro Lab Telecom. Sipro Lab Telecom is an authorized representative of the rights to the G.729 technology and patent portfolio. In a number of countries, it may be required a license fee and/or royalty fee using G.729 The G.729 codec is completely free in Russia.

Based on the above listed, the fact that G.711 is supported by a large number of devices. The systems based on it are easier to use.

We use the NetDoctor module of the program package of OPNET Modeler v.14.5 to test the security of the built wireless network.

For this experiment, we will turn to the main menu OPNET Modeler and clicking on the module NetDoctor we will open its window and run this module. Then we will check its results shown in Figure 5 by modeling WLAN on this module.

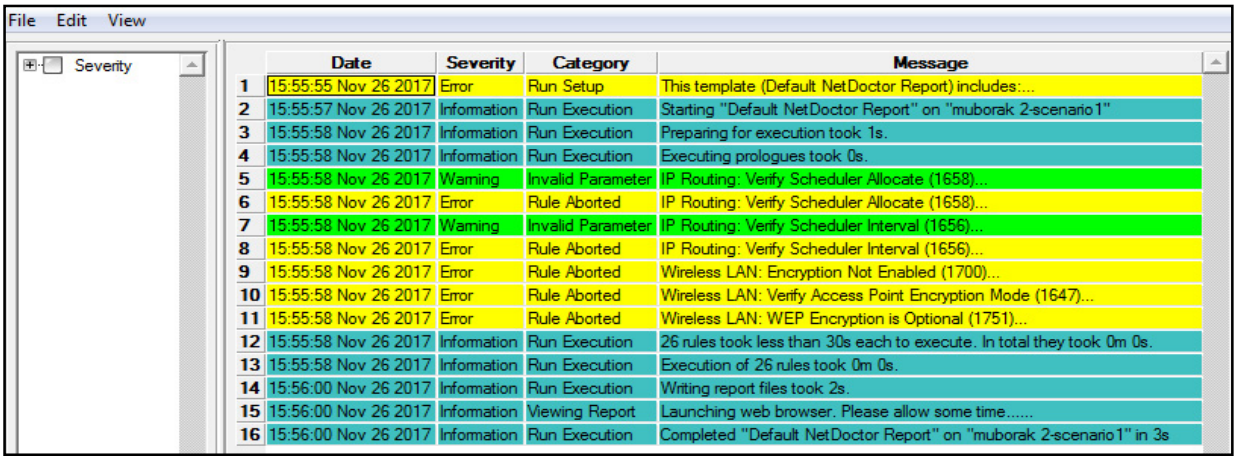

	Date	Severity	Category	Message
1	15:55:55 Nov 26 2017	Error	Run Setup	This template (Default NetDoctor Report) includes:...
2	15:55:57 Nov 26 2017	Information	Run Execution	Starting "Default NetDoctor Report" on "muborak 2-scenario1"
3	15:55:58 Nov 26 2017	Information	Run Execution	Preparing for execution took 1s.
4	15:55:58 Nov 26 2017	Information	Run Execution	Executing prologues took 0s.
5	15:55:58 Nov 26 2017	Warning	Invalid Parameter	IP Routing: Verify Scheduler Allocate (1658)...
6	15:55:58 Nov 26 2017	Error	Rule Aborted	IP Routing: Verify Scheduler Allocate (1658)...
7	15:55:58 Nov 26 2017	Warning	Invalid Parameter	IP Routing: Verify Scheduler Interval (1656)...
8	15:55:58 Nov 26 2017	Error	Rule Aborted	IP Routing: Verify Scheduler Interval (1656)...
9	15:55:58 Nov 26 2017	Error	Rule Aborted	Wireless LAN: Encryption Not Enabled (1700)...
10	15:55:58 Nov 26 2017	Error	Rule Aborted	Wireless LAN: Verify Access Point Encryption Mode (1647)...
11	15:55:58 Nov 26 2017	Error	Rule Aborted	Wireless LAN: WEP Encryption is Optional (1751)...
12	15:55:58 Nov 26 2017	Information	Run Execution	26 rules took less than 30s each to execute. In total they took 0m 0s.
13	15:55:58 Nov 26 2017	Information	Run Execution	Execution of 26 rules took 0m 0s.
14	15:56:00 Nov 26 2017	Information	Run Execution	Writing report files took 2s.
15	15:56:00 Nov 26 2017	Information	Viewing Report	Launching web browser. Please allow some time.....
16	15:56:00 Nov 26 2017	Information	Run Execution	Completed "Default NetDoctor Report" on "muborak 2-scenario1" in 3s

Figure 5. WLAN modeling results using NetDoctor

The Figure 5 shows that positions 6, 8-11 indicate used incorrect technologies in the modeling process beginning with the words «ERROR» in English.

To resolve these errors, we use Configure/Run NetDoctor from the NetDoctor submenu and remove the ticks using IP Multicast and IP Routing and modeling without them as shown in Figure 6.

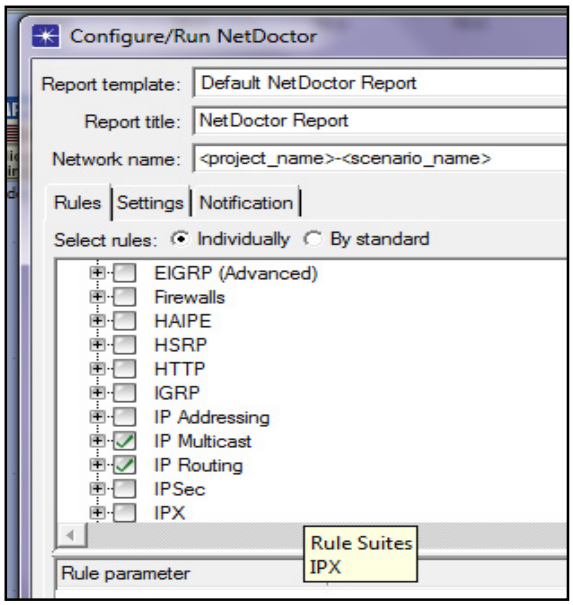

Figure 6. Removal of IP Multicast and IP Routing

As a result, we get the technologies shown in Figures 6–11 where there are no errors

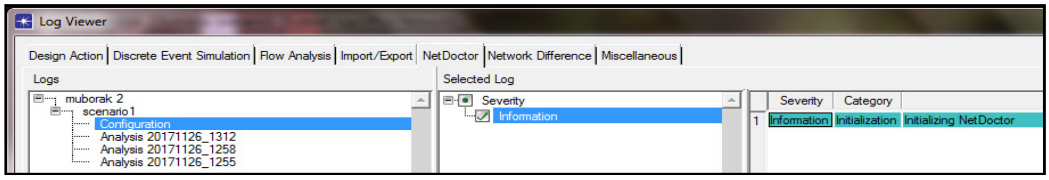

Figure 7. The result of removing the 6th error in the network configuration

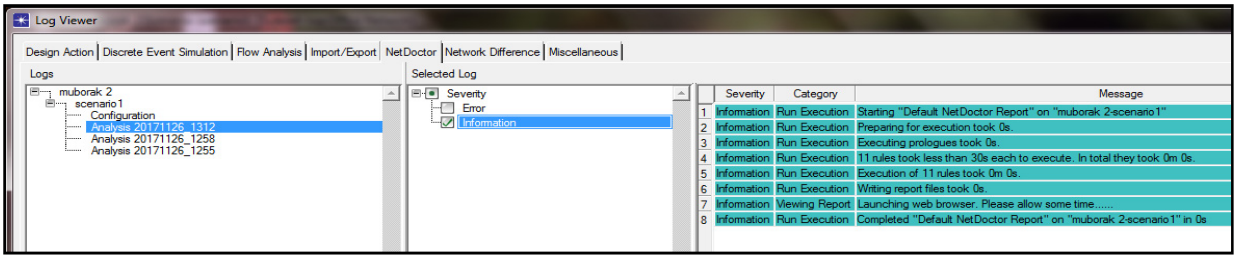

Figure 8. The result of the error 1312 removal analysis

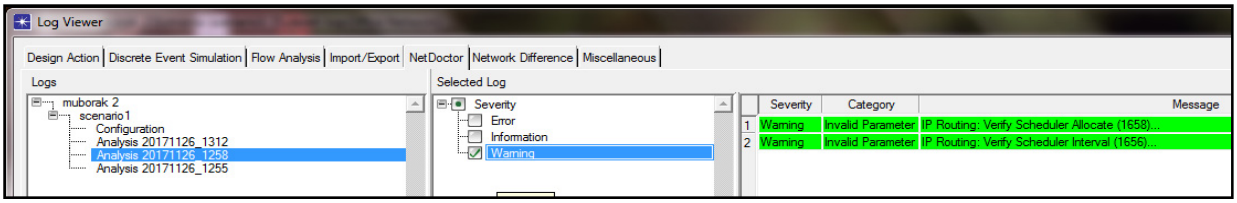

Figure 9. The result of the error 1258 removal analysis

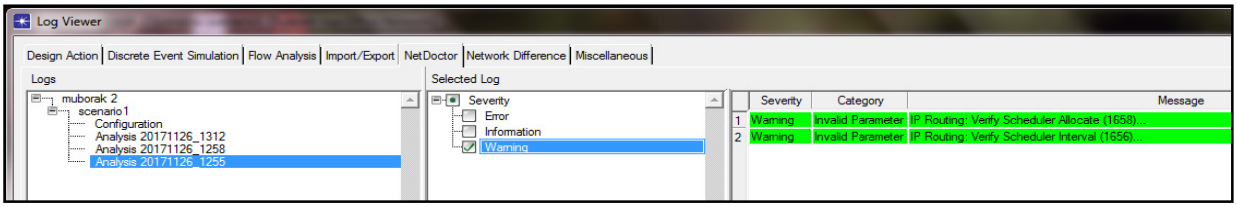

Figure 10. The result of the error 1255 removal analysis

Conclusions

The used codecs in the conducted experiments encrypt data in the researched telecommunication networks.

The G.729 uses less bandwidth for data transmission as opposed to G.711, while the voice quality retains with complex encrypting methods that increase the cost of computational power in encrypting and decrypting processes. Experiments conducted on application program packages show that while comparing the value of the transferred traffic the use of the G729 codec is less than the G711 codec.

Application of the NetDoctor module of the application program package of the APP OPNET Modeller V14.5 showed the errors which were made in the selection of some technologies in modeling, for example, the use of IP Multicast load and the selection of IP technology Routing and others. Detection of used erroneous technologies in the process of building and modeling of telecommunication networks ensures the security of their functioning and predicts their reliable building structure at their design.

References

1 Якубова М.З. Исследование MPLS сетей на основе построения имитационных моделей / М.З. Якубова // Высшая школа Казахстана. — 2016. — № 3. — С. 13–23.

2 Якубова М.З. Имитационное моделирование коммутированных ЛВС / М.З. Якубова // Высшая школа Казахстана. — 2016. — № 3. — С. 30–40.

3 Кислов Д.В. IP-телефония, мобильные телефоны / Д.В. Кислов // ГроссМедиа. — 2007.

4 Сайт журнала «Технологии OPNET» [Электронный ресурс]. — Режим доступа: http://www.opnet.com/services/university/itguru_acadmic_edition.html.

М.З. Якубова, Т.Г. Сериков

NetDoctor модулін қолдану арқылы OPNET Modeler v.14.5 қолданбалы бағдарламасы мен жүйенің қауіпсіздігін қамтамасыз ету

Мақалада құрылған жүйенің қауіпсіздігін құмтамасыз ету үшін NetDoctor модулін қолдану арқылы OPNET Modeler 14.5-те сымсыз абоненттік қатынас жүйесін модельдеу мен оны талдап және зерттеуге арналған. Коммутатордың негізгі кемшілігі — шығыстардың жіберу жолағының шектеулігі. Егер де белгілі бір шығысқа арналған коммутаторға келіп түсіп және оның жылдамдығы және өткізу қабілеттілігінен жоғары болса, пакеттердің қақтығысу проблемасы пайда болады. Бұл жағдайда коммутатор пакеттерді сақтауға немесе пакеттерді кезекке жібереді. Бұл жұмыста екі коммутациялайтын құрылғылардың қолданылуы арқылы, коммутацияланатын жергілікті-есептеуіш желілер құрылады: концентраторлар мен коммутаторлар. Концентратор кірісіне келіп түскен пакеттерді барлық шығыстарына жібереді. Әртүрлі желілерді талдау және модельдеу үшін коммерциялық түрінің қызметін атқаратын OPNET Modeler v.14.5 қолданбалы бағдарламасы пайданылады. Бұл бағдарламада дайын модельдердің көптігіне байланысты қазіргі таңдағы барлық байланыстырушы желілерді модельдеуге және олардың кірістерін өзгертуге мүмкіндік береді.Сонымен қатар OPNET Modeler 14.5 бағдарламасы мен оның кеңейтілуіндегі жергілікті-есептеуіш желілерді модельдеудің тәсілдері мен кеңейтілеген коммутацияланған желілерді зерттеу қарастырылды. Бұл жұмысты зерттеу кезіндегі желілердің жұмыс істеуін тексеру және үлкен коммутацияланатын желілерді құру үшін қолдануға болады.

Кілт сөздер: OPNET Modeler v.14.5 сымсыз жергілікті желі, қосымшалар пакеті, жергілікті желілер, NetDoctor, трафик, модельдеу.

М.З. Якубова, Т.Г. Сериков

Обеспечение безопасности сетей на основе пакета прикладных программ OPNET Modeler v.14.5 с использованием модуля NetDoctor

Статья посвящена моделированию в OPNET Modeler v.14.5 беспроводной сети абонентского доступа, для ее анализа и исследования при использовании и применения модуля NetDoctor для обеспечения безопасности построенной сети. Авторы создавали коммутированные локально-вычислительные сети, с использованием двух различных коммутирующих устройств: концентраторов и коммутаторов. Концентратор передает пакет, прибывший на один из его входов, на все выходы вне зависимости от назначения пакета. Для анализа и моделирования разнообразных сетей применялся пакет прикладных программ OPNET Modeler 14.5, исполняющий собой роль коммерческой версии, предлагаемой бесплатно для использования в образовательных целях. В связи с тем, что у него большая библиотека различных готовых моделей используемых объектов по оборудованию, можно моделировать почти все существующие на сегодняшний момент сети связи и при моделировании можно изменять входные параметры модели. Также рассмотрены методы моделирования локально-вычислительных сетей на OPNET Modeler 14.5 с последующим ее расширением и проведены исследования моделированной расширенной коммутированной сети. Данную работу можно использовать при проведении исследования функционирования сетей с коммутаторами и при построении крупных коммутируемых сетей.

Ключевые слова: OPNET Modeler 14.5, беспроводная локальная сеть, пакет прикладных программ, локально-вычислительные сети, NetDoctor, трафик, моделирование.

References

1 Yakubova, M.Z. (2016). Issledovanie MPLS setei na osnove postroeniia imitatsionnykh modelei [Study of MPLS networks based on the building of simulation models]. *Vysshaia shkola – High School, No. 3,* 13– 23 [in Russian].

2 Yakubova, M.Z. (2016). Immitatsionnoe modelirovanie kommutirovannykh system LVS [Simulation modeling of the switched LAN]. *Vysshaia shkola – High School, No. 3,* 30–40 [in Russian].

3 Kislov, D.V. (2007). IP-telefoniia, mobilnye telephony [IP-Telephony, mobile phones]. *HrossMedia – GrossMedia* [in Russian].

4 Sait zhurnala «Tehnolohii OPNET». [Sait of the magazine «OPNET Technologies»]. *opnet.com.* Retrieved from http://www.opnet.com/services/university/ itguru_acadmic_edition.html [in Russian].

ФИЗИКАНЫ ОҚЫТУ ӘДІСТЕМЕСІ
МЕТОДИКА ФИЗИКИ
METHODOLOGY OF PHYSICS

DOI 10.31489/2019Ph 3/71-77

UDC 378.016

A.B. Iskakova[1], A.K. Kairbayeva[2]

[1]Abai Kazakh National Pedagogical University, Almaty, Kazakhstan;
[2]S. Toraighyrov Pavlodar State University, Kazakhstan
(E-mail: anar_is@mail.ru)

Methodical foundations of the use of project-based technologies in teaching physics to students of technical specialties of higher education institutions

The presented work is devoted to the issues of using project technologies of training in higher education institution based on information technology. The training of highly qualified competitive specialists is the main task for all higher educational institutions. In other words, a graduate of a higher educational institution should design highly efficient, technically advanced engineering systems, analyze the effectiveness of a project in comparison with other projects. The question arises of how to prepare such a specialist in the conditions when the current educational system often lags behind the processes taking place in the global space. In this regard, the authors attach special importance to mini-projects that can be carried out in a short time, while these projects build students' skills such as group work, teamwork management, project reporting, design and research skills. The paper also proposes a general structure of the educational project for one semester. This describes the experience of using the computer program Electronics Workbench version 512 in teaching physics to students of technical specialties. The questions of the effectiveness of innovative creativity of students in the performance of tasks of the mini-project in the course of physics are considered on the example of the simulation of the operation of oscillatory circuits – serial and parallel.

Keywords: project-based training technology, educational project, serial oscillation circuit, parallel oscillation circuit, resonance.

Introduction

The bachelor in the technical field needs to not only possess professional knowledge and skills in its field, but also to have professional competence in design and management activities, that is, be able to apply knowledge and design methods and project management elements when solving professional problems. The attitude to the future specialty is largely determined by the nature of the educational work in which future professional activity must be modeled in a certain way.

Therefore, for the successful formation of bachelors' professional competence, project-based training is the most suitable technology. The basis of this technology is the development of cognitive, creative skills, the ability to independently construct their knowledge, the ability to navigate in the information space, the development of critical thinking.

Main part

Currently, training in higher education involves the wide use of innovative educational technologies: credit, modular, design, problem, etc., which act as methodological foundations of the educational process in a modern university. The idea of project-based training is becoming increasingly popular in the univer-

sity environment. Many authors are developing project models of teaching at the university, which involve the technology of project-based training and building individual trajectories [1, 2].

The project technology is based on the theoretical concepts of «pragmatic pedagogy», which was founded by the eminent American philosopher and educator John Dewey (1859–1952). According to his theory, true and valuable is only that which is useful to people, which gives practical results and is directed to the benefit of the whole society. The main provisions of J. Dewey's theory look as follows:

– in ontogenesis, the child follows the mankind path in cognition development;
– the assimilation of knowledge is a spontaneous uncontrollable process;
– for the assimilation of knowledge, students should be exposed to problem-solving tasks that are real life and meaningful for him;
– training should be conducted through the students' appropriate cognitive and project-based activities, consistent with their personal interests;
– the child learns the material, not just while listening or perceiving the senses, but also due to his need for knowledge.

In natural science undergraduate programs, laboratory work in the general course and special sections of physics plays a very important role. The main idea of laboratory work is the unity of theoretical and practical knowledge, the development of research skills, and the ability to demonstrate acquired knowledge while doing laboratory work. Nevertheless, researchers consider that the traditional method of laboratory work set uphas a number of didactic imperfections. They are as follows: when performing and defending laboratory works, the students do not work independently; the exchange of research results is only between two students, that is, the participants in the laboratory class are isolated [3]; the requirements for the preparation of various categories of graduates are not fulfilled [4]. In this regard, the authors propose the following solutions to this didactic problem – the use of elements of design training technology in the organization of frontal works; conducting a multi-level laboratory workshop using the project-based method.

The concepts and laws of physics studied in the logic of other training courses are not foreign to their conceptual system and cannot be perceived as secondary. It can also be argued that teaching physics is a basic component of the content of the preparation of a future engineer, economist, physics teacher, etc. This means that the following didactic formula applies to it: every basic component of education, for example, as a composite physical practicum, is included in the content of education as a special didactic tool, and not as «additives» in separate chapters and sections. And in this regard, the question arises about how to improve the concept. That is, the improvement on the basis of computer technologies of teaching methods in traditional disciplines of subject preparation of the future engineer based on the internal and external level of coordination of the fundamental and general disciplines of technical specialties of a higher educational institution (physics, chemistry, computer science, mathematics, foreign language, economics, etc.). The internal level is understood as the coordination of separate sections, symbolic designations, the contents of work programs. The external level of coordination contains the psychological and didactic aspects of choosing one or another approach to learning (problem-oriented, project-oriented, context-sensitive, etc.) [5]. The use of computer applications, technologies not only contributes to a more complete implementation of the fundamental goals of these disciplines, but also leads to a more complete and in-depth analysis of physical phenomena and understanding of physics and, in essence, changes the content of training.

Laboratory works are an effective environment for implementing the technology of project-based teaching physics in technical specialties of a higher educational institution. Their use contributes to the formation of a sustainable engineer methodologically motivated and oriented interest in teaching physics, the ability to reclaim and use its scientific content as a methodological experimental and technological means of innovative engineering activity. Despite the high significance of the problem, its comprehensive solution does not exist until now. The organization of a methodological orientation of the educational process in physics is required in that part that concerns the support of an experiment that substantially expands the scope of training and educational research of students.

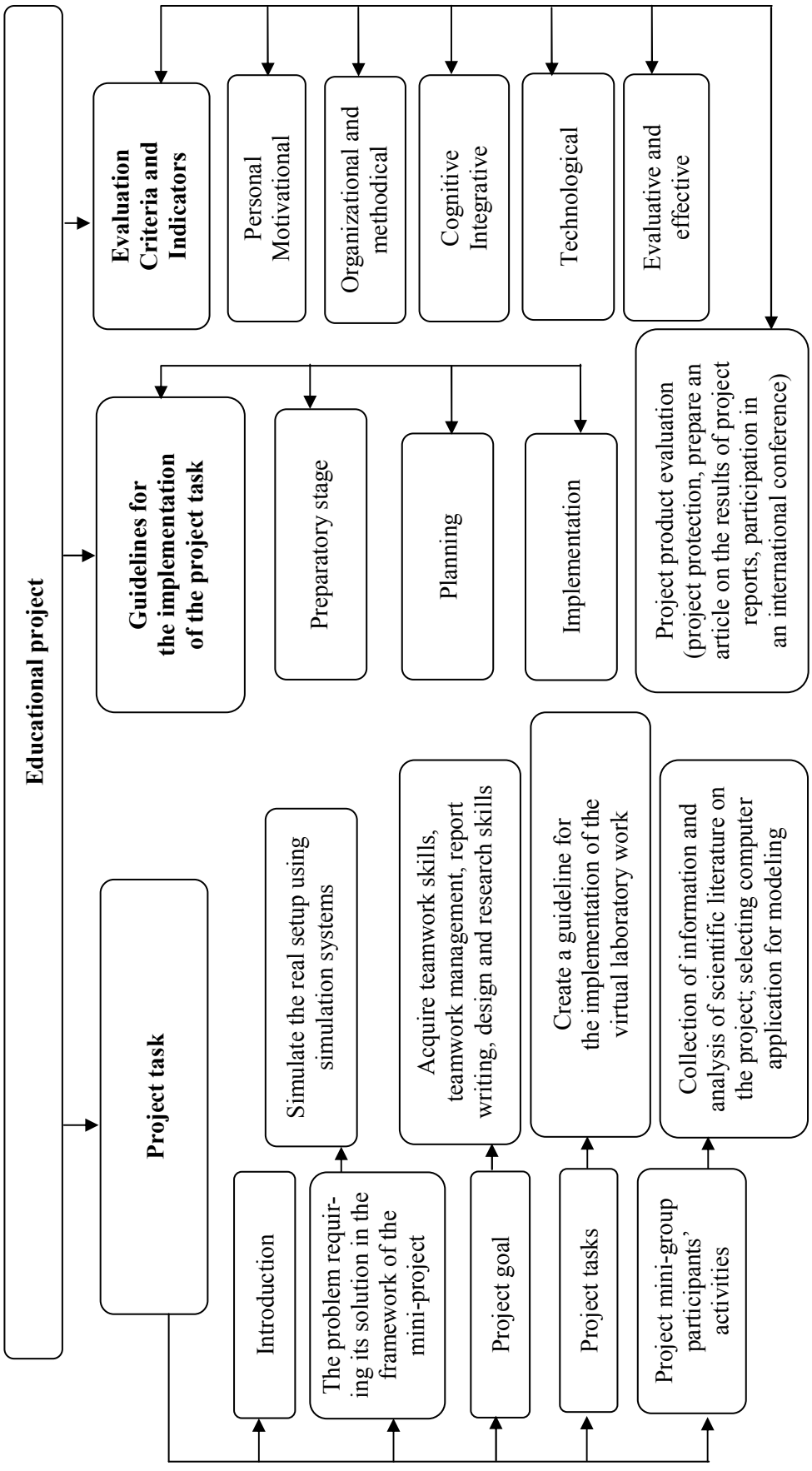

Figure 1. Structure of Educational Project

V. Larionov and A. Leader in their works argue that the combination of virtual and real experiment and simulation in a physical workshop is the main element of the project activity and is necessary in the educational laboratory of the new generation educational laboratory in physics [6]. Taking into account the specifics of a technical specialty when teaching students in physics, which lasts for 2 semesters, educational projects can be compiled on topics that form the professional competencies of the future engineer. The number of participants in mini-projects may consist of 3-5 students. Students themselves can choose the group where they would like to work together and carry out the project. Of course, the teacher, given the abilities of each participant, can make changes in mini-groups. The purpose of the educational project is to create conditions under which students, working in various mini-groups, develop:

– communication skills;
– problem-solving skills;
– the skill of finding information from various sources [7];
– research skills, which include such issues as identifying problems, collecting information, observing, conducting experiments, analyzing, building hypotheses, generalizing);
– systems thinking skills.

In this regard, we propose a general structure of the educational project (Fig. 1).

The use of design technologies with the use of information technologies in teaching physics is given in the works of N. Shiyan, I. Kiseleva, O. Alykova, and others [8–10].

Using this structure of the mini-project, various works were performed by students of the specialty Instrument Making and Information Systems. Let us show one example on the topic «Oscillatory circuit. Free and forced electromagnetic oscillations. Resonance». Electronics Workbench system was used as an application program. With the help of the Electronics Workbench system, students developed a virtual model of the operation of oscillatory circuits – serial and parallel type [11].

The scheme for determining the amplitude-frequency characteristic of a parallel circuit is shown in Figure 2.

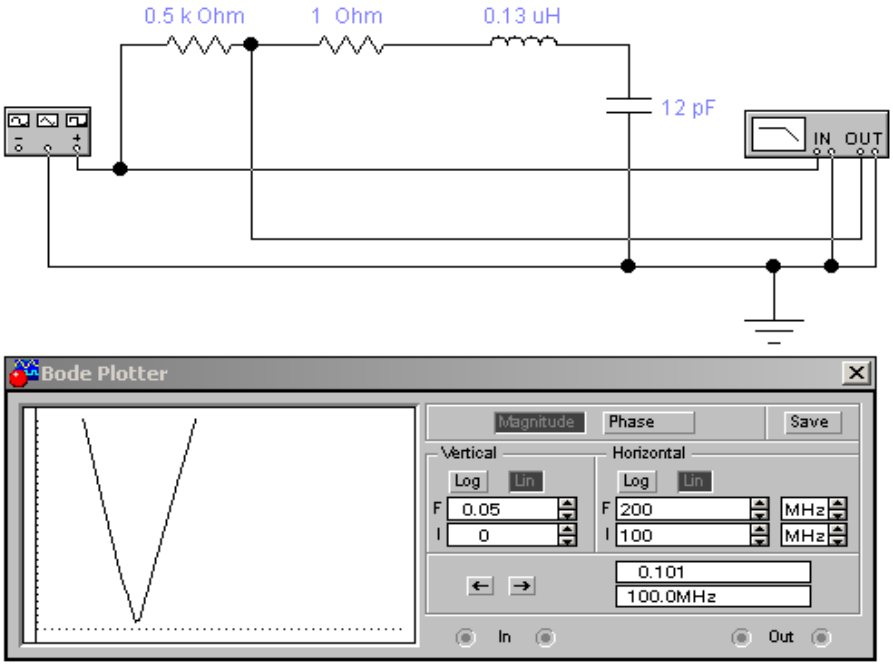

Figure 2. The scheme of obtaining the amplitude-frequency response of the serial circuit and the amplitude-frequency response of the serial oscillating circuit

The quality factor and the resonant frequency of the serial circuit with the parameters shown in the diagram:

$$\nu = \frac{1}{2\pi\sqrt{L \cdot C}} = \frac{1}{2 \cdot 3{,}14\sqrt{0{,}13 \cdot 10^{-6} \cdot 12 \cdot 10^{-12}}} = 128 \text{ Mhz},$$

$$Q = \frac{2\pi \cdot \nu \cdot L}{r} = \frac{2 \cdot 3{,}14 \cdot 128 \cdot 10^{6} \cdot 0{,}13 \cdot 10^{-6}}{1} = 104 .$$

The diagram for determining the amplitude-frequency characteristic of a parallel circuit is shown in Figure 3. Quality factor and resonant frequency of the serial circuit with the parameters indicated on the diagram:

$$\nu = \frac{1}{2\pi\sqrt{L \cdot C}} = \frac{1}{2 \cdot 3{,}14\sqrt{0{,}13 \cdot 10^{-6} \cdot 15 \cdot 10^{-12}}} = 110 \text{ Mhz}$$

$$Q = \frac{R}{2\pi \cdot \nu \cdot L} = \frac{10600}{2 \cdot 3{,}14 \cdot 150 \cdot 10^{6} \cdot 0{,}13 \cdot 10^{-6}} = 100{,}2$$

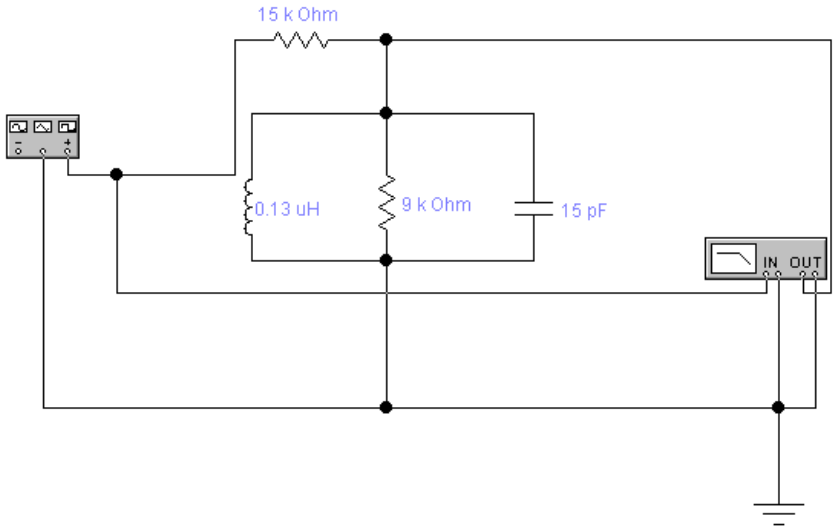

Figure 3. The scheme of obtaining the amplitude-frequency characteristics of the parallel oscillatory circuit

Amplitude-frequency characteristic of a parallel circuit on the screen of a virtual oscilloscope is obtained (Fig. 4).

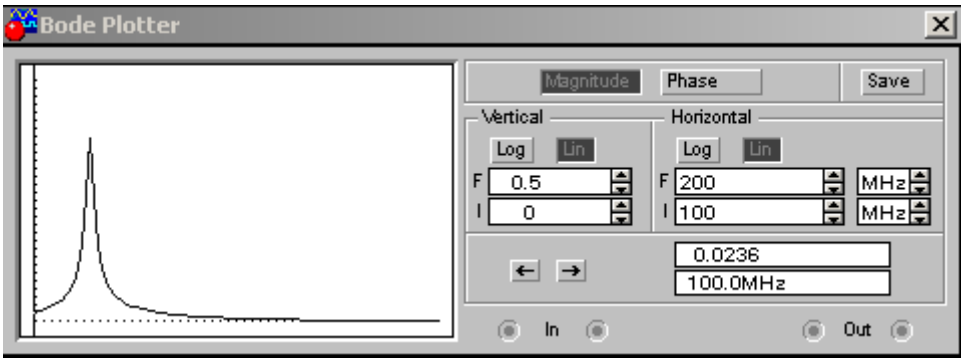

Figure 4. Amplitude-frequency characteristic of the parallel circuit

Conclusion

Thus, the student, working in the information system of modeling Electronics Workbench and showing innovative creativity in the design and modeling of the principle of operation of various electrical circuits, shows sufficient performance of the mini-project.

Of course, at the laboratory work it is impossible to develop a full educational project. Therefore, classes are conducted as full-scale laboratory work, the results of which are used in the implementation of the educational project for comparison with the results obtained on virtual instruments. At the laboratory work, the main methodological guidelines are provided for the educational projects.The main part of the mini-project is performed during the tutorial.

References

1 Дворецкий С. Формирование проектной культуры // Высшее образование в России. — 2003. — № 4. — С. 15–22.

2 Ильин Г.Н. Проективное образование и становление личности // Высшее образование в России. — 2001. — № 4. — С. 85–92.

3 Стародубцов В.А. Лабораторный практикум по курсу физики как проектная обучающая среда // Вестн. ТГПУ. — 2012. — № 4. — С. 151–154.

4 Маслова Ю.В. Профессиональная подготовка студентов радиофизического факультета в рамках лабораторного комплекса «Волоконно-оптические линии связи» [Электронный ресурс] / Ю.В. Маслова, Е.А. Румбешта, А.П. Коханенко // Вестн. ТГПУ. — 2015. — № 8. — С. 120–125. Режим доступа: https://elibrary.ru/item.asp? id=24075535

5 Ларионов В.В. Лабораторно-проектные работы в системе физического практикума технических университетов / В.В. Ларионов, С.Б. Писаренко, А.М. Лидер // Физическое образование в вузах. — 2007. — Т. 13, № 2. — С. 69–77. — Режим доступа: https://elibrary.ru/item.asp? id=9935952 (дата обращения: 1.02.2019).

6 Ларионов В.В. Создание универсального стандарта для выполнения проектно-ориентированных лабораторных работ по физике [Электронный ресурс] / В.В. Ларионов, А.М. Лидер // Фундаментальные исследования. — 2013. — № 6–4. — С. 985–989; URL: Режим доступа https://elibrary.ru/item.asp? id=19043030 (дата обращения: 1.02.2019).

7 Зайнуллина Ф.К. Проектный метод обучения в формировании мотивации образовательного процесса студентов / Ф.К. Зайнуллина // Вестн. КАЗГУКИ. — 2016. — № 4. — С. 164–166.

8 Шиян Н.В. Системные изменения обучения физике в условиях обновления общего образования: дис. ... д-ра пед. наук / Н.В. Шиян. — СПб., 2005. — С. 404.

9 Киселева И.А. Развитие познавательного интереса студентов на основе кластерного подхода в проектной деятельности: дис. ... канд. пед. наук / И.А. Киселева. — Тамбов, 2011. — С. 208.

10 Алыкова О.М. Проектный метод как средство подготовки к будущей профессиональной деятельности [Электронный ресурс] / О.М. Алыкова, А.М. Лихтер, В.В. Смирнов // Изв. РАН. Сер. Физическая. — 2013. — № 10. — С. 1499–1502. — Режим доступа: https://doi.org/10.7868/S0367676513100037

11 Godse, A.P. Electronic Cicuits — II / Godse, A.P., Bakshi U. A. India: Technical Publications, 2010. — 680 p. — ISBN 9788184317688.

А.Б. Искакова, А.К. Каирбаева

Жобалық технологияларды жоо-ның техникалық мамандықтарында білім алатын студенттерге физиканы оқытуда қолданудың әдістемелік негіздері

Мақала жоғарғы оқу орнында жобалық технологияларды ақпараттық технологиялар негізінде қолдану мәселелеріне арналған. Қазіргі уақытта жоғарыбілікті, бәсекеге қабілетті мамандарды даярлау барлық жоғарғы оқу орындарының ең басты міндеттерінің бірі болып табылады. Басқаша айтқанда, жоғарғы оқу орнының түлегі тиімділігі жоғары техникалық жағынан мінсіз болатын инженерлік жүйелерді жобалай, жобаның басқа жобалармен салыстырғандағы тиімділігіне талдау жасай білу керек. Осындай мамандарды қалай даярлау керектігі жайлы сұрақ туындайды. Сол себепті авторлар қысқа уақыт аралығында жүргізуге болатын, минижобалардың негізгі ерекшеліктеріне аса көңіл бөлді. Сонымен қатар авторлар ұсынылып отырған жобалардың студенттердің бойында топта жұмыс жасай білу, ұжымдық топты басқара білу, жобаның есебін дайындай білу, жобалық-зерттеушілік іс-әрекет дағдыларын қалыптастыруға мүмкіндік беретін инновациялық технологиялардың бірі екендігі жайлы айтады. Бұл жобаларды бір семестр аралығында орындаудың жалпы құрылымы келтірілді. Техникалық мамандықтарында білім алатын студенттеріне физиканы оқыту барысында Electronics Workbench 512 қолданбалы компьютерлік бағдарламасын қолданудың тәжірибесі келтірілді.

Кілт сөздер: жобалық оқыту технологиясы, оқу жобасы, тізбекті тербелмелі контур, параллель тербелмелі контур, резонанс.

А.Б. Искакова, А. К. Каирбаева

Методические основы использования проектных технологий при обучении физике студентов технических специальностей вуза

Статья посвящена вопросам использования проектных технологий обучения в высшем учебном заведении на основе информационных технологий. Подготовка высококвалифицированных конкурентоспособных специалистов является основной задачей для всех высших учебных заведений. Другими словами, выпускник высшего учебного заведения должен проектировать высокоэффективные, технически совершенные инженерные системы, анализировать эффективность проекта в сравнении с другими проектами. Возникает вопрос о том, как подготовить такого специалиста в условиях, когда действующая система образования нередко отстает от процессов, происходящих в мировом пространстве.

В связи с этим авторы уделяют особое значение на минипроекты, которые можно проводить за короткое время, при этом эти проекты формируют у студентов такие навыки, как работа в группе, управление коллективной работой, составление отчета проекта, навыки проектно-исследовательской деятельности. Также в работе предложена общая структура проведения учебного проекта на протяжении одного семестра. При этом описывается опыт использования компьютерной программы Electronics Workbench версии 512 в обучении физике студентов технических специальностей. Рассмотрены вопросы эффективности инновационного творчества студентов при выполнении заданий минипроекта по дисциплине «Физика» на примере моделирования работы колебательных контуров – последовательного и параллельного типов.

Ключевые слова: технология проектного обучения, учебный проект, последовательный колебательный контур, параллельный колебательный контур, резонанс.

References

1 Dvoretzsky, S. (2003). Formirovanie proektnoi kultury [Formation of project culture]. *Higher Education in Russia, No. 4,* 15–22 [in Russian].

2 Ilyin, G. (2001). Proektivnoe obrazovanie i stanovlenie lichnosti [Projective education and the formation of personality]. *Higher Education in Russia, no. 4,* 85–92 [in Russian].

3 Starodubtzov, V.A. (2012). Laboratornyi praktikum po kursu fiziki kak proektnaia obuchaiushchaia sreda [Laboratory Workshop on Physics as a Project Learning Environment]. *Vestnik THPU – Bulletin of Tomsk State pedagogical university 4,* 151–154 [in Russian].

4 Maslova, Yu., Rumbeshta, E., & Kokhanenko, A. (2015). Professionalnaia podhotovka studentov radiofizicheskoho fakulteta v ramkakh laboratornoho kompleksa «Volokonno-opticheskie linii sviazi» [Professional training of students of the Faculty of Radio Physics in the framework of the laboratory complex «Fiber-optical communication lines»]. *Vestnik THPU – Bulletin of Tomsk State pedagogical university, No. 8,* 120–125. Retrieved from https://elibrary.ru/item.asp? id=24075535 [in Russian].

5 Larionov, V., Pisarenko, S., & Leder, A. (2007). Laboratorno-proektnye raboty v sisteme fizicheskoho praktikuma tekhnicheskikh universitetov [Laboratory and design work in the system of physical practicum of technical universities]. *Physical education in universities, Vol. 13, No. 2,* 69–77. Retrieved from https://elibrary.ru/item.asp? id=9935952 [in Russian].

6 Larionov, V., & Leder A. (2013). Sozdanie universalnoho standarta dlia vypolneniia proektno-orientirovannykh laboratornykh rabot po fizike [Creating a universal standard for performing design-oriented laboratory work in physics]. *Basic research, No. 6,* 985–989. Retrieved from https://elibrary.ru/item.asp? id=19043030 [in Russian].

7 Zainullina, F. (2016). Proektnyi metod obucheniia v formirovanii motivatsii obrazovatelnoho protsessa studentov [Project training method in shaping the motivation of the educational process of students]. *Vestnik KAZHUKI – Bulletin of Kazan State University of culture and arst, No. 4,* 164–166 [in Russian].

8 Shiyan, N.V. (2005). Sistemnye izmeneniia obuchenia fizike v usloviiiakh obnovleniia obshcheho obrazovaniia [Systemic changes in teaching physics in the context of updating general education]. *Doctor's thesis.* Saint-Petersburg [in Russian].

9 Kiseleva, I.A. (2011). Razvitie poznavatelnoho interesa studentov na osnove klasternoho podkhoda v proektnoi deiatelnosti [Development of students' cognitive interest based on a cluster approach in project activities]. *Candidate's thesis.* Tambov [in Russian].

10 Alykova, O.M., Likhter, A.M., & Smirnov V.V. (2013). Proektnyi metod kak sredstvo podhotovki k budushchei professionalnoi deiatelnosti [Project method as a means of preparing for future professional activities]. *News of the Russian Academy of Sciences. Physical series, No. 10,* 1499–1502. Retrieved from https://doi.org/10.7868/S0367676513100037 [in Russian].

11 Godse, A.P. & Bakshi, U.A. (2010). *Electronic Cicuits – II.* India: Technical Publications. ISBN 9788184317688.

DOI 10.31489/2019Ph 3/78-82

UDC 378.147:372,583

L.F. Ilina, A.S. Kayumova, Ye.R. Zhangbyrbaj, M.M. Bolatbekova

Ye.A. Buketov Karaganda State University, Kazakhstan
(E-mail: aneka.08@mail.ru)

To modernization of physical practicum on molecular physics in the university course

The article is devoted to analysis of the author's work results on the modernization of the physical practicum in Molecular Physics at the Department of physics and nanotechnologies of the physics and technical faculty. High-quality direction of such a physical practicum is impossible without the use of virtual laboratory work, but contact laboratory work is also necessary. Moreover, it is advisable to carry out some laboratory work both contact and virtually. This article presents the essence of work on gas laws and the definition of universal gas constant and Boltzmann constant; three virtual works on statistical physics and one contact laboratory work on transfer phenomena were analyzed. The works were preliminarily analyzed and carried out at the level of teachers and engineers, then by students, moreover of different groups both in the general physics course and in special courses of the corresponding profile. Graduate work and master's dissertation were carried out in some sections; reports were presented at conferences of different levels; published articles and educational and methodical materials.

Keywords: Maxwell distribution, Brownian motion, contact and virtual laboratory works, transfer phenomena.

The structure of the course of molecular physics at the university is as follows: an introduction to molecular physics, the definition of its content and features; molecular kinetic theory; its subject, method, characteristics; fundamentals of the statistical theory of ideal gases (mathematical apparatus, distribution; thermodynamics; transfer phenomena; real gases; molecular kinetic properties of liquids; solids; phase transitions) [1–4].

It is obvious that the physical practicum should be built and organized along the same structure. And this is not true.

Within the framework of one article, it is impossible to present the content of physical practicum in all sections of molecular physics. Let us stay on the first 3 blocks.

The first block includes 2 classical laboratory works: «Determination of the universal gas constant» and «Determination of the Boltzmann constant». These are contact laboratory works that are based on the equation of state of an ideal gas (the Mendeleev-Clapeyron equation) and the basic equation of the molecular-kinetic theory of ideal gases, namely, on one of its consequences, the pressure formula, i.e. 3 basic interconnected universal constants are immediately introduced: R; k (Boltzmann constant) and N_{Av} (Avogadro number).

The results we obtained (and the students), for example, are:

$$R = (8.1 \pm 0.4)\frac{\text{J}}{\text{mol} \cdot \text{K}},$$

i.e. relative fault:

$$\varepsilon = \frac{\Delta R}{R} \cdot 100\,\% \cong 5\,\%.$$

Confidence interval: (7.7 – 8.5) J/mol·K.

Thus, the theoretical value R = 8.31 J/mol·K «fits» into the confidence interval.

Boltzmann's constant:

$$k = (1.2 \pm 0.2) \cdot 10^{-22}\,\frac{\text{J}}{\text{K}}.$$

Relative fault:

$$\varepsilon = \frac{\Delta k}{k} \cdot 100\,\% \cong 17\,\%.$$

Confidence interval:

$$k = (1.0 - 1.4) \cdot 10^{-23} \frac{\text{J}}{\text{K}}.$$

Thus, the theoretical value k = $1.38 \cdot 10^{-23}$ J/K «falls» in the confidence interval, although the measurement error is quite significant.

The experimental setup we use is «assembled» manually and there is no need to rely on the best result [5].

The systems considered in molecular physics are statistical. When analyzing them, the corresponding mathematical apparatus is used: mathematical probability, probability theorems, the concept of averages, theorems of averages, ergodic hypothesis, deviations from the mean [6].

Neutral atoms and molecules obey classical statistics. This is the statistics of distinguishable particles energy of which varies continuously. The main Maxwellian distribution is the velocity or kinetic energy distribution of molecules and the Boltzmann distribution of potential energy molecules in a conservative force field, in particular in the field of the Earth. It is known that they received experimental confirmation several decades after the creation of corresponding theories. We are talking about the experiences of Stern and Perrin.

The velocity distribution of molecules (based on Stern's experiments) and the study of the distribution of Brownian particles in a gravity field and the determination of Boltzmann constant (based on Perrin's experiments) can only be considered using virtual laboratory works in our conditions, they were studied experimentally in due time in the periods from 1906 to 1908 (Perrin's experience) and from 1920 to 1929 (Stern's experience). These experiments are described in educational literature and are well known.

The virtual laboratory work on the Maxwell distribution was carried out in accordance with the MU proposed in [7]. Temperature 1500 K, and the angular velocity of rotation of the cylinder 1000 rad/sec were introduced. The velocities of the particles were set in arbitrary units from 0 to 25 with a step of 50,59 m/sec. Results are presented using a histograms. The experiments were repeated for another temperature (3000 K) with a speed step of 71.34 m/sec.

The results of measurements and calculations are presented in Figure 1.

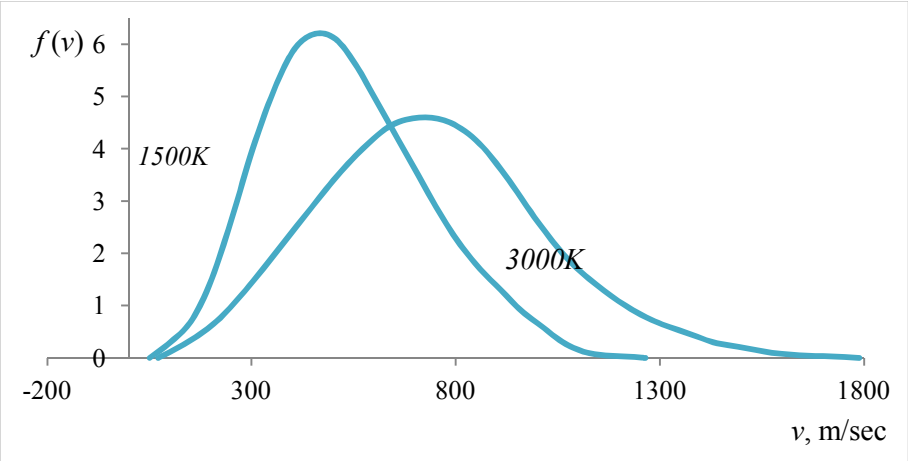

Figure 1. Maxwell distribution of molecules on velocities

The most probable velocities were calculated: in the first case 346 m/sec, in the second – 1264 m/sec.

In addition, students were asked to calculate the molar mass of the filament coating in the experimental setup. Calculations showed that we are talking about silver. It is known from literary sources that silver was used in the first installations of Stern.

On the experiments of Perrin based virtual laboratory work devoted to the study of the distribution of Brownian particles in the field of gravity of the Earth. In the well-known experiments of Perrin, Brownian particles were used in the form of balls (these are gummigut particles) suspended in the environment. In this case, two more conditions were fulfilled: in each experimental series, particles of the same size were used, for which Perrin designed and practically used microcentre. This, firstly, and secondly, the density of the substance of Brownian particles and the environment must be chosen so that the Brownian particles are sus-

pended. In different series of experiments different problems were solved. In one of them, the Avogadro number was calculated on the basis of the Boltzmann distribution. In our chosen laboratory work, the Boltzmann constant was determined.

As an environment was used water ($\rho_0 = 10^3 kg/m^3$); petrol ($\rho_0 = 0{,}88 \cdot 10^3 kg/m^3$); alcohol ($\rho_0 = 790 kg/m^3$). The density of the substance of Brownian particles was set: ($\rho_0 = 1{,}1 \cdot 10^3 kg/m^3$).

To determine the diameter of Brownian particles, a chain is built from them and the total length is measured. The diameter of Brownian particles is d = 0.5 mcm. The number of Brownian particles was determined at zero height and at altitudes: 30 mcm; 60 mcm.

Based on the Boltzmann formula for Brownian particles in a layer of volume $S\Delta h$:

$$\Delta N = n_0 e^{-\frac{\Delta\rho Vgh}{RT}} S\Delta h, \tag{1}$$

where n_0 — concentration of Brownian particles at zero height,

$\Delta\rho$ — density difference between Brownian particles and the environment;

V — Brownian particle volume.

Hence, the Boltzmann constant was determined:

$$k = \frac{\Delta\rho Vgh}{T \ln \frac{n_0}{n}}, \tag{2}$$

The results are:

in water: $k = 1.33 \cdot 10^{-23}$ J/K;

in petrol: $k = 1.17 \cdot 10^{-23}$ J/K;

in alcohol: $k = 1.97 \cdot 10^{-23}$ J/K.

The best result in measurements in water (it was in this environment that Perren's original experiments were conducted), the worst of all is in alcohol.

But in any case, the result is better than the contact definition of the Boltzmann constant.

One of the experimental bases and experimental confirmations of the foundations of the molecular-kinetic theory is the Brownian motion. Therefore, of particular interest is the virtual laboratory work on the determination and analysis of the average free path of Brownian particles [8].

It is known that

$$<\lambda>=\frac{1}{\sqrt{2}\pi d_{eff}{}^2 n} \tag{3}$$

where $<\lambda>$ — average length of free path;

$<d_{eff}>$ — effective diameter (for molecules);

n — their concentration.

The average number of collisions of molecules with other molecules per unit of time is determined as follows:

$$<z>=\frac{<v>}{<\lambda>}, \tag{4}$$

where <v> — average velocity of chaotic particle motion.

Enter the number of particles equal to 25, and the diameter of 350 conventional units at a temperature of T = 1000K.

Conduct 5-6 experiments, changing the diameter from 350 to 100 conventional units, and the number of particles from 25 to 5.

Build graphs of the dependence of $<\lambda>$ on d with n=const (Fig. 2) and $<\lambda>$ on n with d=const (Fig. 3).

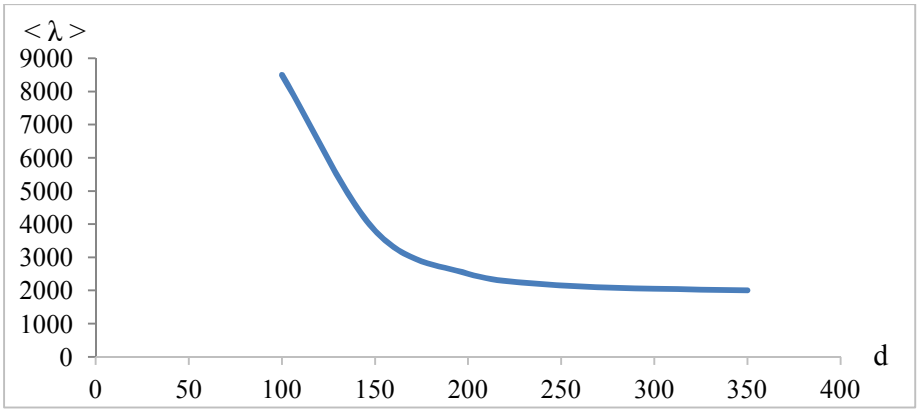

Figure 2. Dependence of average length of free path on the particle diameter at n = const

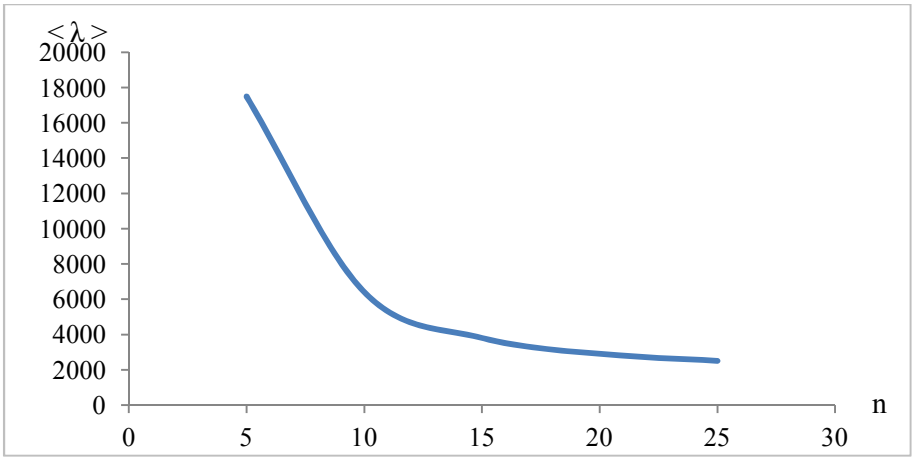

Figure 3. Dependence of average length of free path of particles on their concentration atd = const

Of particular importance in the study of molecular physics are transfer phenomena. Let us stay on one classic laboratory work: «Determination of the coefficient of internal friction of a fluid by the Stokes method». The experimental setup is a long cylindrical glass vessel filled with glycerin. Studying the movements of solid balls of small radius, which are affected by the force of gravity, the buoyant force and the force of internal friction, determined by the Stokes formula.

Work is quite classical, with proper contact and its implementation gives the value of the coefficient of viscosity of glycerol, corresponding to the theoretical.

Work on the modernization of the physics laboratory in molecular physics has been carried out for several years, but it was carried out not systematically, and most importantly, without the active involvement of virtual laboratory work.

The result of the work will be the creation of a physical practicum, covering all basic sections of molecular physics and the publication of relevant guidelines.

References

1 Матвеев А.И. Молекулярная физика / А.И. Матвеев. — М.: Высш. шк., 1987.

2 Иродов И.Е. Физика макросистем. Основные законы / И.Е. Иродов. — М.; СПб.: Лаборатория баз знаний, 2001.

3 Кикоин И.К. Молекулярная физика / И.К. Кикоин, А.К. Кикоин. — М.: Наука, 1976.

4 Телеснин Р.В. Молекулярная физика / Р.В. Телеснин. — М.: Высш. шк., 1973.

5 Физический практикум; Механика и молекулярная физика / под ред. В.И. Ивероновой. — Ч. 1. — 1988.

6 Ильина Л.Ф. Физика. Механика и молекулярная физика: учеб.- метод. пос. / Л.Ф. Ильина, Л.С. Бадаева. — Караганда: Изд-во КарГУ, 2014.

7 Толстик А.М. Виртуальные лабораторные работы / А.М. Толстик. — Томск: Томск. ун-т, 2007.

8 Жанбырбай Е.Р. Система организации СРС и СРСП на примере раздела «Явления переноса» / Е.Р. Жанбырбай, Л.Ф. Ильина // Вестн. Караганд. ун-та. Сер. Физика. — 2018. — № 3 (91). — С. 93–102.

Л.Ф.Ильина, А.С.Каюмова, Е.Р.Жаңбырбай, М.М.Болатбекова

Жоғарғы оқу орны курсында молекулалық физика бойынша физпрактикумның модернизация мәселесі

Мақала физика және нанотехнологиялар кафедрасында молекулалық физика бойынша физикалық практикумды жаңғыртуына байланысты авторлардың жұмыстарының нәтижелерін талдауға арналған. Мұндай физикалық практикумды сапалы орындау үшін виртуалды зертханалық жұмыстарды пайдаланбау мүмкін емес, бірақ түйіспелі зертханалық жұмыстар да қажет. Сонымен қатар кейбір зертханалық жұмыстарды түйіспелі және виртуалды түрде орындау қажет. Мақалада газ заңдары мен әмбебап газ тұрақтысы және Больцман тұрақтысын анықтау бойынша жұмыстардың мәні баяндалған; статистика бойынша үш виртуалды жұмыс және тасымалдау құбылыстары бойынша бір түйіспелі зертханалық жұмыс талданды. Жұмыстар алдын ала талданып, оқытушылар мен инженерлер деңгейінде, одан кейін жалпы физика курсында, сондай-ақ тиісті бейіндегі арнайы курстарда әртүрлі топтарда жүргізілді. Кейбір бөлімдер бойынша дипломдық жұмыстар мен магистрлік диссертациялар орындалды; түрлі деңгейдегі конференцияда баяндамалар ұсынылды; мақалалар мен оқу-әдістемелік құралдар жарияланды.

Кілт сөздер: максвелл түрлендіруі, броундық қозғалыс, түйіспелі және виртуалды зертханалық жұмыстар, тасымалдау құбылыстары.

Л.Ф. Ильина, А.С. Каюмова, Е.Р. Жанбырбай, М.М. Болатбекова

К модернизации физпрактикума по молекулярной физике в вузовском курсе

Статья посвящена анализу результатов работы авторов по модернизации физпрактикума по молекулярной физике на кафедре физики и нанотехнологий физико-технического факультета. Качественная постановка такого физпрактикума невозможна без использования виртуальных лабораторных работ, но контактные лабораторные работы также необходимы. Более того целесообразно некоторые лабораторные работы выполнять как контактно, так и виртуально. Авторами изложена суть работ по газовым законам и определению универсальной газовой постоянной и постоянной Больцмана; проанализированы три виртуальные работы по статистической физике и одна контактная лабораторная работа по явлениям переноса. Работы предварительно анализировались и выполнялись на уровне преподавателей и инженеров, затем студентами, причем разных групп как в курсе общей физики, так и в спецкурсах соответствующего профиля. По некоторым разделам выполнялись дипломные работы и магистерские диссертации; представлялись доклады на конференциях разных уровней; опубликованы статьи и учебно-методическое пособие.

Ключевые слова: максвелловское распределение, броуновское движение, контактные и виртуальные лабораторные работы, явления переноса.

References

1 Matveev, A.I. (1987). *Molekuliarnaia fizika [Molecular physics]*. Moscow: Vysshaia shkola [in Russian].

2 Irodov, I.E. (2001). *Fizika makrosistem. Osnovnye zakony [Physics of macrosystems. Basic laws]*. Moscow-Saint-Petersburg: Laboratoriia bazovykh znanii [in Russian].

3 Kikoin, I.K., & Kikoin, A.K. (1976). *Molekuliarnaia fizika [Molecular physics]*. Moscow: Nauka [in Russian].

4 Telesnin, R.V. (1973). *Molekuliarnaia fizika [Molecular physics]*. Moscow: Vysshaia shkola [in Russian].

5 Iveronova, V.I. (1988). *Fizicheskii praktikum. Mekhanika i molekuliarnaia fizika [Physical practicum. Mechanics and Molecular physics]*. Moscow: Nauka [in Russian].

6 Ilina, L.F., & Badaeva, L.S. (2014). *Fizika. Chast 1. Mehanika. Molekulyarnaia fizika. [Physics. Part 1. Mechanics. Molecular physics]*. Karaganda: Izdatelstvo Karahandinskoho hosudarstvennoho universiteta [in Russian].

7 Tolstik, A.M. (2007). *Virtualnye laboratornye raboty [Virtual laboratory works]*. Tomsk: Tomskii universitet [in Russian].

8 Zhangbyrbaj, Ye.R., & Ilina, L.F. (2018). Sistema orhanizatsii SRS i SRSP na primere razdela «Yavleniia perenosa» [The system of organization of the IWS and IWST studies by the example of «Transport phenomena»]. *Vestnik Karahandinskoho universiteta. Seriia fiziki – Bulletin of the Karaganda University, Physics Series, 3(91)*, 93–102 [in Russian].

ЕСКЕ АЛУ
ПАМЯТИ УЧЕНОГО
IN MEMORY OF THE SCIENTIST

Жизнь, посвященная науке

7 мая 2019 г. после тяжелой продолжительной болезни ушел из жизни доктор педагогических наук, профессор, академик Академии педагогических наук Республики Казахстан Арынгазин Канапия Мубаракович.

Вся жизнь Канапии Мубараковича была посвящена служению педагогической науке. Свой трудовой путь он начал школьным учителем физики и математики после окончания казахской средней школы Майского района Павлодарской области в 1952 г. В 1954–1955 гг. был избран секретарём райкома комсомола Майского района. С 1955 по 1958 гг. являлся курсантом Первого Чкаловского военно-авиационного училища лётчиков в г. Оренбурге, в котором, кстати, учился первый космонавт Ю.А. Гагарин.

Однако любовь к педагогическому труду оказалась сильнее, и в 1958 г. Канапия Мубаракович поступает в Казахский педагогический институт имени Абая, по окончании которого в 1963 г. был направлен на работу в Карагандинский педагогический институт. Затем была учеба в аспирантуре Казахского государственного университета имени С.М. Кирова и защита кандидатской диссертации, после чего К.М. Арынгазин вновь возвращается в Караганду, где сначала работает заместителем декана, затем деканом физико-математического факультета.

В 1972 г. Карагандинский педагогический институт был преобразован в университет, и Канапия Мубаракович, будучи первым деканом уже физического факультета университета, а затем и заведующим кафедрой теоретической физики, внес значительный вклад в его становление и развитие. К.М. Арынгазин более 10 лет являлся деканом ФПК ОНО КарГУ, проректором по науке ИПК РО при КарГУ и заведующим кафедрой педагогического менеджмента.

В 2001 г. успешно защитил диссертацию на соискание учёной степени доктора педагогических наук, в 2005 г. был избран действительным членом Академии педагогических наук Казахстана. В последние годы жизни являлся профессором кафедры физики и нанотехнологий.

Вклад К.М. Арынгазина в развитие образования Республики Казахстан получил высокую оценку: он награжден 4 медалями, Знаком отличника образования КазССР, Грамотой Минвуза КазССР.

Им были опубликованы более 160 печатных работ, 7 монографий, часть из них — в дальнем зарубежье. Его книги по смысловой педагогике для естественнонаучных дисциплин пользуются большим спросом не только в Казахстане, но и далеко за пределами страны. На протяжении многих лет он являлся членом коллегии Карагандинского областного департамента образования, Ученого совета КарГУ, Объединенного диссертационного совета по защите докторских диссертаций по специальности «Общая педагогика, история педагогики и образования, этнопедагогика и профессиональное образование» при КарГУ им. Е.А. Букетова, членом редакционной коллегии серии «Физика» научного журнала «Вестник Карагандинского университета». Под его научным руководством выполнялись и были успешно защищены диссертационные работы на соискание ученой степени кандидата педагогических наук.

К.М. Арынгазин был высококвалифицированным специалистом в области теоретической физики и педагогики. Он являлся образцом не только для студенческой молодежи, но и для молодых преподавателей и сотрудников.

Светлая память о Канапие Мубараковиче Арынгазине навсегда останется в сердцах его учеников и коллег.

Редакционная коллегия серии «Физика»
журнала «Вестник Карагандинского университета»

АВТОРЛАР ТУРАЛЫ МӘЛІМЕТТЕР
СВЕДЕНИЯ ОБ АВТОРАХ
INFORMATION ABOUT AUTHORS

Afanasyev, D.A. — PhD, Senior researcher of the Institute of Applied Mathematics, Ye.A. Buketov Karaganda State University, Kazakhstan.

Ahmetzhanov, B. — Candidate of physical and mathematical sciences, docent, S. Amanzholov East Kazakhstan State University, Ust-Kamenogorsk, Kazakhstan.

Alikhaidarova, E.Zh. — PhD student, Ye.A. Buketov Karaganda State University, Kazakhstan.

Alkina, A.D. — Master, senior lecturer, Karaganda State Technical University, Kazakhstan.

Azimkhanov, A.S. — Deputy chief of research reactor complex «Baikal-1», National Nuclear Center of the Republic of Kazakhstan, Kurchatov, Kazakhstan.

Belukha, I. — Leading researcher, candidate of biological sciences, National Medical Research Center of Radiology, Obninsk, Russia.

Bogacheva, V. — Engineer, National Medical Research Center of Radiology, Obninsk, Russia.

Bolatbekova, M.M. — Master student, Ye.A. Buketov Karaganda State University, Kazakhstan.

Chaizhunusova, N.Z. — Professor, Semey State Medical University, Kazakhstan.

Çopuroğlu, E. — Gaziosmanpaşa University, Tokat, Turkey.

Endo, S. — Professor, PhD, Hiroshima University, Japan.

Fujimoto, N. — Professor, Hiroshima University, Japan.

Gnyrya, V.S. — Head of research reactor complex «Baikal-1», National Nuclear Center of the Republic of Kazakhstan, Kurchatov, Kazakhstan.

Hoshi, M. — Professor, PhD, Hiroshima University, Japan.

Ibrayev, N.Kh. — Doctor of physical and mathematical sciences, professor, Ye.A. Buketov Karaganda State University, Kazakhstan.

Ilina, L.F. — Candidate of physical and mathematical sciences, docent, Ye.A. Buketov Karaganda State University, Kazakhstan.

Iskakova, A.B. — PhD student, Abai Kazakh National Pedagogical University, Almaty, Kazakhstan.

Ivanov, S. — Doctor of medical sciences, deputy director, National Medical Research Center of Radiology, Obninsk, Russia.

Kairbayeva, A.K. — Candidate of pedagogical sciences, Head of International Relations Department, S. Toraighyrov Pavlodar State University, Kazakhstan.

Kalygulov, D. — PhD student, D. Serikbayev East Kazakhstan Technical University, The Faculty of Energy, Ust-Kamenogorsk, Kazakhstan.

Kaprin, A. — Director general, corresponding member of RAS, doctor of medical sciences, professor, National Medical Research Center of Radiology, Ministry of Health, Obninsk, Russia.

Kawano, N. — Professor, PhD, Hiroshima University, Japan.

Kayumova, A.S. — Senior lecturer, Ye.A. Buketov Karaganda State University, Kazakhstan.

Kim P.M. — Director, LLP «Konstruktor — 2014», Karaganda, Kazakhstan.

Klinovitskaya, I. — PhD student, D. Serikbayev East Kazakhstan Technical University, Ust-Kamenogorsk, Kazakhstan.

Kolyzhenkov, T. — Senior researcher, candidate of biological sciences, National Medical Research Center of Radiology, Obninsk, Russia.

Kutum, B.B. — PhD student, L.N. Gumilyov Eurasian National University, Nur-Sultan, Kazakhstan.

Lay, P. — PhD, Technical Director ECM Technologies, France, Grenoble.

Mehmetoğlu, T. — M.Sc., Amasya University, Taşova Vocational School, Turkey.

Mekhtiyev, A.D. — Candidate of technical sciences, associate professor, Karaganda State Technical University, Kazakhstan.

Muratbekov, B.M. — Master student, S. Amanzholov East Kazakhstan State University, Ust-Kamenogorsk, Kazakhstan.

Nurumkanov, D.K. — Master student, S. Amanzholov East Kazakhstan University, Ust-Kamenogorsk, Kazakhstan.

Ohtaki, M. — Professor, Hiroshima University, Japan.

Otani, K. — Professor, Hiroshima University, Japan.

Petukhov, A.D. — Research assistant, National Medical Research Center of Radiology, Obninsk, Russia.

Plotnikov, S.V. — Doctor of physical and mathematical sciences, professor, D. Serikbayev East Kazakhstan Technical University, Faculty of Energy, Ust-Kamenogorsk, Kazakhstan.

Sakaguchi, A. — Associate professor, PhD, Tsukuba University, Japan.

Serikov, T.G. — PhD, senior lecturer, Karaganda State Technical University, Kazakhstan.

Shabdarbaeva, D.M. — Doctor of medical sciences, professor, head of Departament, Semey State Medical University, Kazakhstan.

Shaikhova, G.N. — PhD, docent, L.N. Gumilyov Eurasian National University, Nur-Sultan, Kazakhstan.

Shevchuk, E.P. — Master, senior lecturer, S. Amanzholov East Kazakhstan University, Ust-Kamenogorsk, Kazakhstan.

Shichijo, K. — Professor, Nagasaki University, Japan.

Stepanenko, V.F. — Doctor of biological sciences, professor, National Medical Research Center of Radiology, Obninsk, Russia.

Yaskova, E. — Leading researcher, candidate of biological sciences, National Medical Research Center of Radiology, Obninsk, Russia.

Yugay, V.V. — PhD, associate professor, Karaganda State Technical University, Kazakhstan.

Zhangbyrbaj, Ye.R. — Master student, Ye.A. Buketov Karaganda State University, Kazakhstan.

Zhumadilov, K.Sh. — PhD, head of Department, L.N. Gumilyov Eurasian National University, Nur-Sultan, Kazakhstan.

Zhunussov, Y.T. — Professor, Semey State Medical University, Kazakhstan.